MOLECULAR CLONING, EXPRESSION AND ENZYMATIC CHARACTERIZATION OF CYTOSOLIC GLUTATHIONE S-TRANSFERASE FROM *Acidovorax* sp. KKS102

DAYYABU SHEHU

FACULTY OF SCIENCE
UNIVERSITY OF MALAYA
KUALA LUMPUR

2018

MOLECULAR CLONING, EXPRESSION AND ENZYMATIC CHARACTERIZATION OF CYTOSOLIC GLUTATHIONE S-TRANSFERASE FROM *Acidovorax* sp. KKS102

DAYYABU SHEHU

THESIS SUBMITTED IN FULFILMENT OF THE REQUIREMENTS FOR THE DEGREE OF DOCTOR OF PHILOSOPHY

INSTITUTE OF BIOLOGICAL SCIENCES
FACULTY OF SCIENCE
UNIVERSITY OF MALAYA
KUALA LUMPUR

2018

UNIVERSITY OF MALAYA

ORIGINAL LITERARY WORK DECLARATION

Name of Candidate: Dayyabu Shehu

Matric No: SHC140117

Name of Degree: Doctor of Philosophy

Title of Project Paper/Research Report/Dissertation/Thesis ("this Work"): MOLECULAR CLONING, EXPRESSION AND ENZYMATIC CHARACTERIZATION OF CYTOSOLIC GLUTATHIONE S-TRANSFERASE FROM *Acidovorax* sp. KKS102

Field of Study: Biochemistry

I do solemnly and sincerely declare that:

(1) I am the sole author/writer of this Work;
(2) This Work is original;
(3) Any use of any work in which copyright exists was done by way of fair dealing and for permitted purposes and any excerpt or extract from, or reference to or reproduction of any copyright work has been disclosed expressly and sufficiently and the title of the Work and its authorship have been acknowledged in this Work;
(4) I do not have any actual knowledge nor do I ought reasonably to know that the making of this work constitutes an infringement of any copyright work;
(5) I hereby assign all and every right in the copyright to this Work to the University of Malaya ("UM"), who henceforth shall be owner of the copyright in this Work and that any reproduction or use in any form or by any means whatsoever is prohibited without the written consent of UM having been first had and obtained;
(6) I am fully aware that if in the course of making this Work I have infringed any copyright whether intentionally or otherwise, I may be subject to legal action or any other action as may be determined by UM.

Candidate's Signature Date:

Subscribed and solemnly declared before,

Witness's Signature Date:

Name:

Designation

MOLECULAR CLONING, EXPRESSION AND ENZYMATIC CHARACTERIZATION OF CYTOSOLIC GLUTATHIONE S-TRANSFERASE FROM *Acidovorax* sp. KKS102

ABSTRACT

Glutathione S-transferases (GSTs) are a family of enzymes that function in the detoxification of a variety of electrophilic substrates. In this study, cloning and biochemical characterization of GSTs from *Acidovorax* sp. KKS102 were carried out. Database suggests that there are eleven putative GSTs in *Acidovorax* sp. KKS102. Phylogenetic analysis showed that the GSTs were distributed into Beta, Nu, zeta, Chi, while some did not show any particular class. Two GSTs (KKSG6 and KKSG9) were selected for further study. Sequence alignment showed that KKSG6 is closely related to BphK, a GST found within the operon responsible for PCB biodegradation in some organisms and showed dechlorination function against metabolites of polychlorobiphenyl degradation. The substrate specificity of KKSG6 included reacting with CDNB, ethacrynic acid, hydrogen peroxide and cumene hydroperoxide. Molecular docking, sequence alignment, and site-directed mutagenesis studies revealed some key amino acids that were found to play a crucial role in the catalytic activity of the protein. The C10F and A180P mutants displayed an increase in catalytic activity of the enzyme against CDNB and ethacrynic, however, the peroxidase activities did not show any significant change. In contrast, the K107T mutant displayed variable results toward various substrates suggesting its possible role in determining substrate specificity in this enzyme. Analysis of kinetic parameters using CDNB and GSH as substrates showed a high K_m value of the enzyme for CDNB when compared to GSH. C10F and A180P mutants also displayed a decrease in the affinity of both CDNB and GSH to KKSG6 with a corresponding increase in V_{max} and k_{cat}, however, K107T showed decrease in V_{max} and k_{cat}. The enzyme also

displayed dechlorination function against 2, 3, and 4-chlorobenzoates and 2,4-dichlorobenzoate. The C10F and A180P mutants both showed an increase in dechlorination function while K107T showed a variable result. The same trend of dechlorination activity was observed against DDT, endosulfan, and permethrin. Phylogenetic analysis revealed that KKSG9 is closely related to zeta class, however, it has possessed low sequence similarity to known zeta class GSTs. Functional analysis showed that the enzyme exhibits wider substrate specificity compared to most zeta class GSTs by reacting with 1-chloro-2,4-dinitrobenzene (CDNB), *p*-nitrobenzyl chloride (NBC), ethacrynic acid (EA), hydrogen peroxide, and cumene hydroperoxide. The enzyme also displayed dehalogenation function against dichloroacetate in addition to permethrin, and dieldrin. The mutant (Y12C) displayed low catalytic activity and dehalogenation function against all the substrates when compared with the wild type. Kinetic analysis using NBC and GSH as substrates showed that the mutant (Y12C) displayed a higher affinity for NBC when compared with the wild type, however, no significant change in GSH affinity was observed. The presence of a tyrosine residue in KKSG9 motif instead of commonly known Cys, Thr, Ser or Ala might represent an evolutionary trend toward improving the catalytic activity of the enzyme. These enzymes could be useful in the bioremediation of various classes of organochlorine pollutants.

Keywords: glutathione S-transferase, *Acidovorax* sp. KKS102, cloning, dechlorination, bioremediation.

EKPRESI PENGKLONAN MOLEKULAR DAN PENCIRIAN ENZIMATIK GLUTATION S-TRANFERASE SITOSOLIK DARI *Acidovorax* sp. KKS102

ABSTRAK

Glutathione S-transferase (GST) merupakan keluarga enzim dengan fungsi utama untuk mendetoksifikasi pelbagai substrat elektrofilik. Dalam kajian ini, proses pengklonan dan pencirian biokimia GST dari organisma degradasi bifenil/poliklorobifenil (PKB) *Acidovorax* sp. KKS102 telah dijalankan. Maklumat data memperlihatkan bahawa *Acidovorax* sp. KKS102 mengandungi 11 GST diduga. Analisis filogenetik menunjukkan GST tersebut terdiri daripada kelas Beta, Nu, Zeta dan Chi, dengan sebahagian lagi tidak mempunyai kelas yang khusus, justeru mencadangkan kewujudan kelas GST yang baharu. Dua kelas GST, iaitu KKSG6 dan KKSG9 telah dipilih untuk kajian lanjutan. Analisa jujukan identiti menunjukkan KKSG6 adalah berkait rapat dengan GST yang dikenali sebagai BphK. BphK wujud di dalam operon yang bertanggungjawab dalam proses biodegradasi PKB pada sesetengah organisma di samping fungsi penyahklorin terhadap metabolit degradasi poliklorobifenil. Ciri-ciri ini disumbangkan dari kemampuan yang tinggi untuk mendegradasi sebilangan organisma degradasi PKB. Ujian substrat spesifik KKSG6 memperlihatkan reaksi terhadap CDNB, asid etakrinik, hidrogen peroksida, dan kumin hydroperoksida. Keputusan pengdokan molekular, analisa jujukan identiti dan mutagenesis site-directed mendedahkan beberapa asid amino utama yang berperanan penting di dalam aktiviti katalitik di dalam protein tersebut. Mutan C10F dan A180P menunjukkan peningkatan di dalam aktiviti katalitik enzim terhadap CDNB dan asid etakrinik, namun, tiada perubahan signifikan terhadap aktiviti peroksida. Sebaliknya, mutan K107T menunjukkan reaksi yang berbeza di dalam aktiviti terhadap pelbagai substrat, mencadangkan peranannya di dalam penentuan spesifikasi substrat enzim tersebut. Analisa parameter kinetik menggunakan CDNB dan

GSH sebagai substrat memperlihatkan enzim tersebut mempunyai afiniti yang tinggi terhadap GSH jika dibandingkan dengan CDNB. Mutan C10F dan A180P juga menunjukkan pengurangan afiniti terhadap CDNB dan GSH kepada KKSG6, selaras dengan peningkatan V_{max} dan K_{cat}, namun K107T menunjukkan pengurangan V_{max} dan K_{cat}. Enzim tersebut juga mempamerkan fungsi deklorinasi terhadap 2, 3, dan 4-klorobenzoat serta 2,4-diklorobenzoat. Terdapat peningkatan di dalam fungsi deklorinasi yang diperlihatkan oleh kedua-dua mutan C10F dan A180P, namun keputusan terhadap K107T adalah pelbagai. Paten aktiviti diklorinasi ini turut dilihat terhadap DDT, endosulfan dan permethrin. Analisa filogenetik mendedahkan bahawa KKSG9 adalah berhubung rapat dengan kelas Zeta, namun, GST mempunyai jujukan identiti yang rendah, dengan ciri-ciri biokimia yang sama terhadap kelas Zeta GST. Analisis fungsi menunjukkan spesifikasi substrat yang lebih luas berbanding kebanyakkan kelas Zeta GST, melalui reaksinya terhadap 1-kloro-2,4-dinitrobenzena (CDNB), *p*-nitrobenzil klorit (NBK), asid etakrinik, hidrogen peroksida, kumin hidroperoksida. Enzim tersebut juga memperlihatkan fungsi dehalogenes terhadap dikloroasetat, permethrin dan dieldrin. Mutan (Y12C) menunjukkan aktiviti katalitik dan fungsi dehalogenes yang rendah terhadap kesemua substrat, berbanding jenis liar. Analisis kinetik menggunakan NBK dan GSH sebagai substrat mempamerkan mutan (Y12C) mempunyai afiniti yang tinggi terhadap NBK, berbanding jenis liar, namun didapati tiada perubahan signifikan terhadap afiniti GSH. Kehadiran residu tirosina pada motif KKSG9, berbanding pada sistin, treonina, tirosina dan alanina, menunjukkan kemungkinan aliran evolusi terhadap peningkatan aktiviti katalitik enzim. Enzim-enzim ini membawa kebolehan untuk fungsi bioremediasi terhadap pelbagai kelas agen pencemar organoklorin.

Katakunci: glutathione S-transferase, *Acidovorax* sp. KKS102, pengklonan, deklorinasi bioremediasi.

ACKNOWLEDGEMENTS

In the name of Allah most gracious most merciful. My thanks will surely go to almighty Allah first for seeing me through this process, indeed it is a blessing and may almighty Allah make the knowledge acquired to be of benefit to the entire humanity at large. My parents deserve a lot of recommendation and in fact, I can only say may almighty Allah bless them with Jannatul Firdaus for their kindness, prayers and patience toward us. May their gentle souls rest in perfect peace ameen. My profound gratitude will also go to Kaduna state government for offering me the PhD scholarship and the committee that piloted and oversees the overseas scholarship scheme. Bayero University Kano also deserved a lot of recommendation for offering me the fellowship award for this study.

I also wish to express my gratitude to our able supervisor in person of Associate Prof. Dr. Zazali Alias. No doubt I benefitted with a lot of inspiration, guidance, advice and encouragement from you Sir in the course of this research. I also cannot forget the person behind my coming to join this laboratory, Nasiru Abdullahi, you have really helped me, offered word of encouragement and in the end, I have benefitted a lot from you. Other colleagues in the lab cannot be forgotten as well, Haizatul Akmal, surely, I cannot forget you. Christina, Abiramy, and lots of undergraduate students, we really had a very nice stay. To my friends generally back at home, thank you very much for your prayers.

I wish to express my gratitude to my wife and the children for your perseverance and understanding. To my siblings: Yusuf, Nura, Ibrahim, Suraj, Nasir, Bintas, Hauwa, etc, I will also like to say thank you for your support. May Allah rewards you abundantly ameen. To my Friends in struggle: Murtala Ya'u, Hafeez Yakasai, Abba Babandi, Isah Fakai, Shehu Habibu and lots of others, I say thank you all for your support and prayers

My tribute also goes to my dear mother who passed away on 9th April, 2018. May almighty Allah forgive your short comings and may Jannatul Firdaus be your final abode.

TABLE OF CONTENTS

LIST OF FIGURES

LIST OF TABLES

LIST OF SYMBOLS AND ABBREVIATIONS

Abbreviations	Description
H_2O_2	Hydrogen peroxide
CDNB	1-Chloro-2,4-dinitrobenzene
CuOOH	Cumene hydroperoxide
DCA	Dichloroacetate
DCNB	1,2-Dichloro-4-nitrobenzene
DDT	Dichlorodiphenyltrichloroethane
EA	Ethacrynic acid
EPNP	3,4-epoxy-3-methyl-1-butene
GR	Glutathione reductase
GSH	Reduced glutathione
GST	Glutathione S-transferase
HCCA	2-Hydroxychromene-2-carboxylic acid
IPTG	Isopropyl-β-thiogalactoside
LB	Luria Bertani
MAPEG	Membrane-associated proteins involved in eicosanoid
NADPH	Nicotinamide adenine dinucleotide phosphate
NBC	Nitrobenzyl chloride
NCBI	National Center for Biotechnology Information
PCB	Polychlorobiphenyls
PCP	Pentachlorophenol
RMSD	Root mean square deviation
SDS-PAGE	Sodium deodecyl polyacrylamide gel electrophoresis
TCHQ	Tetrachlorohydroquinone

LIST OF APPENDICES

CHAPTER 1: INTRODUCTION

1.1 Research Background

Glutathione S-transferases (GSTs) constitute several different classes of enzymes which deals with detoxification, and, in some instances, activation of different classes of substrate through catalytic conjugation with tripeptide glutathione (GSH) and thereby increasing their solubility and subsequent excretion from the body (Alias & Clark, 2010; Dainelli et al., 2002; Hayes, et al., 2005; Oakley, 2005; Clemens, 2006). GSTs serves to reduce the reactivity of electrophilic compounds to cellular macromolecules by forming a water-soluble glutathione conjugate which can be easily removed or degraded (Sheehan et al., 2001; Chee et al., 2014; Vignesvaran & Alias, 2016). GSTs have a staggering range of substrate to react with including drugs, pesticides, herbicides, environmental toxicants/carcinogens and other endogenously produced molecules (Allocati et al., 2009; Hayes & Pulford, 1995). Bacterial GSTs were also found to have other unique functions, such as dehalogenation of dichloromethane and pentachlorophenol as well as biodegradation of atrazine and lignin (Allocati et al., 2009; Bader & Leisinger, 1994; Favaloro et al., 1998; Favaloro et al., 2000; Sonoki et al., 2002). GSTs have both positive and negative effects, they serve to protect the organism from dangerous environmental substances, while at the same time they are implicated in resistance phenomenon (Hayes et al., 2005; Hamilton et al., 2003; Sies, 1999).

GSTs are classified based on location as cytosolic, mitochondrial, microsomal and bacterial specific fosfomycin resistant protein (Allocati et al., 2009; Armstrong, 2000; Hayes et al., 2005). However, other factors such as immunological properties, kinetic features, and similarity in crystal structure played a great role in determining a GST class (Hayes et al., 2005; Sheehan et al., 2001). Cytosolic GSTs currently contained the largest members so far discovered in both prokaryotic and eukaryotic organisms. In bacteria, at least seven different members were discovered to date, these are; Beta, Chi, Theta, Zeta,

Rho, Eta, and Nu classes (Pandey et al., 2015; Rossjohn et al., 1998; Sheehan et al., 2001; Skopelitou et al., 2012; Stourman et al., 2011; Vuilleumier, 1997; Wiktelius & Stenberg, 2007).

A significant number of the techniques applied for environmental clean-up are either partially effective or prohibitively expensive (Das, 2014; Zhao & Poh, 2008). This, however, points to the need to develop effective and economically feasible waste remediation technologies that could be rapidly deployed in a range of physical settings (Das, 2014; Singh et al., 2017). The metabolic potential of the microbial community to transform various compounds provides a safe and economic alternative to eliminating pollutants in a less costly way. Microorganisms possessed various characteristics which make them an ideal target to be utilized for bioremediation purposes. These include; short life cycles, high rates of genetic mutation, ease of genetic exchange, small size, a range of resting or protective stages and well-developed detoxification and co-metabolic strategies which allow them to exist in environments that are refractory to higher plants and animals (Watanabe, 2001; Zhang et al., 2017). Furthermore, they can be found in oil spills, chlorinated hydrocarbon mixtures, mixed pyrogenic wastes, hot acid sulfur springs, Antarctic permafrost layer, sediments containing high levels of polycyclic aromatic hydrocarbons, nitrogen-containing aromatics, heavy metals and trace elements (Chanal et al., 2006; Edwards et al., 1998; Horikoshi, 1998). The ability of microbial flora to survive in such extreme environments suggests that over evolutionary times, the organisms are endowed with broadly specific mechanisms for detoxifying and metabolizing a wide range of materials found in anthropogenic pollutant mixtures (Dash et al., 2013).

Acidovorax sp. KKS102 formerly known as *Pseudomonas* sp. KKS102 is a biphenyl/polychlorinated biphenyl (PCB) degrading organism isolated from a soil sample

containing biphenyl/PCB hydrocarbons (Ohtsubo et al., 2012). PCBs are synthetic and very stable organic molecules that carry multiple chlorine atoms on a biphenyl carbon skeleton. They have excellent properties and as such they are used industrially for various applications; however, they are among the persistent pollutants that can remain in soil and water bodies for up to decades (Borja et al., 2005). Also, because of their lipophilic nature, they tend to magnify and bioaccumulate in higher trophic level organisms where they cause a serious threat to the natural ecosystem and human health. Many PCBs are endocrine disrupting chemicals, carcinogenic and have effects on liver function and nervous system (Kaushik & Kaushik, 2007). Although they are banned, the compounds still exist in the environment at present and pose a great threat to humans, wildlife and the environment (Barakat et al., 2013). They are volatile and have long-range of transport in the atmosphere period. As such, they can be found even in environments where they have never been used or produced, such as Antarctic and Arctic (Cabrerizo et al., 2012). PCBs are among the twelve chemicals classified in the Stockholm convention to be prioritized for eventual elimination by 2025 (Borja et al., 2005).

Bacterial GSTs played a role also in the biodegradation of several exogenous molecules in addition to playing a significant role in detoxification of endogenously produced molecules such as free radicals and other products of oxidative stress (Hayes et al., 2005; Vuilleumier, 1997). Some bacterial GSTs were found to be situated in many degradative pathways signifying their role in the biodegradation of several other exogenous molecules (Hofer et al., 1994; Lloyd-Jones & Lau, 1997). One of such important function is the dehalogenation exhibited by various classes of bacterial GST. The dehalogenation reaction renders many halogenated compounds either less toxic or more soluble thereby helps in eventual biodegradation of such pollutants. These include; dichloromethane dehalogenases, dichloroacetate dehalogenases, in atrazine metabolism

and polychlorobiphenyl degradation pathways (Favaloro et al., 2000; Scholtz et al., 1988; Seeger & Pieper, 2010; Thom et al., 2001)

A specific bacterial GST was found to be situated within an operon termed *bph*, which is responsible for biphenyl/PCB biodegradation is some organisms (Seeger & Pieper, 2010). This GST termed BphK was found to be responsible for dehalogenation of toxic metabolites such as chlorobenzoates, 4-chloro-2-hydroxy-6-oxo-6-phenyl-2,4-dienoate(HOPDA), 3-chloro-2-hydroxy-6-oxo-6-phenyl-2,4-dienoate (HOPDA), and 2,6-dichloro-2,3-dihydroxy biphenyl generated during the biodegradation process (Abraham et al., 2002; Dai et al., 2002; Seah et al., 2000). The existence of BphK in some biphenyl degraders was attributed to the high degradation capability of PCBs in some biphenyl/PCB degraders such as *Burkholderia xenovorans* LB400, considered as a model organism for PCB biodegradation (Seeger & Pieper, 2010). However, biochemical characterization of BphK in *Burkholderia xenovorans* LB400 showed that the GST has limited substrate specificity and low catalytic activity (Bartels et al., 1999; Fortin et al., 2006). One promising way of improvement is to screen various BphK homologs present in biphenyl utilizing strains with potential dehalogenase activities. It has been suggested that some of this GST homologs might have had desired and sufficient activity against chlorinated benzoates that hamper the complete metabolism of PCBs.

1.2 Research Question

Even though *Acidovorax* sp. KKS102 has shown a very promising application in the biodegradation of polychlorobiphenyls, the *bph* operon in this organism is lacking a BphK gene. There were various attempts to improve on the biodegradation capability of *Acidovorax* sp. KKS102 including the insertion of a constitutive promoter that enhances the overexpression of *bph* genes (Ohtsubo et al., 2003). The symbiotic relationship of *Acidovorax* sp. KKS102 and *Pseudomonas fluorescence* KKL101 in which, the latter

utilizes the biodegradation product of the former (benzoate) as its source of carbon was also well studied (Kikuchi et al., 1995; Kimbara et al., 1988). However, it was found that while biphenyls can be fully degraded by the concerted action of *Pseudomonas fluorescens* KKL101 and *Acidovorax* sp. KKS102, polychlorobiphenyls were found not to be fully degraded by these organisms. By-products such as chlorobenzoates were found as dead-end metabolites in the biodegradation process (Kikuchi et al., 1995). Information from the complete genome sequence of *Acidovorax* sp. KKS102 showed that the organism contained many putative GSTs. Studies on these GSTs might open a way for their eventual utilization in the engineering of a strain with better degradation capability. Because bacterial GSTs also showed a promising application in the dechlorination of many organochlorine pesticides and herbicides, the research will as well look at the possibility of the interaction between the GSTs and some organochlorine pesticides.

1.3 Research Objectives

(a)To investigate the properties of glutathione S-transferases in *Acidovorax* sp. KKS102 through bioinformatics analysis

(b)To clone, express and purify the recombinant GSTs from *Acidovorax* sp. KKS102

(c)To biochemically characterize the recombinant GSTs

1.4 Research Linkages and Correlation Between the Chapters

The thesis writes up is in a conventional format which progressively coordinates each chapter with the one preceding it. There is a total of six chapters. Chapter 1 is the (general introduction) which explained the general background of the study, research question as well as research objectives. Chapter two covered the (literature review) which explained extensively a review of the related literature, current classification of bacterial cytosolic

GSTs, previous and current works on glutathione S-transferase in bacteria, and the role played by bacterial GST in various dehalogenation reactions. Chapter three deals with the methodology section. This chapter explained in detail, the materials including equipment, reagents and the methodologies employed in answering the research question. Chapter four deals exclusively with the results obtained This chapter tried to pull out information on the putative GSTs identified in *Acidovorax* sp. KKS102 including their probable distribution into various classes, their molecular weight, isoelectric points and the relationship between the putative GSTs. The GSTs in *Acidovorax* sp. KKS102 were also analyzed through bioinformatic analysis in order to identify a suitable BphK homologue and other GST for further studies. The chapter then explained the processes of cloning the identified gene (KKSG6), confirmation of the clone, transformation, expression and characterization of the gene using available known GST substrates. The chapter further explained the kinetic analysis of the KKSG6 using CDNB and GSH as substrates. Site-directed mutagenesis and characterization of the mutants were also carried out in this chapter in order to investigate the functional role of some amino acids in the catalytic activity of the protein. Investigation of possible interaction between the BphK homolog and various chlorobenzoate substrates and some organochlorine pesticides through molecular docking study was carried out in chapter five. Dehalogenation function of the identified BphK homolog against various chlorobenzoate substrates and some organochlorine pesticides was also investigated in this chapter. Furthermore, cloning and characterization of another gene; a novel zeta-like glutathione s-transferase (denoted as KKSG9) was also carried out. Investigation of the kinetic properties of the KKSG9 using *p*-nitrobenzyl chloride and GSH as substrates was also carried out. Site-directed mutagenesis was carried out on Tyr12 in order to investigate the functional role of the amino acid in the catalytic activity of the protein. The possible interaction and dehalogenation function of KKSG9 against dichloroacetate, permethrin, and dieldrin as

substrates were also investigated. Finally, chapter six is the conclusion and recommendation chapter. The chapter summarizes the major findings in the research and gives a suggestion on the future direction of further research.

CHAPTER TWO: LITERATURE REVIEW

2.1 Glutathione S-transferase

Glutathione S-transferases (GSTs) comprises many classes of enzymes that catalyze the conjugation reactions between the tripeptide glutathione (GSH) and several classes of electrophilic non-polar substrates yielding water-soluble, less toxic product which can be degraded or excreted from the cell (Sherratt & Hayes, 2001; Atkinson & Babbit, 2009). The potential substrates for GSTs includes: drugs, hormones, pesticides, products of oxidative stress and several other xenobiotics (Allocati et al., 2009). Furthermore, GSTs were found to participate and catalyze other reductive reactions during the transformation of organic and inorganic peroxides and isomerization reactions during metabolism of some amino acids (Benson et al., 1977; Ketterer et al., 1990). GSTs played also a key role in resistance to chemotherapy in which their polymorphism is implicated in cancer chemotherapy (Hall et al., 1989). Several other non-catalytic functions are also associated with GSTs such as intracellular transport of hydrophobic ligands, sequestration of carcinogens and regulation of signal transduction pathways (Hayes et al., 2005). They also participate in leukotriene as well as prostaglandins biosynthesis (Jakobsson et al., 1997; Kanaoka et al., 1997; Shigeki et al., 1987). They are ubiquitously present in the majority of species such as plants, animals, and bacteria. In mammals, GSTs constitute about 4% of total soluble proteins in the liver and most of them are soluble enzymes with the exception of some microsomal GSTs (Hayes et al., 2005).

GST monomers are about 25,000 Da proteins and they form either homo or heterodimer (Figure 2.1). The subunits for both homo and heterodimer are derived from the same class of isoenzyme and the process occurred naturally (Frova, 2006). Each monomer has a G-site which binds the co-substrate glutathione (GSH) and H-site which bind different hydrophobic substrates (Oakley, 2005). The G-site is an essential pocket

that is specific for GSH and was found to be conserved among all GST classes. It is formed as a result of dimerization between the N and C-terminal domains of the two subunits. Moreover, the formation of heterodimer one subunit from each of the two isoenzyme increases the catalytic repertoire of the protein because each subunit can now bind to its preferred substrate (Vargo & Colman, 2004). The C-terminal contains the H-site and unlike the G-site, it varied among GSTs, this allows different electrophilic substances both the endogenous and the exogenous to bind to the site (Dourado et al., 2008). Catalytic active monomers have not been observed in GST and whether the formation of dimers is coupled to an increase in the activity of the enzyme is a subject of investigation (Oakley, 2005). Some studies using pi isoenzyme suggests that dimerization results in stabilization of the tertiary structure of the individual subunits and this can presumably be extended to each of the domains of the subunit (Erhardt & Dirr, 1995). However, positive cooperativity was observed with respect to GSH binding and CDNB activity in mutant pi enzyme by the disruption of ion pair between Cys 47 and Lys 54 (Bello et al., 1995). Secondary catalytic activities of some GSTs were also observed. These GSTs have selenium independent steroid isomerization as well as peroxidase activity with organic hydroperoxides (Hurst et al., 1998; Prabhu et al., 2004).

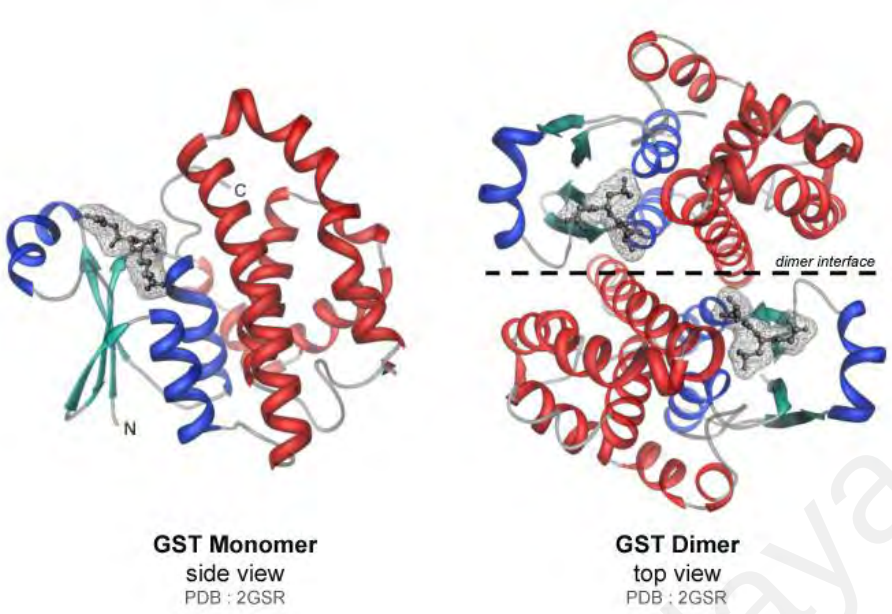

Figure 2.1: Structure of GST monomer and dimer (Frova, 2006).

2.2 Discovery of GSTs

The discovery of GST was dated as far back as 1961 when conjugation reactions between GSH and 1,2-dichloro-4-nitrobenzene (DCNB) or bromosulfophthalein in the rat liver cells were observed to be facilitated under the influence of certain enzyme (Booth et al., 1961; Combes & Stakelum, 1961). The enzyme was later found to be ubiquitously distributed in almost all organisms including; microbes, insect, plants, fish, birds, and mammals (Hayes & Pulford, 1995).

2.3 GST substrates

Various substrates were used to measure GST activity in living organisms including 1-chloro-2,4-dinitrobenzene, ethacrynic acid, para-nitrobenzyl chloride, hydrogen peroxide, cumene hydroperoxide, 1,2-epoxy-3-p-nitrophenoxypropane, fosfomycin, dichloromethane, tetrachloro-p-hydroquinone and much more (Vuilleumier, 1997). The structures of some standard and physiological substrates for GSTs are presented in (Figure 2.2 and 2.3) respectively.

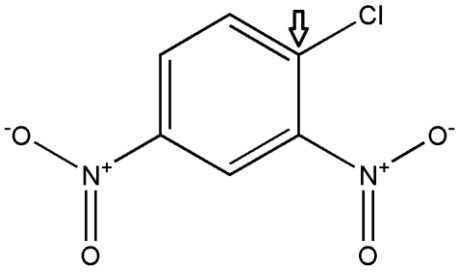

1-chloro-2,4-dinitrobenzene

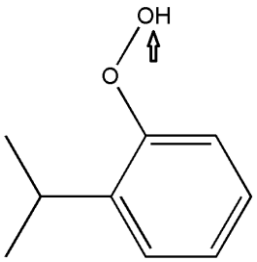

cumene hydroperoxide

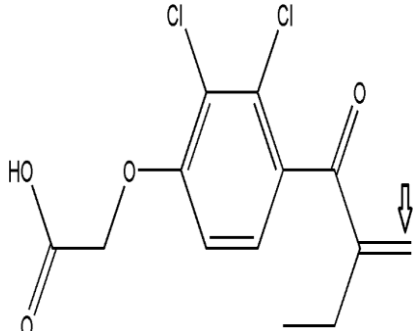

Ethacrynic acid

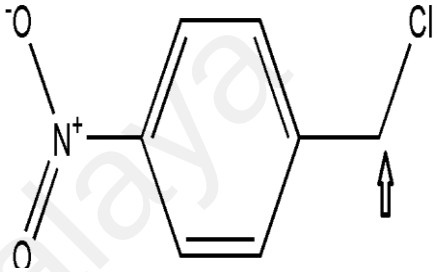

para-nitrobenzyl chloride

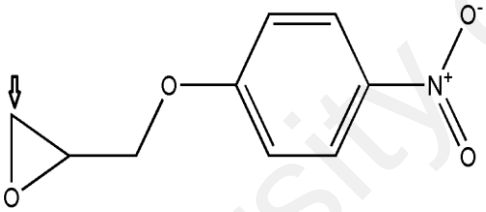

1,2-epoxy-3-p- nitrophenoxypropane

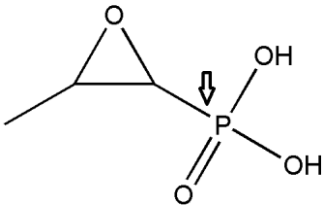

Fosfomycin

Figure 2.2: Structure of some standard substrates used to measure GST activity. The arrow indicates the point of attack by the GSH.

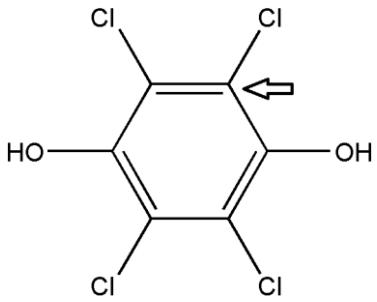

Tetrachloro-p-hydroquinone

dichloromethane

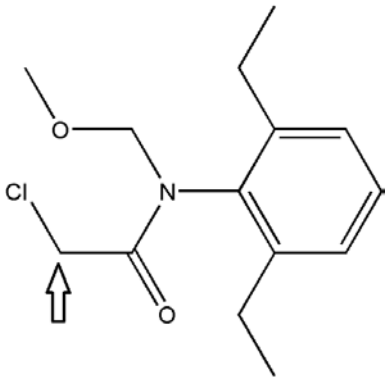

Alachlor

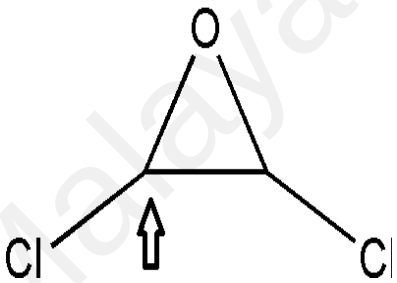

2,3-dichlorooxirane

Figure 2.3: Structure of some physiological substrates for GSTs. The arrows indicate the point of GSH attachment.

2.3 Role of GSTs in the metabolism of xenobiotics and endobiotics

Advances in agricultural practices, industrialization, and many other activities have resulted in a sharp increase in non-nutritional foreign chemical species which living organisms are continuously exposed (Glick, 2015). The interaction of organisms with the chemical species is mostly deleterious, cancer and carcinogenic effects are some widely noticed effects (Ames et al., 1990). Plant and fungal toxins, superoxide radical and hydrogen peroxide (H_2O_2) are among the naturally occurring toxic compounds. One of the fundamental requirements necessary for survival is the ability to overcome the threats posed by both the endogenously produced and or xenobiotic compounds (Hayes & Pulford, 1995; Vuilleumier, 1997). Generally, living organisms have evolved various strategies to catalytically transform a given toxic substance to a less toxic product which

includes binding, sequestration, and scavenging (Koppel et al., 2017). The scheme for the phase I and phase II of xenobiotic metabolism is presented in (figure 2.4). Phase I of xenobiotic metabolism is often characterized by the introduction of a functional group to the chemically inactive xenobiotic thereby creating an electrophilic center that is attacked by the reduced GSH in phase II. The phase II reaction is catalyzed by glutathione S-transferase in which Conjugation of xenobiotic with GSH served as a molecular flag which renders the molecule more soluble and allows it to be excreted (Jakoby, 2012).

The glutathione (GSH) react with the electrophilic substrate to form a more soluble and less toxic compound (GSR). The rate-limiting reaction is measured by the product released and is controlled by the C-terminal region of the enzyme (Armstrong, 1997). Activation of GSH to form anionic thiolate (GS^-) is the first stage of the reaction. Binding of the GSH to the G-site of the enzyme results in deprotonation and a concomitant decrease in the pKa of the thiol group from 9.2 to 6.2-6.6 pH units (Caccuri et al., 2002).

From the chemical point of view, GST substrates encompass all classes of compounds that can be able to react with the thiol moiety of GSH. This includes both the naturally synthesized and man-made compounds. They include herbicides, pesticides, environmental pollutants, drugs carcinogens, methyl parathion, muconaldehyde, atrazine, DDT, lindane, Malathion, and tridiphane are all detoxified by GST (Hamilton et al., 2003; Hayes & Pulford, 1995; Lien et al., 2002). Epoxides such as those that formed from aflatoxin B1, polycyclic aromatic hydrocarbons (PAH) and fosfomycin are also substrates for GSH conjugation (Hayes & McLellan, 1999; Vos et al., 1989). Some GST substrates are activated by CYP_{450}, some are activated by cyclooxygenase while isothiocyanates are formed as a result of combustion of vegetables (Marnett, 1994; Verhoeven et al., 1997).

Some metabolic reactions in the living organism such as aerobic respiration produce reactive oxygen species through oxidative phosphorylation which are detrimental to the

body system. These include; peroxide radicals, anion radicals and superoxide anions (Finkel & Holbrook, 2000). Other processes such as cyclooxygenase, lipooxygenase, CYP_{450} and xanthine oxidase-catalyzed reactions also contribute to their formation. These free radicals can attack macromolecules such as DNA, proteins, lipids, and carbohydrates to inflict damages and further produces secondary reactive metabolites (Marnett et al., 2003). The attack on membrane lipids is the most detrimental because it results in a free radical chain reaction which would amplify the damage to the membrane and hence destroy cells (Slater, 1988). Enzymatic defense system such as glutathione peroxidase, superoxide dismutase, and catalase neutralize the effect of these free radicals. However, some of them ultimately react with these macromolecules especially the membrane lipid leading to the formation of a free radical chain reaction. Unstable hydroperoxides are produced in the process which is further broken down to form secondary products such as ketoaldehydes, epoxyaldehydes and 2-alkenals some of which are genotoxic (Marnett et al., 2003). Enzyme systems such as alcohol dehydrogenase, aldehyde dehydrogenase, aldo-keto reductase and glutathione peroxidases catalyze the degradation of these secondary products into harmless substances (Hayes & McLellan, 1999). Metabolism of catecholamines (epinephrine and nor-epinephrine) also results in the formation of O-quinones which are reactive compounds, they are detoxified by GST (Baez et al., 1997).

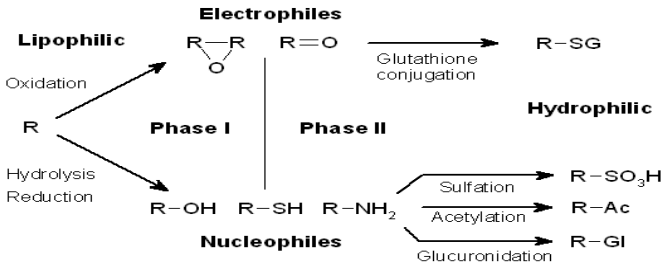

Figure 2.4: Phase I and II of xenobiotics metabolism (Retrieved from: https://www.ncbi.nlm.nih.gov/pubmed/8461038).

Conjugation of glutathione with various compounds does not necessarily mean detoxification. However, in some cases, the conjugate is even more toxic than the parent compound. Typical examples are seen with ethylene dibromide (EDB) and dichloromethane (DCM) (Guengerich et al., 2003; Wheeler et al., 2001). The formation of an electrophilic center which can potentially react with DNA to form adduct was also observed during conjugation of dichloromethane with GST (Wheeler et al., 2001). In the case of ethylene dibromide, the glutathione conjugates undergo rearrangement reaction to produce episulfonium intermediate capable of modifying DNA (Wheeler et al., 2001).

Some GST conjugates exert their toxic effects by depleting the cell GSH pool. A typical example is seen in plant glucosinolates metabolites such as sulforaphane and isothiocyanates of allyl, benzyl, and phenethyls (Xu & Thornalley, 2001). They reversibly form thiocarbamates by conjugation with GSH and following export from the cell by multidrug resistance proteins (MRPs), the thiocarbamates can undergo spontaneous degradation and the resulting isothiocyanates can be re-taken up by the cell and undergo another conjugation with GSH. The intracellular GSH level will be depleted in the process especially in those cells with low level of GSH and the isothiocyanates distribute themselves in the body, conjugate with other proteins and results in cell death (Xu & Thornalley, 2001). However, in some cases, the depletion of GSH level in the cell is of advantage. Many kinds of literatures have shown that overexpression of GST in a tumor is the basic mechanism associated with tumor resistance to drugs (Morrow et al., 1998). Anticancer drugs such as cyclophosphamide, thiotepa, and melphalan are ultimately metabolized and rendered inactive by GST before carrying out their functions (Hayes & Pulford, 1995; Tew, 1994). One way to circumvent this problem is to develop inhibitors of GST or employ mechanisms that would deplete the cell's GSH level, this will allow the drugs to function properly without being inactivated (Sherratt & Hayes, 2001).

2.5 Special functions of bacterial GSTs

In addition to the above-mentioned functions of GSTs, bacterial GSTs were found to have many other functions including; dehalogenation reaction of chlorinated compounds, biodegradation of several organic compounds both aromatic and aliphatic which are widely used in industries as well as biodegradation of potentially dangerous polycyclic aromatic hydrocarbons (Allocati et al., 2009).

2.5.1 Dehalogenation reactions

Halogenated organic compounds comprise diverse classes of compounds which are lipophilic and thus have a great tendency for bioaccumulation in food chains (Sims et al., 2014). They include; polycyclic aromatic hydrocarbons, pesticides, herbicides and several other industrial chemicals (Rigét et al., 2016). They are among the most heavily used compounds in the environment, however, some of them appeared to be recalcitrant and therefore causes a great threat to the environment and animal health as well (Fiedler, 2002). The toxicity and persistent of halogenated compounds is quite related to the number of halogen atoms attached to the carbon skeleton. The higher the number of halogens attached the greater the lipophilic nature and persistent of the organic compound (Harrad, 2010). Some halogenated compounds such as chloroacetate and 1-chlorobutane are easily biodegradable by microbial flora that is available in almost all environments, others such as dichloromethane and 1,2-dichloroethane the degradative organism can only be isolated after prolong exposure to the halogenated compound i.e., as a result of adaptation (Janssen et al., 2005; Leisinger, 1996).

2.5.1.1 Dehalogenation of dichloromethane

Dehalogenation reaction represents one of the most important and initial steps during the biodegradation of chlorinated compounds. Even though there are many dehalogenases

with activity towards chlorinated compounds, however, not all of them are GSTs (Hug et al., 2013; Yamamoto et al., 2005). Dichloromethane (DCM) is one of the widely used solvents and as a result, it appeared to be one of the common waste water contaminants (Copley, 1998). DCM dehalogenases in bacteria belong to GST superfamily and they are classified as theta class GST because of their close relation to the eukaryotic theta GSTs (Allocati et al., 2009). DCM dehalogenase catalyzes a reaction in which the GSH attack DCM to form unstable thioester linkage which decomposes spontaneously to form formaldehyde and regenerate GSH (Figure 2.5) (Blocki et al.,1994). Two DCM dehalogenases isolated from *Methylobacterium dichloromethanicum* (DM4) and *Methylophilus leisingeri* (DM 11) with 56% sequence identity are among the most extensively studied and characterized GSTs (Scholtz et al., 1988; Stourman et al., 2003). They both have the same essential serine residue at the N-terminal sequence (Allocati et al., 2009). The difference between the two dehalogenases lies in the fact that DM11 quickly out-compete DM4 when grown in the same millimolar concentration of DCM, that is, the former has a greater rate of dechlorination than the latter. However, these are the properties expected considering the origin of the two DCMDs, DCM11 was isolated from sample that was exposed to high level of DCM for long period (Scholtz et al., 1988) while DM4 was isolated from the site with a presumably low concentration of DCM (Gisi et al., 1998).

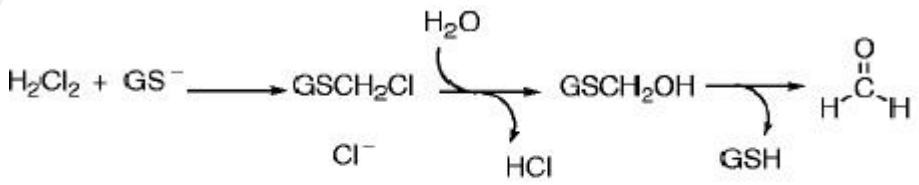

Figure 2.5: Mechanism of dehalogenation of dichloromethane by methylotrophic DCM degraders (Copley, 1998).

2.5.1.2 Dehalogenation of tetrachlorohydroquinone (TCHQ)

Tetrachlorohydroquinone (TCHQ) dehalogenase is another enzyme with significant identity to microbial zeta class GST superfamily (McCarthy et al., 1996). The best-studied TCHQ dehalogenase is from *Sphingobium chlorophenolicum* (Kiefer & Copley, 2002; Kiefer et al., 2002). The enzyme is involved in the biodegradation of pentachlorophenol, a fungicide used for wood preservation (Habash et al., 2002). TCHQ dehalogenase catalyzes the reductive dehalogenation of TCHQ to form dichlorohydroquinone utilizing two GSH molecules in the process (Xun et al., 1992). The proposed mechanism of dehalogenation by TCHQ dehalogenase was quite similar to that of GST catalyzed reactions (Figure 2.6).

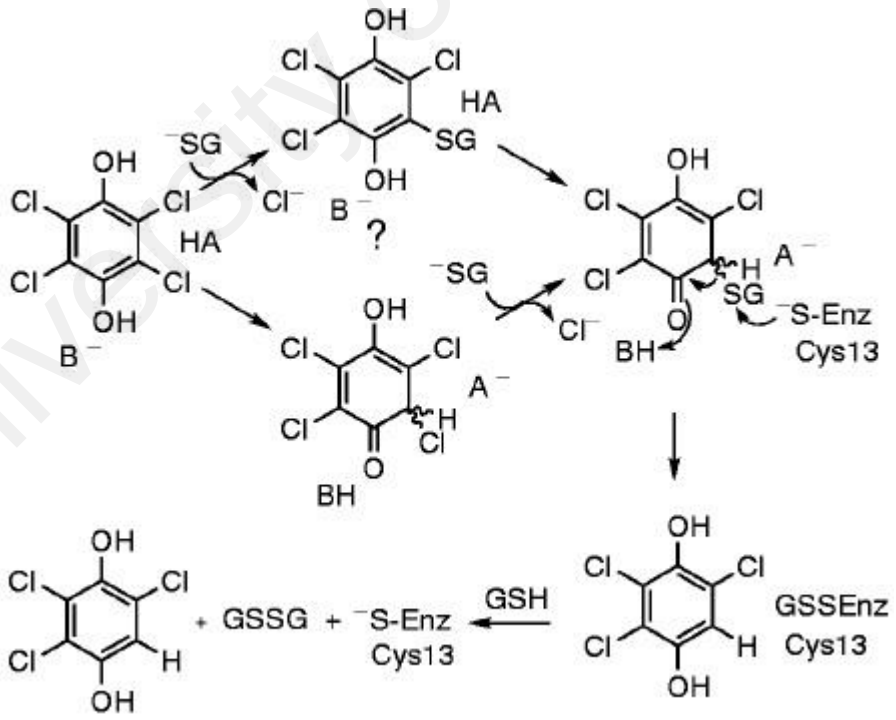

Figure 2.6: Mechanism of TCHQ dehalogenase during reductive dechlorination of TCHQ (Copley, 1998).

2.5.1.3 Dehalogenation of atrazine

Atrazine is a synthetic chlorinated compound and one of the most widely used herbicide after glyphosate for controlling grassy weeds and is relatively persistent in the soil (De Souza et al., 1998). Biodegradation of atrazine is carried out by a single microorganism or microbial consortium (Smith et al., 2005). The best-studied response of microbial population on exposure to atrazine is derived from *Pseudomonas* strain ADP (Sadowsky et al., 1998). This strain responded by producing enzymes that degrade the atrazine to cyanuric acid (Sadowsky et al., 1998). The first step involves the removal of chlorine atom through conjugation with GSH and this is subsequently followed by additional three enzymatic steps that degrade the compound to cyanuric acid (Figure 2.7) (Allocati et al., 2009). Bacterial glutathione S-transferase catalyzes the initial dehalogenation reaction and this produces the substrate for the next enzymatic steps (De Souza et al., 1998). The cyanuric acid is then further metabolized to carbon dioxide and ammonia by *Pseudomonas* sp. ADP and many other soil bacteria (Cook, 1987; Mandelbaum et al., 1995).

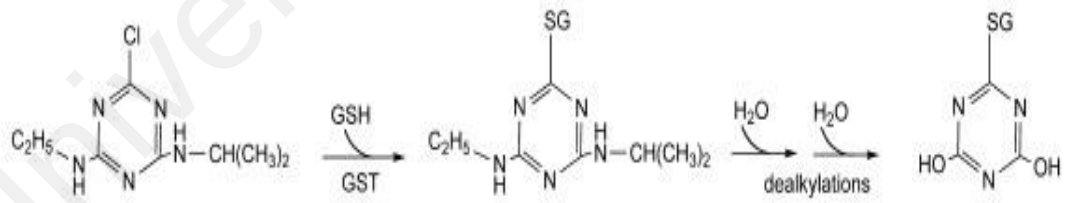

Figure 2.7: Degradation of atrazine to cyanuric acid by *Pseudomonas* sp. strain ADP. GST catalyzes the first dehalogenation reaction (Allocati et al., 2009).

2.5.1.4 Dehalogenation of organochlorine pesticides and herbicides

A specific glutathione S-transferase situated within the operon of some biphenyl/polychlorobiphenyl degrading organisms termed BphK was also found to show dechlorination activity against many pesticides and herbicides. The enzyme was shown

to be a potential candidate that could be employed in plants growth promoting bacteria so as to help in protecting the plants against the pesticides and provide a cleaner environment (McGuinness et al., 2007).

2.5.1.5 Dehalogenation of dichloroacetate

Dichloroacetate (DCA) is a water contaminant that is believed to be carcinogenic and can cause liver damage. A newly discovered Rho class GST was found to have a dichloroacetate dechlorinating activity against this chemical which is eventually converted into glyoxylate with the release of chloride ions (Pandey et al., 2015). The proposed pathway for complete DCA metabolism is presented below (Figure 2.8).

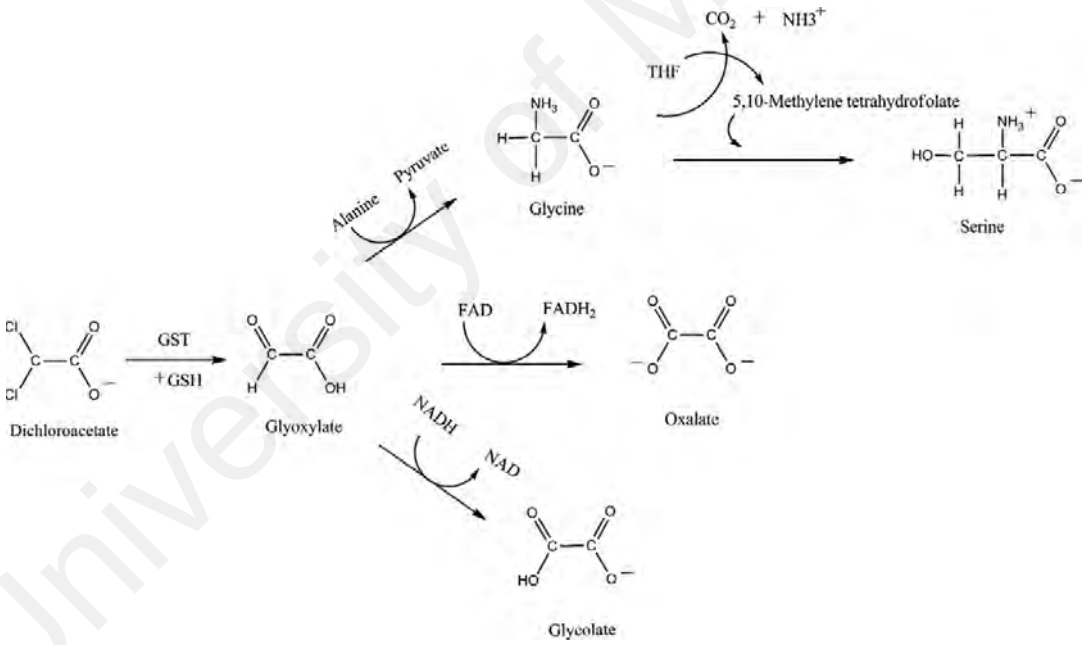

Figure 2.8: Fate of DCA and metabolic degradative pathway of glyoxylate (Pandey et al., 2015).

2.5.2 Other conjugation reactions

2.5.2.1 Isoprene metabolism

Isoprene (2-methyl-buta-1,3-diene) is a volatile compound emitted from plants especially under the thermal condition and from several other bacteria. Isoprene plays a

major role in atmospheric chemistry because of its involvement in the generation of ozone, carbon monoxide and organic peroxides (Thompson, 1992). Isoprene is produced industrially as a byproduct of naphtha or as a side product in the synthesis of ethylene. The compound is shown to be carcinogenic and with effects on skin and respiratory system making it imperative to be removed from the environment (Ashworth et al., 2010). Two GST genes (isoI and isoJ) from *Rhodococcus* sp. strain AD45 were found to be involved in isoprene metabolism and their functional properties were characterized (van Hylckama Vlieg et al., 1998). The organism degrades isoprene and utilizes the compound as a source of energy (van Hylckama Vlieg et al., 1998). Two glutathione S-transferases are involved in the biodegradation of isoprene. The first GST catalyzes the opening of the epoxide ring in isoprene monoxide with subsequent formation of the conjugation product. The second GST is a lyase that catalyzes the removal of the GSH conjugated in the first reaction (Figure 2.9) (van Hylckama Vlieg et al.,1999).

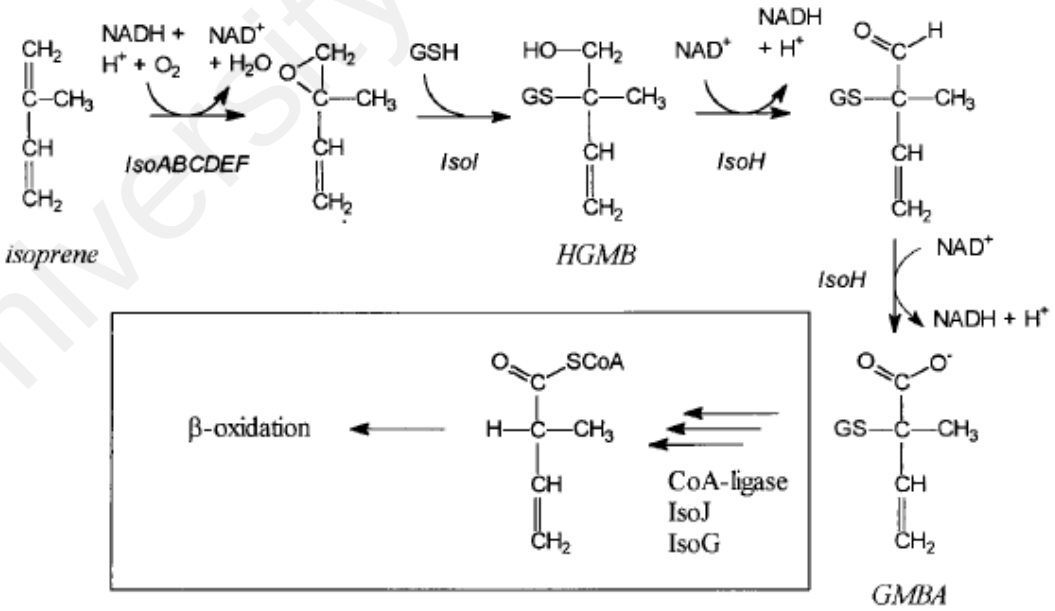

Figure 2.9: Pathway of isoprene degradation in *Rhodococcus* sp. strain AD45 (van Hylckama Vlieg et al., 2000).

2.5.2.2 Lignin degradation

Lignin is one of the most abundant aromatic material in nature. In order to achieve effective commercial utilization of lignin, the polysaccharide component of lignocellulose needs to become fully accessible (Camarero et al., 2014). The degradation of lignin is achieved by the concerted action of both the bacterial and fungal enzymes. The product can then be used for various applications such as ethanol production, in the paper industry, and animal feeding (Camarero et al., 2014). LigE, LigF and LigG in *Sphingomonas paucimobilis* SKY-6 were found to be GSTs involved in the degradation of β-aryl ether linkages (Masai et al., 2003). LigE and LigF are transferases that utilize glutathione (GSH) to cleave the β-aryl linkages while LigG is a lyase that catalyzes the regeneration of GSH from the conjugated product of LigF (Figure 2.10) (Masai et al., 2003).

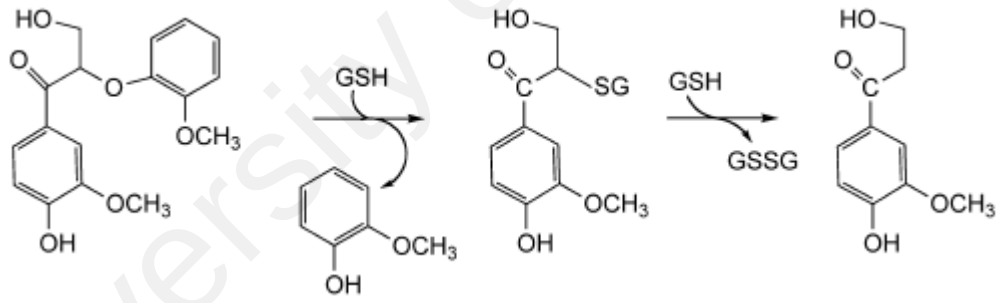

Figure 2.10: Pathway for lignin degradation by GST (Allocati et al., 2009).

2.5.2.3 Naphthalene degradation

Naphthalene is one of the persistence polycyclic aromatic hydrocarbons (PAHs) released either from a natural source or as a result of human activities (Yu et al., 2015). The natural source of naphthalene includes volcanic eruptions and incomplete combustion of fuels while industrial effluents and petroleum spills constitute the greater part of human activities that release naphthalene into the environment (Edema et al., 2013; Keck et al., 2006). They are of great concern because to their toxicity and the threat they

pose to human health and animals in general (Edema et al., 2015). They are carcinogenic and therefore are among the sixteen pollutants classified as priority pollutants by the United State Environmental protection agency (Al-Majed et al., 2012). Bacterial GST has been shown to play a key role during the bioremediation of naphthalene. Kappa class GST has been shown to play a role during the biotransformation of naphthalene by *Pseudomonas putida* G7 strain. The strain converts naphthalene into salicylate in a series of six reactions that involve GST in the fourth step (Figure 2.11) (Eaton, 1994). The GST catalyzes cis-trans isomerization reaction between C7-C8 of 2-hydroxychromene-2-carboxylic acid (HCCA). This reaction produces trans-O-hydroxybenzylidene pyruvic acid before forming the final product salicylate (Thompson et al., 2007).

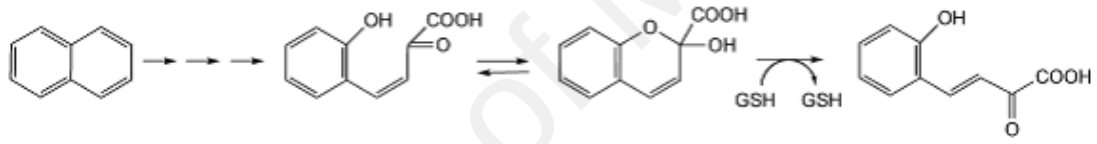

Figure 2.11: Conversion of naphthalene to salicylate by *Pseudomonas putida* G7. GST catalyzes the fourth step of the reaction (Allocati et al., 2009).

2.5.3 Bacterial GST catalyzing the reduction of arsenate to arsenite using GSH

Beta class glutathione s transferase (GSTB) in *Escherichia coli* was found to be involved in conferring arsenate resistance thereby allowing the organism to overcome the effect of the heavy metal (Chrysostomou et al., 2015). Toxic heavy metalloid arsenic predominantly exists as oxyanion either in pentavalent or trivalent oxidation states. To be able to detoxify arsenate, the heavy metal must first be reduced to arsenite by arsenate reductases present in some organisms (Messens & Silver, 2006). However, in the absence of arsenate reductase, GSTB in *Escherichia coli* was found to be able to affect the reduction process using reduced GSH thereby converting the arsenate into arsenite which can then be exported by specific arsenate transporters (Chrysostomou et al., 2015).

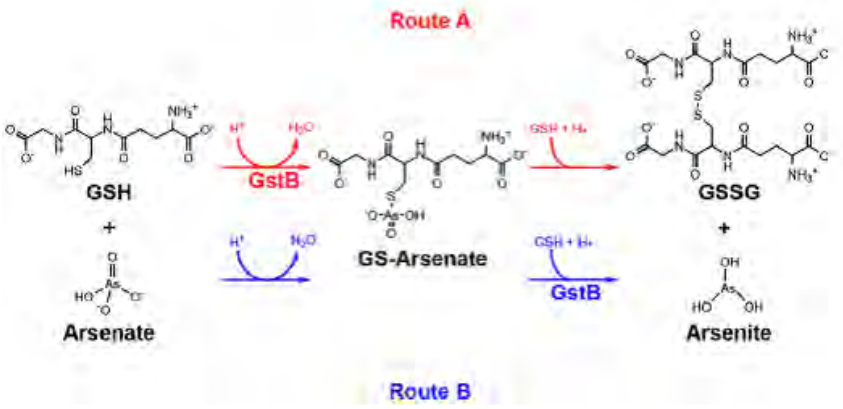

Figure 2.12: Proposed mechanism of arsenate reduction by GSTB (Chrysostomou et al., 2015).

Two pathways were proposed to explain the GSTB mediated arsenite reduction processes (Chrysostomou et al., 2015). In the first pathway, GSTB catalyzes the conjugation of GSH with arsenate and the intermediate then spontaneously reacts with second GSH molecule to form reduced arsenite and oxidized GSSG. In the second pathway, arsenate spontaneously reacts with one molecule of GSH and GSTB then catalyze the addition of second GSH molecule forming arsenite and oxidized GSH (Figure 2.12) (Chrysostomou et al., 2015).

2.6 Classification of GSTs

Unveiling the complete genome sequence of many organisms greatly enhances understanding of genome organization in several different organisms. The process also reveals the presence of GSTs in several different organisms and this necessitates the need for a homogenous classification and nomenclature of GST genes (Edwards et al., 2000). Based on the recommendation of the committee for human gene nomenclature, the existing mammalian system for classification and nomenclature was also adopted in a non-mammalian system. Using this system, three letter prefix donates the species from which the GST is derived followed by the abbreviation GST. The class of the GST is indicated next by a letter while the order of gene discovery in a given species is followed

by a number (Chelvanayagam et al., 2001). For example, hsaGSTM1 represent the first mu-class GST gene reported in man, however, some variations are still in use in which a single letter is used to represent the species in mammals and two letter prefixes in other organisms (Edwards et al., 2000).

Several different criteria were used in GST classification however, the most prominent one is based on amino acid percentage sequence identity. In this criterion, greater than 40% or less than 20% was set as a bench mark for classifying GST into either same or different class respectively. However, other properties such as immunological reactivity, kinetic features, and crystal structure similarity provide additional properties being considered (Sheehan et al., 2001). Based on the above properties, GSTs are classified into four families namely; cytosolic, microsomal, mitochondrial and bacterial fosfomycin resistance protein (Armstrong, 2000). Cytosolic GSTs were further sub-divided into many classes and they constitute the largest family of GSTs (Hayes et al., 2005; Sheehan et al., 2001). Kappa class GSTs is a typical example of mitochondrial GST characterized in eukaryotes while Microsomal GSTs (MAPEG) are membrane-bound proteins that function during metabolism of eicosanoids. The fourth family exclusively present in bacteria is bacterial fosfomycin resistance protein (Allocati et al., 2009).

2.6.1 Cytosolic GST (cGST)

Cytosolic GSTs abbreviated as cGSTs are soluble GSTs that occurred as dimers with an average amino acid length between 200-250 and molecular weight between 23-30 kDa. Each subunit in the dimer is made up of domain I and domain II known as the N-terminal and C-terminal respectively. Domain I consist of α-helices and β-strands while domain II consists of helical segments only (Allocati et al., 2009). They occur as a homodimer (between the same subunits) or heterodimer (between different subunit). Formation of heterodimer is mainly observed to occur between subunits of the same class due to the

fact that interfacial residues' incompatibility prevents monomers from different classes to dimerize (Oakley, 2005). Each subunit appeared to be catalytically independent because it possessed both the G (Glutathione) and H (Hydrophobic substrate) binding sites necessary for catalytic activity, however, catalytic active GSTs always occurred as dimers (Frova, 2006). Some monomers in plant's lambda and DHAR appeared to possess catalytic activity even though these monomers lack GSH dependent conjugating and peroxidase activities with standard substrates, still, they possessed glutathione transferase activity (Dixon et al., 2002).

Among all the GST subfamilies, cGST are by far the most abundant found in almost all species (Frova, 2006). In bacteria, Cytosolic GSTs are composed of six different classes namely: beta, chi, theta, eta, zeta and rho (Allocati et al., 2009; Pandey et al., 2015; Skopelitou et al., 2012).

2.6.1.1: Beta class GSTs

The prototype of beta class GST was first identified from *Proteus mirabilis* after carefully analyzing that the GST display certain structural and biochemical properties that distinguished it from other known GST classes (Rossjohn et al., 1998). Beta class GST was found to occur only in bacteria and currently, four crystal structures of beta class GST belonging to different organisms were already analyzed (Allocati et al., 2009). The overall crystal structures in all the four classes consist of an N-terminal domain which resembles the thioredoxin-like protein fold. The C-terminal domain was found to be all helical and is separated by a short linker. In addition, a unique structural motif discovered only in beta class GST was also identified from *Onchobactrum antrophi* GST (OaGST) (Allocati et al., 2009). This motif was found at the G-site and it consists of a network of hydrogen bondings that function to zipper the end of the C-terminal domain and the starting helix of the thioredoxin-like domain. Beta-class GSTs have characteristics

reactivity with 1-chloro-2,4- dinitrobenzene (CDNB), the existence of cysteine at the glutathione binding site and their ability to be separated using GSH matrix (Rossjohn et al., 1998). Furthermore, they were found to conjugate antibiotics therefore helps in conferring antibiotic resistance to the organisms (Perito et al., 1996). Recently, a beta class GST termed BphK was also found to be located within the operon for biphenyl/polychlorobiphenyl degradation pathway. This enzyme was shown to catalyze the dechlorination of some metabolites released during the biodegradation process thereby helps in improving the efficiency of biphenyl/polychlorobiphenyl degraders (Gilmartin et al., 2003).

2.6.1.2: Theta class GSTs

Theta class GSTs in bacteria were first identified from facultative methylotrophic bacteria *Methylobacterium* sp. Strain DM 11 (Scholtz et al., 1988). Later, the enzyme was also identified from another strain called *Methylobacterium* sp. DM 4 (La Roche & Leisinger, 1990). Theta class GST have dichloromethane dehalogenase (DCM) activity, they lack reactivity with DCNB and they do not bind to GSH affinity matrix (Bader & Leisinger, 1994). Several other DCM dehalogenases were also identified from different bacterial strains. Analysis of sequence variations among different DCM dehalogenases revealed highly conserved sequences that affect catalytic properties of the proteins (Vuilleumier, 2001). Other dichloromethane dehalogenases are increasingly being discovered from other organisms (Yu et al., 2017).

2.6.1.3: Zeta class GSTs

Zeta class GSTs was recognized in eukaryotic sequences by the presence of distinct motif SSCX(W/H) RVRIAL situated at the N-terminal part of the protein. The motif in bacteria was later recognized as RSSASYRVRIAL whereby the cysteine residue is

replaced with either Ala, Ser or Thr residues. The distinguishing characteristic of zeta class GSTs is that they possessed tetrachlorohydroquinone (TCHQ) dehalogenase and isomerase activities (Anandarajah et al., 2000; Copley, 2000; McCarthy et al., 1996). They were also found to have dichloroacetate dechlorinating activities (Tong et al., 1998; Zeen et al., 1998).

2.6.1.4 Chi class GSTs

Chi class GSTs are among the newly discovered cytosolic GSTs from bacteria. The GST was first identified from cyanobacteria called *Synecochoccus elongates* PCC 6301 and *Thermosynechococcus elongates* BP-1 (Wiktelius & Stenberg, 2007). The proteins were found to exhibit low sequence similarity to other known GST classes. Crystal structure of any of the members was not determined, however, online structural prediction using other known GST classes showed that the enzyme displayed typical structural features that were found to be present in other cytosolic GSTs. This includes; the presence of Pro53, Ile 68 identified in what is called motif I and the N-capping box containing "Ser/Thr-Xaa-Asp" residues which played a role in the folding of GSTs. Further secondary structural analysis predictions using known crystal structures of other GST classes also showed that chi class adopts the usual βαβαββα and all helical structures found in N and C-terminal domain of all GSTs respectively. However, one distinguishing feature of this class of GST is the absence of essential cysteine residue found in beta class GST, though other potential candidates such as Ser and Tyr are present around the N-terminal position that might fulfill the function. The chi class GST have distinguishing characteristic by exhibiting activity towards isothiocyanates (a plant-based compound which act as defense mechanism in response to injury or stress caused by pathogens) and they completely lack cysteine residue. The enzyme was also found to exhibit moderate activities against wide range of GST's standard substrates (Wiktelius & Stenberg, 2007).

2.6.1.5: Eta class GSTs

The GST termed Eta class was first identified from a pathogenic soil bacterium *Agrobacterium tumefaciens* C58. The protein was found to exhibit very low sequence similarity with all known cytosolic GST classes, it was designated as (Atu GSTH1-1) and called Eta class GST. The crystal structure of Eta class GST was determined in complex with S-(P-nitrobenzyl)-glutathione. The structure showed a typical overall fold of GSTs with N-terminal domain resemble the thioredoxin like protein fold and an all α-helical segment in the C-terminal domain. Comparison of the crystal structure of Atu GSTH1-1 with the crystal structures of other known cGSTs showed that it closely resembles YfcG; a Nu class GST from *E. coli*. One special feature that was observed in Atu GSTH1-1 is the absence of essential Tyrosine, Cysteine or Serine residues at the glutathione binding site of the protein. These residues were found to play an essential role in the binding and activation of GSH in various GST classes. However, site-directed mutagenesis studies showed that Phe 22, Ser 25, Arg 34 and Arg 187 contributed significantly to catalysis. The enzyme was found to show significant activity toward aryl halides as well as strong peroxidase activity toward organic hydroperoxides (Skopelitou et al., 2012).

2.6.1.6: Rho class GSTs

This class of cytosolic GST was first reported from a cyanobacterium *Synechocystis* PCC 6803. The enzyme was found to display very low sequence similarity, showing the highest similarity of 21% with representatives from zeta, theta, and alpha classes. Based on percentage sequence similarity, the enzyme was designated as rho class GST. Furthermore, while the average molecular weight of cytosolic GSTs is around 25KDa, this protein was found to have a molecular weight of about 30 kDa. Biochemical characterization showed that the enzyme has strong dehalogenase activity towards dichloro-acetate and glutathione-dependent peroxidase activity (Pandey et al., 2015).

2.6.1.7 Nu class GSTs

Nu class GST was first identified from *Escherichia coli* after observing a unique structural and catalytic properties not previously seen in other GST classes (Stourman et al., 2011; Wadington et al., 2009). Two representative members currently identified are designated as YfcG *also* known as (GST N1-1) and YghU also labeled as (GST N2-2). YfcG was found to show very low activity with standard GST substrate, 1-chloro-2,4-dinitrobenzene (CDNB). The peroxidase activity of the enzyme was only detected with cumene hydroperoxide but not with other peroxides. Structurally, YfcG was found to possessed typical GSH transferase features with N-terminal domain resembling that of thioredoxins like proteins and all α-helical domain at the C-terminal part of the protein. Crystal structure of YfcG was grown in the presence of reduced glutathione (GSH), but surprisingly an oxidized glutathione GSSG was found occupying the active site between the two subunits of the dimer. The disulfide bond was also found to be on the surface of the protein, similar to what was observed in glutaredoxins and thioredoxins. This suggests that the protein might be involved in oxidoreductase activities, however, no cysteine residue is present at the active site of the protein. This further shows that the sulfhydryl groups are not involved in the redox chemistry of the reaction. Furthermore, this suggests a unique disulfide-bond reductase activity from the members of YfcG family (Wadington et al., 2009).

The crystal structure of YghU reveals somewhat interesting and completely new phenomenon with regards to GSH binding. The enzyme exhibited an unusual behavior by binding to two molecules of GSH in each of its active sites, one tight and one weak binding. The binding behavior observed is consistent with their kinetic behavior which suggests either negative cooperativity or differences in the affinity of the two GSH molecules to their respective active sites. Overlay of the two crystal structures from YfcG

and YghU showed very close similarity and even in the superposition of the two GSH from YghU and the GSSG from YfcG. Another interesting scenario observed in the crystal structures of both YfcG and YghU is the presence of threonine and arginine residues at the opposite subunits of their crystal structures. The threonine residue interacts with the first GSH molecule in YfcG and GSSG in YghU, while the arginine residue interacts with the second molecules of GSH and GSSG in YfcG and YghU respectively. Just like YfcG, YghU enzyme failed to show transferase activities using most standard GST substrates, however, it did show modest peroxidase activities toward several organic hydroperoxides (Stourman et al., 2011).

2.6.2 Mitochondrial GSTs (Kappa Class GSTs)

Kappa class GST was first identified in rat liver mitochondria and was initially placed in theta class based on N-terminal sequence analysis (Harris et al., 1991). The enzyme has been shown to be present in peroxisomes as well as endoplasmic reticulum in adipose tissue (Raza, 2011). After full sequence analysis of its protein, the enzyme was later discovered to be completely different and was named kappa class (Pemble & Taylor, 1992). Also, molecular cloning and crystallography had provided additional evidence that the protein belongs to a different class of transferase (Ladner et al., 2004; Robinson et al., 2004). Amino acid comparison using sequence homology showed that kappa GST is completely different from all other GST classes (Ladner et al., 2004; Robinson et al., 2004).

Kappa GSTs showed some catalytic properties of other GSTs such as reactivity with the model substrate CDNB (Morel et al., 2004). The presence of kappa GST in mitochondria and peroxisomes suggest its role in detoxification of peroxides produced during lipid metabolism as both the two organelles are involved in β-oxidation of fatty acids des (Frova, 2006).

2.6.3 Microsomal GSTs (MAPEG Enzymes)

Microsomal GSTs constitute the third class of transferases, in other words, they are called membrane associated proteins involved in eicosanoid and glutathione metabolism (MAPEG). Sequence homology studies with other GSTs showed that they have less than 10% similarity with other GST classes and their subunits contained an average of 150 amino acids (Frova, 2006). The protein superfamily of MAPEG is sub-grouped into four (I-IV) with less than 20% protein identity between subgroups (Hayes et al., 2005). Subgroup I is made up of MGST2, FLAP and LTC_4S, subgroup II contain MGST3 and other members from plants and fungi, members of subgroup III are normally found in *Escherichia coli* and *Vibrio cholera* and they are called microsomal GST-like proteins while the last subgroup contain MGST1 and PGES1 (Hayes et al., 2005). They are ubiquitously distributed in organisms and are mostly involved in the synthesis of eicosanoids, leukotrienes, and prostaglandins. They are also involved in GSH-dependent catalyzed transferase or isomerase reaction (Frova, 2006). Others such as MGST1 have no biosynthetic activities but they are involved in GSH dependent catalyzed conjugation of halogenated arenes, various halogenated hydrocarbons, and CDNB (Andersson et al., 1994). MGST1 also catalyzes the reduction of organic hydroperoxides and those produced as a result of fatty acid and phospholipid metabolisms (Mosialou et al., 1995). In view of the above fact, MGST1 seems to function solely as detoxication enzyme (Mosialou et al., 1995).

MGST2 and MGST3 in contrast to MGST1 were found to have a synthetic function in addition to the detoxication function. Both enzymes were found to play a role in the synthesis of LTC4 by conjugating LTA4 to GSH and they also have peroxidase activity against hydroperoxides produced during fatty acid and lipid metabolism (Jakobsson et al., 1997). FLAP is a non-catalytic protein in the sense that it is only involved in the

activation of catalytic enzyme 5-lipoxygenase by binding to arachidonic acid, 5-lipoxygenase is responsible for the formation of all leukotrienes from arachidonic acid (Mandal et al., 2004). The major function of LTC_4S is to catalyze the synthesis of LTC_4 from LTA_4 and reduced glutathione hence it has glutathione transferase activity, however, both FLAP and LTC_4S lacks peroxidase activity (Jakobsson et al., 1997). PGES1 is an isomerase which catalyzes the GSH dependent isomerization of PGD2 to PGE2 and unlike FLAP and LTC4S, the enzyme has peroxidase activity (Jakobsson et al., 1999).

2.6.4 Bacterial fosfomycin resistance protein

Fosfomycin is an antibiotic produced naturally by *Streptomyces* strain and is effective against wide range of both gram-positive and gram-negative bacteria as well as pathogens that affect animals and human health (Falagas et al., 2008). Fosfomycin specifically inhibits UDP-N-acetylglucosamine-3-enolpyruvyltransferase (MurA), an enzyme that catalyzes the transfer of phosphoenolpyruvate to UDP-N-acetylglucosamine (Thompson et al., 2015). With this inhibition, the biosynthesis of peptidoglycan in the cell wall of bacteria is inhibited and therefore the growth of the bacteria halted (Thompson et al., 2015). The clinical efficiency of fosfomycin is compromised by both the genomic and plasmid-encoded resistance proteins known as fosfomycin resistance proteins (Nilsson et al., 2003). There are different types of fosfomycin resistant proteins known as Fos A, Fos B, and Fos X. They all confer resistance to fosfomycin by enzymatic modification of the oxirane ring of fosfomycin thereby inactivating the antibiotic (Figure 2.13), Fox A add GSH while Fos B and Fos X add either L-cysteine or hydroxyl group (Allocati et al., 2009).

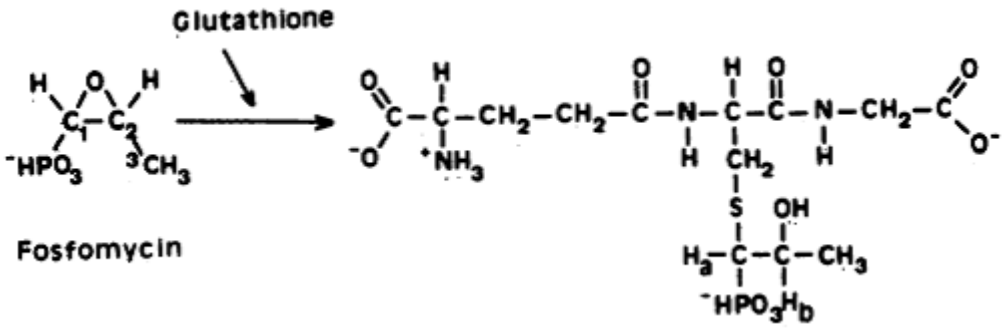

Figure 2.13: The proposed reaction of modification of fosfomycin based on NMR data **(**Arca et al., 1988).

2.6.4.1 Fos A

Fos A is a plasmid-borne gene initially isolated from clinical samples in *Serratia marcescens* and later shown to be present in both the clinical and environmental samples (Arca et al., 1990; Garcia-Lobo & Ortiz, 1982). It is a metalloenzyme that requires K^+ and also contains mononuclear Mn^{2+} center which bind with the antibiotic. Fos A is considered as glutathione S-transferase because of its specificity for glutathione as a substrate and its detoxifying function (Mannervik et al., 1988). Unlike other GSTs, Fos A has no reactivity with the model substrate CDNB and does not bind to the GSH-agarose matrix (Arca et al., 1990). The protein had been well characterized biochemically and spectroscopically from opportunistic *Pseudomonas aeruginosa* (Rife et al., 2002). The protein fold of Fos A resembles that of vicinal oxygen chelate superfamily (VOC) (Rife et al., 2002). It contained the metal binding site located in the cavity of the paired βαββββ motif while the K^+ is located at a distance of about $6.5A^0$ from the Mn^{2+} binding site (Allocati et al., 2009). The mechanism of inactivation is by modification of the oxirane ring (Figure 2.14).

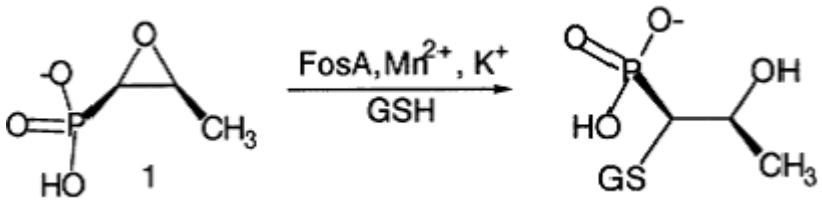

Figure 2.14: Enzymatic modification of oxirane ring by FosA (Rife et al., 2002).

2.6.4.2 Fos B

Fos B is encoded by either genome or by plasmid as seen in *Staphylococcus* strain (Etienne et al., 1991) and Bacillus substilis (Cao et al., 2001) respectively. It is a metalloprotein that uses Mg^{2+} instead of Mn^{2+} as a metal cofactor. It is less efficient than Fos A when GSH is used as a substrate however, they are equally active when L-cysteine is used as thiol donor (Cao et al., 2001). This is probably because most gram-positive bacteria including *Bacillus substilis* lacks a detectable level of GSH (Allocati et al., 2009).

2.6.4.3 Fos X

Fox X is genomically encoded and just like Fox A, it also requires Mn^{2+} for its activity. The enzyme is a hydrolase which catalyzes the hydrolysis of epoxide ring in fosfomycin thereby inactivating the antibiotic (Figure 2.15) (Allocati et al., 2009). Fos X structure determined from *Mesorhizobium loti* and *Lysteria monocytogenes* is closely related to Fos A from Pseudomonas aeruginosa (Rife et al., 2002). However, Fox X lacks βαβββ motif for binding K^+ and therefore the binding of fosfomycin to Fos X enzymes appeared in a completely different orientation to that of Fos A (Fillgrove et al., 2003; Fillgrove et al., 2007).

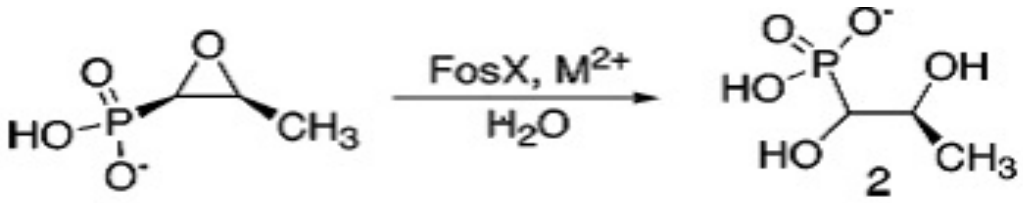

Figure 2.15: Hydration of fosfomycin by FosX (Fillgrove et al., 2003).

According to (Allocati et al., 2009), another fosfomycin resistance protein with a completely different mechanism of inactivation called fosfomycin C was also discovered from *Pseudomonas syringae* strain. The enzyme uses ATP in the presence of Mg^{2+} to phosphorylate the antibiotic thereby inactivating it. Sequence alignment between Fos C and other fosfomycin resistance proteins showed no any relationship.

2.7 Polychlorinated biphenyls

Polychlorinated biphenyls abbreviated as (PCBs) (Figure 2.16) are synthetic organic chemicals that contain several chlorine atoms attached to the biphenyl carbon skeleton (Chemicals, 1999; Loganathan et al., 2016). PCBs contain several different isomers known as congeners and it has been estimated that about 20-60 different congeners are present in commercial formulations (Ohtsubo et al., 2004). Several million tons of PCBs were estimated to have been produced worldwide with significant amount found itself deposited into the environment causing a great threat to human health and animals (Faroon et al., 2003; Sericano et al., 1995; Kawano et al., 2014). PCBs produced in the U.S are marketed under the trade name Aroclor, they have very excellent properties including thermal stability, chemical inertness, and high electrical resistivity and therefore are being used extensively in many industrial applications. (Borja et al., 2005). They are also used industrially for several applications such as; in hydraulic fluids equipment, dielectrics in capacitors, heat exchange liquids and much more. PCBs are also used to a lesser extent as pesticides, carbon-less copy paper inks, plasticizers, waxes, and

dyes (Feng et al., 1998). Several other countries such as Japan, Italy, and Germany also produced the same product with different trade names called Kaneclor, Fenclor and Pyralen respectively. They have very high degree of hydrophobicity and versatility in composition as well as chemical stability and these make it difficult for PCBs to undergo natural degradation as such, they remain deposited for decades in the environment (Borja et al., 2005). Also, their volatility and long range of transport ensured their distribution into almost all sorts of environment irrespective of whether it has ever been produced or used in that environment (Cabrerizo et al., 2012).

Even though their production has been banned for decades, however, a large proportion of PCBs are still in use as dielectrics in transformers and capacitors (Wu et al., 2012). The rest are in storage waiting to be disposed of or have already been released into the environment (Wu et al., 2012).

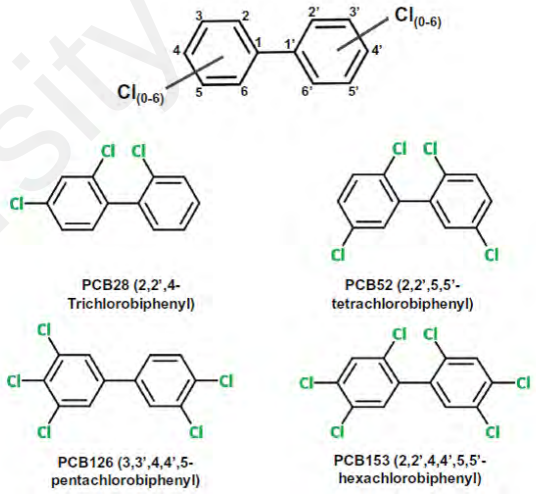

Figure 2.16. Structure of polychlorinated biphenyl (PCB). The chlorine atom is substituted for hydrogen atoms in any of the numbered positions (Ludewig & Robertson, 2013).

The number of chlorine atoms attached to the biphenyl carbon skeleton determines the toxicity of a given PCBs. Generally, the higher the number of chlorine atom attached to the biphenyl carbon skeleton the more toxic is the PCB congener. Highly toxic PCBs

mostly carries between five to ten chlorine atoms. Most of the chorine substituent are found at the *para* and *meta* positions and are considered to be less toxic, however, those substituted at *ortho* positions are considered to be more toxic (Albro & McKinney, 1981; Sylvestre et al., 1985).

The hydrophobicity of PCBs makes them difficult to be degraded by either the natural soil or aquatic biota to any significant rate. Several studies have shown that the compound can be degraded aerobically or anaerobically to yield less toxic or mineralized by-product (Cookson Jr, 1995). Aerobic organisms degrade PCBs through oxidative degradation while anaerobic organisms degrade the compounds through reductive dehalogenation (Cookson Jr, 1995).

2.7.1 Health implications of polychlorobiphenyls

Toxicity of polychlorobiphenyls to humans and other animals occurs as a result of either excessive bioaccumulation by plant and subsequent consumption of such plants by animals or as a result of direct exposure (Johnson et al., 1999; Falandysz, 2001; Kannan et al., 1994). Direct exposure of polychlorobiphenyls may lead to their adsorption through lungs, skin and gastrointestinal tract where they accumulate in adipose tissues (Johnson et al., 1999). PCBs have been implicated in a lot of diseases in both humans and animals. Studies have shown that PCBs are responsible for mass mortalities in sea birds as well as gross reduced reproductive capacity in the birds as a result of their anti-estrogen like properties which prevent calcium deposition during egg shell development (Borja et al., 2005). The anti-estrogen like properties was found to be responsible for reduced male reproductive capabilities in both birds and animals (Borja et al., 2005).

PCBs were considered before as probable carcinogens in humans, however, some studies recently classified one of the congeners as a carcinogen, this prompt complete re-

evaluation of PCBs (Humans, 2012; Lauby-Secterian et al., 2016). Many epidemiological studies performed on animals also implicated PCBs in the development of liver cancer and malignant melanoma (Cogliano, 1998). A meta-analysis performed on Yucheng and Yusho populations in Taiwan and Japan respectively exposed to polychlorinated biphenyls and dibenzofurans over 40 years ago showed a significant elevation in many types of cancers, heart diseases and hepatic disease mortalities exposed in men (Li et al., 2015). Furthermore, elevated mortality as a result of liver cancer in women was also identified (Li et al., 2015). Other studies as well implicated higher chlorinated congeners to be efficacious promoters of cancer while the lower chlorinated congeners as potential initiators (Robertson & Hansen, 2015). Exposure to high concentration of PCBs was also found to cause acute toxicity and other health implications ranging from impaired immune function, weight loss, hepatitis, depression, dizziness, behavioral alteration and thyroid gland injuries (Cogliano, 1998).

2.7.2 Aerobic biodegradation and biotransformation of polychlorobiphenyls

There are several efforts as to the selection of proper way for the destruction of PCBs. One of the best option being used is incineration however, it has the disadvantage of producing another set of pollutants such as dibenzofurans and dibenzodioxins as a result of incomplete combustion and it is also very expensive (Borja et al., 2005). Another alternative is the use of microorganisms, a technique popularly referred to as bioremediation. Several microorganisms have displayed capability for PCBs biodegradation by using enzymes to catalytically transform the organic pollutant to simpler products with lesser negative effects (Liu et al., 2016; Lopez-Echartea et al., 2016). This is done in two ways i.e. mineralization and co-metabolism. Mineralization of PCBs by microbial community results in complete degradation of pollutant to its constituent element by transforming the pollutants to its energy source (Dobbins, 1995),

however, even in such cases metabolism of PCB isomers containing several chlorine atoms is accomplished by the co-metabolic process (Komancová et al., 2003). PCBs transformation by co-metabolism requires the organism to use other sources of energy as it cannot make use of the pollutant to derive energy, this result in incomplete degradation and accumulation of metabolites that could be toxic to the organism itself (McEldowney et al., 1993).

The *bph* operon is responsible for the degradation of biphenyl/PCB in *Acidovorax* sp. KKS102 and other biphenyl/PCB degrading organisms. The organization of *bph* operons in *Acidovorax* sp. KKS102 and other biphenyl degrading strains are presented in (Figure 2.17). In *Acidovorax* sp. KKS102, the *bph* operon is made up of 13 cistrons; bphEGF (orf4) A1A2A3BCD (orf1) A4R (Figure 2.19) (Fukuda et al., 1994; Kikuchi et al., 1994; Kimbara et al., 1988). From comparison with operons of other bacteria, the *bph* operon seems to be evolved by fusion of three segments, bphABC, bphD, bphEFG (Furukawa, 2000). The PCBs degradation is accomplished through co-metabolism by bipheyl degrading enzymes (Furukawa & Fujihara, 2008). The proposed pathway for biphenyl degradation by *Acidovorax* sp. KKS102 is presented in (Figure 2.18). The enzymes are classified into the upper and lower pathway enzymes. The upper pathway enzymes are responsible for the conversion of biphenyl/PCBs to form 2-hydroxypenta-2,4-dienoate and benzoate. They are made up of biphenyl dioxygenase (BphA) which consist of four subunits (BphA1, BphA2, BphA3 and BphA4), dihydrodiol dehydrogenase (BphB), 2,3-dihydroxybiphenyl dioxygenase (BphC) and 2-hydroxy-6-oxo-6-phenylhexa-2,4-dieonate HOPDA hydrolase (BphD). The lower pathway enzymes are made up of BphE, BphF and BphG. They catalyze the conversion of the final product of upper pathway enzymes to form acetyl CoA and pyruvate (Kikuchi et al., 1994).

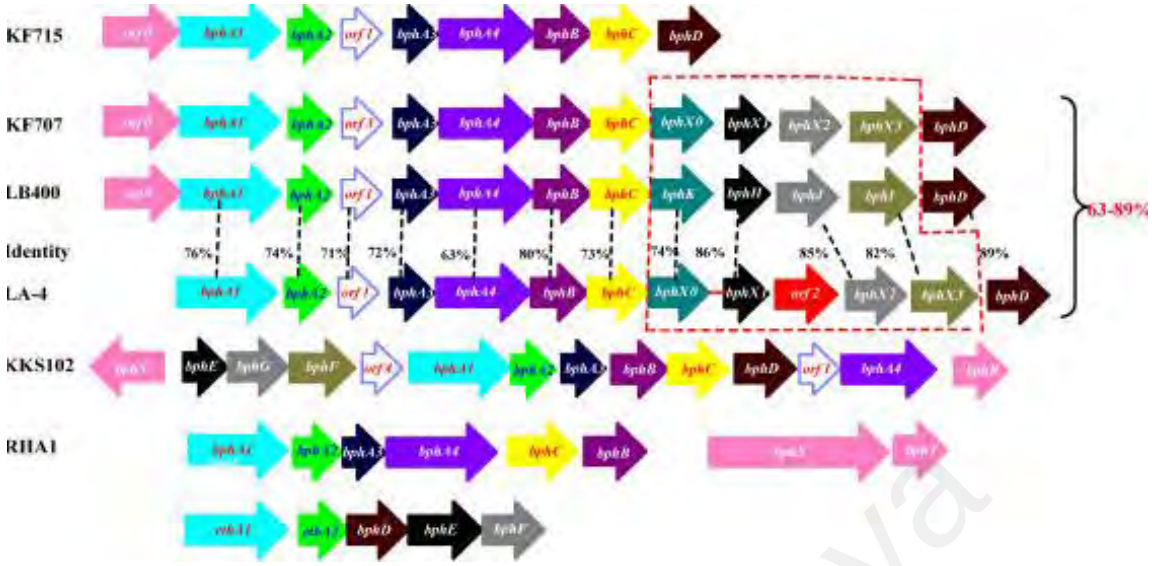

Figure 2.17. Organization of bph gene clusters from various strains. LA-4, *Dyella ginsengisoli* LA-4 *bph* gene cluster; LB400, *B. xenovorans* LB400 bph gene cluster; KF707, *P. pseudoalcaligenes* KF707 *bph* gene cluster; KF715, *P. putida* KF715 *bph* gene cluster; KKS102, *Acidovorax* sp. KKS102 *bph* gene cluster; RHA1, *Rhodococcus jostii* RHA1 *bph* gene cluster. Homologous genes with the same function are depicted in the same color (Li et al., 2012).

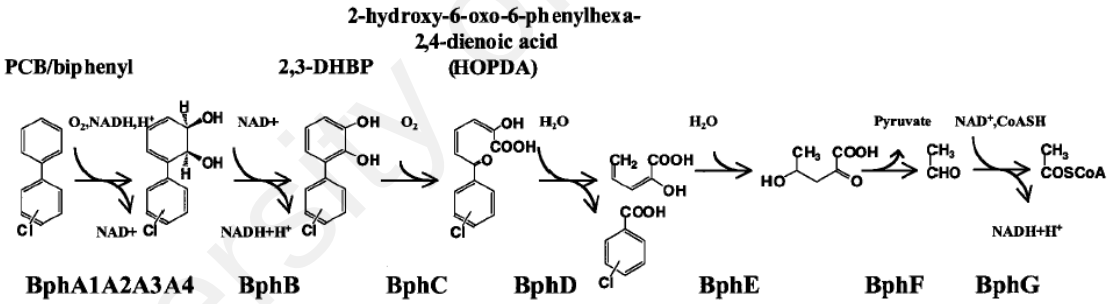

Figure 2.18: Proposed pathway for the conversion of biphenyl/PCB to acetyl CoA and pyruvate in *Acidovorax* sp. KKS102 (Delawary et al., 2003).

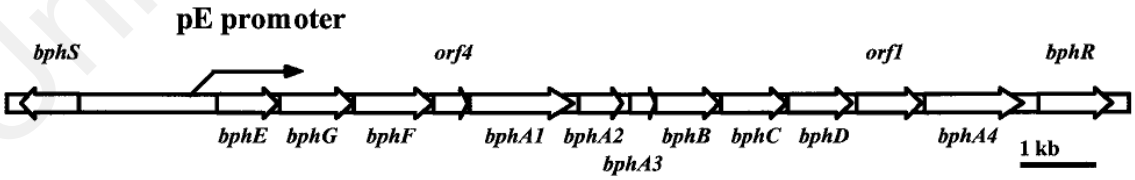

Figure 2.19: Organization of bph operon in *Acidovorax* sp. KKS102, previously *Pseudomonas* sp. KKS102 (Delawary et al., 2003).

2.7.2.1 Upper pathway enzymes

2.7.2.1.1 Biphenyl 2,3-dioxygenases (BphA1A2A3A4)

Biphenyl 2,3-dioxygenase is a non-heme iron and multicomponent oxygenase that initiates the degradation of biphenyls/PCBs (Gibson & Parales, 2000; McKay et al., 2003). They are made up of two components; iron-sulfur protein and different electron transport proteins. Their main function is to introduce one or atoms of diatomic oxygen into biphenyl/PCBs (Wackett, 2002). They catalyze the formation of cis-2,3-dihydro-2,3-dihydroxybiphenyl/PCB from their main substrates (Biphenyls/PCBs). BphA1A2 are the terminal oxygenases that accept electrons from NADH catalyzed by ferredoxin (BphA3) reductases (BphA3A4) (Seeger & Pieper, 2010). The enzyme also determines the region of the substrate to be attacked and this places them as the most important enzyme that determines and select the type of congener to be degraded by a given strain (Seeger & Pieper, 2010).

2.6.2.1.2 Cis-2,3-dihydro-2,3-dihydroxybiphenyl dehydrogenases (BphB)

The second reaction in the biodegradation of biphenyls/PCBs is dehydrogenation reaction catalyzed by a cis-2,3-dihydro-2,3-dihydroxybiphenyl dehydrogenase. This second reaction produces 2,3-dihydroxy biphenyl/PCB. The enzyme can be able to transform a wide range of dihydrodiol compounds because of its broad substrate specificity (Seeger & Pieper, 2010).

2.7.2.1.3: 2,3-Dihydroxybiphenyl 1,2-dioxygenases (BphC)

2,3-dihydroxybiphenyl dioxygenase belongs to sub-family 3A of type I extradiol dioxygenases. It catalyzes the transformation of 2,3-dihydroxybiphenyls to 2-hydroxy-6-oxo-6-phenylhexa-2,4-dieonate (McKay et al., 2003). However, the enzyme is susceptible to inactivation by a specific chlorosubstituted 2,3-dihydroxybiphenyls. The

enzyme contains ferrous ion at its active site and oxidation of the ferrous to ferric ion results in the loss of activity by the enzyme (Vaillancourt et al., 2002).

2.7.2.1.4: 2-Hydroxy-6-phenyl-6-oxohexa-2,4-dienoate (HOPDA) hydrolases (BphD)

The fourth step in the of biphenyl degradation involves hydrolytic degradation of HOPDA to produce 2-hydroxypenta-2,4-dienoate and benzoate (Seeger & Pieper, 2010). It was observed that chlorosubstituted HOPDAs on phenyl moiety are efficiently transformed while chlorosubstituted HOPDAs on dienoate were found to competitively inhibit BphD (Bhowmik et al., 2007).

2.7.2.2 Lower pathway enzymes

BphE, BphF and BphG are hydratase, aldolase and dehydrogenase respectively which constitutes the lower pathway enzymes in *Acidovorax* sp. KKS102. Collectively, these enzymes convert 2-hydroxypenta-2,4-dienoate into final products; pyruvate and acetyl CoA. These products can enter the Krebs cycle and help the strain grow by providing some of the necessary carbon. The process is feasible only when the PCB is chlorinated in one of the biphenyl rings which gives room for the formation of pyruvate and acetyl CoA in the non-chlorinated ring. The chlorinated ring produces chlorobenzoate with either one, two or even tree chlorine atoms as dead-end products (Pieper & Seeger, 2008).

2.7.3 Toxicity of PCBs and their metabolites

One of the major challenges in the bioremediation of PCBs is the toxicity of the PCBs themselves and some of their metabolites (Blasco et al., 1995). In most cases, bacterial degradation of a specific congener of PCB is incomplete and therefore toxic intermediates are accumulated in the process (Figure 2.20) (Seeger & Pieper, 2010). PCBs themselves

are lipophilic as such they tend to accumulate in the bacterial membranes and decreases cell viability. Also, some of the metabolic intermediates such as dihydrodiols and dihydroxybiphenyls are even more toxic than the PCBs themselves (Cámara et al., 2004). Dihydroxybiphenyls, in particular, inhibits bacterial cell separation by affecting the DNA content of the bacteria (Hiraoka et al., 2002).

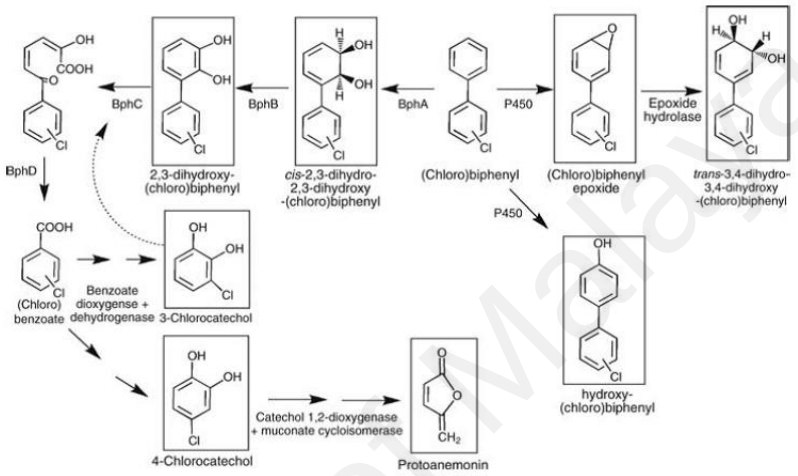

Figure 2.20. Biodegradation of PCBs, accumulation of toxic metabolites (boxed) (Seeger & Pieper, 2010).

Transformation of Chlorobenzoate also results in the formation of downstream toxic product protoanemonin. Other products such as 3-chlorocatechol are inhibitors of 2,3-dihydroxybiphenyl-1,2-dioxygenase and this is detrimental to the upper pathway enzymes (Vaillancourt et al., 2002). Moreover, protoanemonin is an antibacterial compound that kills PCB degraders and is formed from 4-chlorocatechol channeled into 3-oxoadipate pathway (Blasco et al., 1995). Formation of protoanemonin was thought to be responsible for poor performance and survival of PCB degraders in soil microcosm studies (Blasco et al., 1997).

2.7.4 Research needs

In one of the PCB degrading organism, *Burkholderia xenovorans* LB 400 considered to be a model organism in PCB degrading bacteria, the function of one enzyme coded by

a gene termed BphK organism was initially obscure. This gene is located within the *bph* operon for biphenyl/PCB degradation in some organisms. It was later discovered that the enzyme has dechlorinating function against some of the toxic metabolites generated during the PCB biodegradation (Bartels et al., 1999; Gilmartin et al., 2003). The enzyme was found to catalyze the dehalogenation of the dead-end product, chlorobenzoate, suggesting that the enzyme was recruited by some species in order to facilitate the degradation of PCBs (Figure 2.21) (Gilmartin et al., 2003). The enzyme was also found to catalyze the dehalogenation of HOPDAs at a much significant rate than Chlorobenzoates (Fortin et al., 2006). However, it was discovered that the enzyme has very limited substrate specificity as it can react only with CDNB (Brennan et al., 2009). Furthermore, the dechlorinating activity against these substrates was found to be very low and therefore, it has been suggested that one possible way of improvement is to screen various BphK homologs from other PCB utilizing bacteria for potential dehalogenase activity. It is possible that a better enzyme with better dehalogenase function and wider substrate specificity could be discovered that can be used against these toxic metabolites (Cao et al., 2013; Agullo et al., 2017).

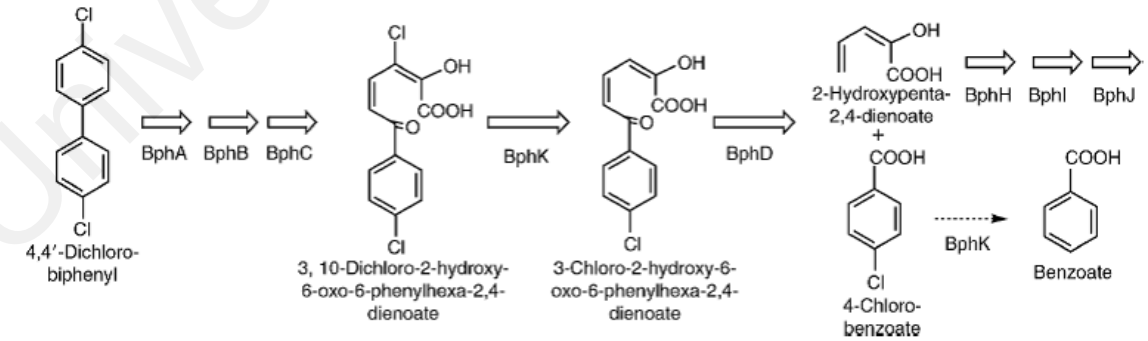

Figure 2.21: Formation of 4-chlorobenzoate and its conversion to benzoic acid by BphK (Seeger & Pieper, 2010).

There were various attempts for enzyme optimization in order to facilitate the PCB biodegradation by microorganisms. However, most of the researches dwelled much on

BphA i.e. bihenyl-1,2-dioxygenases as it is the key enzyme that determines the type of PCB congener to be degraded by a given PCB degrader (Seeger & Pieper, 2010; Suenaga et al., 2002; Vézina et al., 2007; Zielinski et al., 2006). Recently, some efforts were also put toward identifying enzymes that can deal with the bottlenecks generated during PCB biodegradation. In this vein, a HOPDA hydrolase was identified from *S. wittichii* RW1 with novel activity toward 3-chlorinated HOPDAs (inhibitor of BphD (Seah et al., 2007). Also, a mutant BphK (A180P) was identified from *Burkholderia xenovorans* LB 400 which has improved activity toward dechlorination of several organochlorine compounds (McGuinness et al., 2007). However, there was no effort toward identifying a homolog of BphK that could have wider substrate specificity and much higher catalytic activity than the already identified BphK. This type of homolog if identified, will be valuable in genetic engineering of strain with better degradation capability or be used against the metabolites of PCB biodegradation.

CHAPTER THREE: METHODOLOGY

3.0 Materials

3.1 Organism (*Acidovorax* sp. KKS102)

The organism was obtained in freeze-dried form from the Japan Collection of Microorganisms (JCM No. 17234) and revived using Luria-Bertani broth according to the JCM's instructions. Putative GST protein sequences were retrieved from the NCBI database and they were designated as KKSG1-KKSG11 based on their location (from 5'-3') in the chromosome of the organism. This is in order to create a way of identifying the individual GSTs from *Acidovorax* sp. KKS102 for further studies.

3.2 Chemicals

The chemicals used in this research are of high purity grade obtained from various companies. They include: 30% Acrylamide/Bis-acrylamide (29:1), Ammonium persulphate, Tetramethylethylenediamine (TEMED) (Bio-Rad, USA). Ammonium iron(III) sulfate dodecahydrate, Tetraoxosulfate (VI) acid, Trioxonitrate (V) acid (Merck KGaA, Germany). Cell lysis buffer, Coomassie Brilliant Blue G-250, DL-Dithiothreitol (DTT), Ethylenediaminetetraacetic acid (EDTA), Mercuric thiocyanite, N-phenylthiourea, Sodium deodecyl sulphate, (Sigma Aldrich, USA). Isopropyl β-D-thiogalactoside (IPTG) (Gold Bio.Com, USA). Sodium Chloride, Sodium dihydrogen phosphate, Sodium hydroxide (Systerm).

3.3 Kits

Prepease gel extraction kit (USB Corp, Germany). Prepease genomic DNA extraction kit (USB Corp, Germany). Prepease plasmid extraction kit (USB Corp, Germany). Quickchange Lightning Site-Directed mutagenesis kit (Agilent technologies,

USA). Rosetta-gami 2(DE3) competent cells (Novagen, Germany). TOPO Cloning and expression kit (Invitrogen, USA).

3.4 Molecular Biology Consumables

1Kb DNA ladder (Lucigen, USA). 6× Loading dye, Nuclease free water (Fermentas, USA). Agarose LE Analytical grade (Promega, USA). Ampicillin (Nacalai Tesque, Japan). Chloramphenicol, Tetracycline (Duchefa Biochem, Netherlands). Kanamycin sulphate (Calbiochem, Canada). Luria Bertani Agar, Luria Bertani Broth (Friendemann Schmidt, Germany). Lysozyme, Protease inhibitor, Bovine Serum Albumin (Sigma Aldrich, USA). Phusion flash high fidelity polymerase, Taq DNA polymerase (Thermo Fisher Scientific, USA). Red safe nucleic acid staining solution (Intron Biotechnology). Benchmark protein ladder, SOC medium (Invitrogen, USA).

3.5 Substrates for enzyme assay

1,2- dichloro-4-nitrobenzene (DCNB), 1-Chloro-2,4-dinitrobenzene (CDNB), Dichloroacetate, Dichlorodiphenyltrichloroethane DDT, Endosulfan, Dieldrin, Hexa-2,4-dienal, Hydrogen peroxide, Permethrin, *p*-Nitrobenzyl Chloride, Trans trans-Hepta-2,4-dienal, Trans-2-hexenal, Trans-2-octenal, Trans-4-phenyl-3-butene-2-one (PBO), Glutathione reductase, Nicotinamide Adenine Dinucleotide Phosphate (NADPH), Reduced glutathione (GSH) (Sigma Aldrich, USA). 2-chlorobenzoate, 3-chlorobenzoate, 4-chlorobenzoate, 2,4-dichlorobenzoate, 2,5-dichlorobenzoate, 2,6-di chlorobenzoate (Merck KGaA, Germany).

3.6 Buffers

0.5M Tris-HCl buffer pH 6.8, 1.5M Tris-HCl buffer pH 8.8, 25mM Tris buffer pH 7.4, TAE Buffer (0.09M Tris-Borate), TBE Buffer (0.09M Tris-Borate, Tris/glycine

SDS running buffer (25Mm tris, 192Mm glycine and 0.1% (W/V) SDS, pH 8.3 (Biorad, USA). 2Mm EDTA (Sigma Aldrich, USA).

3.7 Instrumentation

Air clean PCR station (ISC Bioexpress). AKTA purifier FPLC (GE Healthcare, Sweden). Alpha imager mini gel documentation system (Alpha Innotech). Cary 60 UV-Visible spectrophotometer (Agilent technologies, USA). Centrifugal concentrator Vivaspin 20 (Sartorius Stedim). Centrifuge (Eppendorf Germany). GSTrap^{TM} HP (GE Healthcare). JASCO V60 Spectrophotometer (Jasco, Japan). Laminar hood (SASTEC). Microprossecor pH meter (Hann instruments, USA). Microwave (Pensonic, Japan). Mini-PROTEAN Electrophoresis with Biorad power supply (Biorad, USA). Mixing block (Biocher). Mycycler thermal cycler (Biorad, USA). Nanodrop spectrophotometer (Thermo-Scientific, USA). Orbital shaker (Protech). Sonicator (Roop Ultrasonic Powersonic 603). Temperature controlled shaking incubator (Wisebath). Vortex Mixer (Labnet international Inc, USA)

3.8 Methods

3.8.1 Bioinformatic analysis

Sequence alignment study was carried out using ClustalW2 (Larkin et al., 2007). Phylogenetic analysis was carried out using molecular evolutionary genetic analysis (MEGA) software version 6.0 (Tamura et al., 2013). Neighbor-joining method was used to trace the evolutionary history of the GSTs (Saitou & Nei, 1987). The Reltime method was used to calculate the divergence time for all the branch points (Tamura et al., 2012). Bootstrap values were set at 1000 replications by the method of Felsenstein (1985). Predicted molecular weight and isoelectric point were determined using ProtParam tool (http://us.expasy.org/tools/ protparam.html).

3.8.2 DNA extraction from *Acidovorax* sp. KKS102

DNA extraction was carried out using prep-ease genetic DNA isolation kit. About 1.5ml of a culture of stationary phase of *Acidovorax* sp. KKS102 grown in LB-medium was transferred to pre-weighed and sterilized microcentrifuge tube and centrifuged at 13,000g for 1 minute. The procedure was repeated until about 30 mg of the pellet was obtained. 0.24 ml of homogenization buffer was then added and the mixture was homogenized using micro homogenizer until the sample was completely homogenized. This was then transferred to a clean 1.5 ml microcentrifuge tube. 0.2 ml of chloroform/isoamyl alcohol (24:1 v/v) and 0.8 ml of protein precipitation buffer were then added to the lysate. The mixture was vortexed 10 pulses at full speed for 3 minutes. This was then centrifuged at 13,000 × g for 4 minutes. 0.88 ml of the upper aqueous phase was then transferred to a clean 1.5 ml microcentrifuge tube containing 0.62 ml of isopropanol. The solution was mixed by inverting the tube 15 times and then centrifuged at 13,000g for 4 minutes. The supernatant was carefully aspirated and the pellet was washed once with 1 ml of 70% ethanol by vortexing. This was then centrifuged at 13,000g for 2 minutes. The supernatant was carefully aspirated and the pellet was dried at for 5 minutes at 37ºC. The extracted DNA was then re-suspended in 150 µl of DNA resuspension buffer and vortexed to dissolve the DNA. The concentration of the extracted DNA was measured using nanodrop spectrophotometer and kept at -20ºC for downstream application.

3.8.3 Agarose gel electrophoresis of extracted DNA

Agarose gel electrophoresis of extracted DNA was carried out in order to examine the integrity of the extracted DNA. 1 g of molecular biology grade agarose was dissolved in 100 ml of 1 × TAE buffer in order to prepare 1 % (w/v) TAE agarose. The solution was micro waved until the agarose was completely dissolved. This was allowed to cool to

about 50°C and 5 µl of red safe staining solution was added. The gel was then poured into the gel tank containing 1.5 mm of gel comb and allowed to cool and hardened. 1 × TAE buffer was then poured into the tank until the gel was completely covered. 5 µl of the extracted DNA was then mixed with 2 µl of DNA loading dye and pipetted into the well. 5 µl of gel ready DNA marker was also pipetted into the adjacent well. The electrophoresis was performed at 80V for 1 hour 30 minutes. The DNA was visualized using AlphaImager mini.

3.8.4 PCR amplification of KKSG6 and KKSG9

The KKSG6 gene was successfully amplified using Thermo Fisher Scientific phusion flash high-fidelity master mix using primers; (Forward: 5' CACCATGAAGCTCTACTACGCCCCCGGT3' and Reverse: 5'TCACGACAGCAACCCCTCAGCCCGCA3'). PCR reaction was set using 3 step PCR-set up. 1) one cycle of initial denaturation at 98°C for 10 seconds, 2) thirty cycles of denaturation at 98°C for 1 second, 68.5°C annealing for 5 seconds and 72°C extension at 15s/1kb, 3) One cycle of final extension at 72°C for 10 minutes. The amplified products were purified and cloned into pET101 D-TOPO vector. The successful clone was isolated and sequenced for further confirmation.

The KKSG9 gene was successfully amplified using Thermoscientific phusion flash high-fidelity master mix. The pair of primers used were; Forward: 5' CACCATGCTCGCCCTCTACGGCCA3' and Reverse: 5'TCAGTCGCGGTCGGGTGCTCCT3'. The 20 µl reaction mixture consist of 6 µl nuclease free water, 1 µl each of 10 µM forward and reverse primers, 2 µl of 47 ng/µl DNA and 10 µl phusion flash high-fidelity master mix. The PCR reaction was set using 3 step PCR-set up. 1) one cycle of initial denaturation at 98°C for 10 seconds, 2) thirty

cycles of denaturation at 98ºC for 1 second, 67.1ºC annealing for 5 seconds and 72ºC extension at 15s/1kb, 3) one cycle of final extension at 72ºC for 10 minutes.

3.8.5 Agarose gel electrophoresis and purification of amplified KKSG6 and KKSG9

The amplified products of KKSG6 and KKSG9 were run in agarose gel electrophoresis as described for the electrophoresis of DNA in section (3.2.3) and visualized under U.V. illumination using AlphaImager mini. The gel was purified using PrepEase gel purification kit as follows. About 100 mg of the fragment was excised from the gel using a clean, nuclease free scalpel and excess agarose was cut off to minimize the gel volume. It was weighed and transferred into a clean microcentrifuge tube. 200 µl of NT buffer was then added in order to solubilize the gel and the mixture was incubated at 50ºC until the gel was completely dissolved. To bind the DNA to the column, PrepEase clean-up column was then placed into a 2 ml collecting tube and the sample was directly added to the center of the clean-up column. This was centrifuged at 11,000g for 1 minute and the flow-through discarded. 600 µl of NT3 buffer was then added directly to the clean-up column and then centrifuged at 11,000g for 1 min in order to wash the column. In order to dry the column and remove excess NT3 buffer, the column was further centrifuged at 11,000 × g for 2 minutes. This was then incubated at 70ºC for 3 minutes in order to completely remove the residual ethanol from NT3 buffer. The PrepEase clean-up column was then placed into a clean 1.5 ml microcentrifuge tube and 25 µl of NE buffer pre-heated at 70ºC was added. This was incubated at room temperature for 1 minute and the DNA was eluted by centrifugation at 11,000g for 1 minute. The concentration of the eluted DNA was quantified using nanodrop spectrophotometer and adjusted for subsequent procedures.

3.8.6 TOPO cloning reaction of KKSG6 and KKSG9 into a pET 101 D-TOPO vector

KKSG6 and KKSG9 were cloned into pET 101 D-TOPO vector (Appendix E). The genes were situated between nucleotides 297-310 in 5'-3' direction of the D-TOPO vector using the following set up. About 3 ng of fresh PCR product in 2 µl volume was added into 1 µl of 15 ng pET 101 D-TOPO vector to a clean microcentrifuge tube. 1 µl of salt solution was added and the mixture was made up to 6 µl by the addition of 3 µl sterile water. The mixture was gently mixed and incubated at room temperature for 5 minutes. The reaction was then kept on ice.

3.8.7 Transformation of recombinant plasmids of KKSG6 and KKSG9 into One Shot TOP10 chemically competent E-*coli* cells

3 µl each of the TOPO cloning reactions were then added to one vial each of the one Shot TOP10 chemically competent E-*coli* cells. The reaction mixtures were mixed and incubated on ice for 15 minutes. The cells were then heat shocked at 42°C water bath for exactly 30 seconds. The tube was immediately transferred to ice and 250 µl of room temperature S.O.C. medium was added. The tubes were tightly capped and shaken horizontally (200 rpm) at 37°C for 60 minutes. 100 µl from each tube was then spread unto LB medium supplemented with 100 µg/ml ampicillin and incubated overnight at 37°C.

3.8.8 Colony PCR

A colony PCR was performed in order to isolate successful clones from the TOPO cloning reactions using both the T7 specific primers and a combination of T7 and KKSG6 specific primer. The procedure involved picking a small amount from the colony of transformed TOP10 and then added it unto the PCR reaction mixture containing forward

and reverse primers and master mix. The initial heating step causes the release of plasmid DNA so that it can serve as a template for the amplification reaction. Four different combination of primers were employed in order to make sure that the colony contain the successful recombinant gene with the expected size. The first colony PCR was carried out using gene specific forward and reverse primers. The second colony PCR was carried out using T7 forward and T7 reverse primers. The third and fourth colony PCR was carried out using a combination of T7 forward and gene specific reverse and T7 reverse and gene specific forward primers respectively.

The reaction mixture consists of 8 µl nuclease free water, 1µ each of the forward and reverse primer and 10µl of Taq DNA polymerase. For KKSG6, the PCR cycling condition involved one cycle of an initial denaturation for 10 seconds at 98ºC, 20 cycles of denaturation for 1 minute at 98ºC, annealing at 68.5ºC, 50ºC, 59.0ºC and 60.0ºC for the four different primer combinations as stated above respectively, then 1 cycle of final extension at 72ºC. For KKSG9, the reaction mixture consists of 8 µl nuclease free water, 1 µl each of the forward and reverse primer and 10µl of Taq DNA polymerase. The PCR cycling condition involved one cycle of an initial denaturation for 10 seconds at 98ºC, 20 cycles of denaturation for 1 minute at 98ºC, annealing at 67.1ºC, 50ºC, 57.1ºC and 60.5ºC respectively for the four different primer combinations as stated above respectively, then 1 cycle of final extension at 72ºC. The amplified products were run on an agarose gel as described for the electrophoresis of DNA in section (4.4.3) and visualized under U.V. illumination using AlphaImager Mini.

3.8.9 Plasmid extraction

The plasmid was extracted using PrepEase MiniSpin plasmid extraction kit as follows. About 5 ml of bacterial culture was harvested in a clean 1.5 ml microcentrifuge tube by centrifugation at 11,000g for 30 seconds. The pellet was then resuspended in 250 µl of

RNase A-A1 buffer by vigorous vortexing. The suspension was then lysed by addition of 250 µl of A2 buffer, mixed gently by inverting the tube 6-8 times and the mixture incubated at room temperature for 3 minutes. The lysate was then neutralized by adding 300 µl of A3 buffer and the mixture was immediately mixed until a white homogenous suspension containing an off-white flocculate was formed. This was then centrifuged at 11,000g for 10 minutes at 4ºC. To bind the plasmid to the column, PrepEase MiniSpin column was then placed into a 2 ml collecting tube and the clarified lysate was added unto the column. This was centrifuged at 11, 000g for 1 minute and the flow-through was discarded. In order to remove all nucleases, the PrepEase MiniSpin column was placed back into the 2 ml collecting tube and 500 µl of AW buffer (heated to 50ºC) was added. This was centrifuged at 11, 000g for 1 minute and the flow-through was discarded. To wash the column, the PrepEase MiniSpin column was placed back into the 2 ml collecting tube and 600 µl of A4 buffer was added. This was also centrifuged at 11,000g for 1 minute and the flow-through was discarded. In order to completely dry the column, the PrepEase MiniSpin column was placed back into the 2 ml collecting tube and centrifuged at 11,000g for 2 minutes. The final elution step was done by placing the PrepEase MiniSpin column into a clean 1.5 ml microcentrifuge tube and thereafter 30 µl of AE buffer (heated to 70ºC). The eluted plasmid was quantified using nanodrop spectrophotometer and kept at -20ºC for further use.

3.8.10 Site-directed mutagenesis

The method of Liu and Naismith (2008) was adopted in site directed mutagenesis studies. The 50µl PCR reaction mixture contained the following components; 35 µl nuclease free water, 5 µl of 10× reaction buffer, 4 µl of 23 ng/ µl recombinant plasmid, 1.5 µl of quick solution, 1.25 µl containing 10 mM each of both forward and reverse primers, 1 µl of dNTP mix, and 1 µl of QuickChange enzyme solution.

For KKSG6, the pair of primers used during the PCR reaction and the cycling condition were as follows; for the Cys10Phe mutation, the primers are; forward 5'-CCGGTGCCT**T**CTCGCTCGCCGTCCACATTGCCTTG-3' and reverse 5'-GAGCGAG**A**AGGCACCGGGGGCGTAGTAGAGCTTCAT-3'. The cycling conditions used are; (1) one cycle of initial denaturation at 95ºC for 7 minutes, (2) twelve (12) cycles of denaturation at 95ºC for 1 minute, 53.0ºC annealing for 1 minute and 68ºC extension for 3.5 minutes, (3) three cycles of denaturation at 95ºC for 1 minute, 51.0ºC annealing for 1 minute and 68ºC extension for 3.5 minutes (4) three cycles of denaturation at 95ºC for 1 minute, 71.0ºC annealing for 1 minute and 68ºC extension for 3.5 minutes (5) final extension at 68.0ºC for 20 minutes.

For the Lys107Thr mutation, the primers are; forward 5'-CTGCACA**C**GGGCTTCAGCCCCTGGCTGTGGCAC-3' and reverse 5'-GAAGCCC**G**TGTGCAGTTCGGTGCTGACGAAGGTG-3'. The cycling conditions used are; (1) one cycle of initial denaturation at 95ºC for 7 minutes, (2) twelve (12) cycles of denaturation at 95ºC for 1 min, 57.0ºC annealing for 1 minute and 68ºC extension for 3.5 minutes, (3) three cycles of denaturation at 95ºC for 1 minute, 41.0ºC annealing for 1 minute and 68ºC extension for 3.5 minutes, (4) three cycles of denaturation at 95ºC for 1 minute, 72.0ºC annealing for 1 minute and 68ºC extension for 3.5 minutes and (5) final extension at 68.0ºC for 20 minutes.

For the Ala180Pro mutant; Forward 5'-ACCTGCAG**C**CCTGGATGGCACGCGTGGCGGCCCGCCC -3' and reverse 5'-CCATCCAGG**G**CTGCAGGTGCGGGTAGGCAGTGAGCGGG-3'.The 50µl PCR reaction mixture consists of PCR reaction for all the three different mutants was set as follows 1) one cycle of initial denaturation at 95 ^{0}C for 7 minutes, 2) twelve (12) cycles of denaturation at 95ºC for 1 minute, 66.0ºC annealing for 1 min and 68ºC extension for

3.5 min, 3) three cycles of denaturation at 95ºC for 1 minute, 51.0ºC annealing for 1 minute and 68ºC extension for 3.5 minutes 4) three cycles of denaturation at 95ºC for 1 minute, 78.0ºC annealing for 1 minute and 68ºC extension for 3.5 minutes and (5) final extension at 68.0ºC for 20 minutes.

For KKSG9, the pair of primer used during the PCR reaction for the Y12C mutation are as follows; forward 5'-TTTCCTCCTGCACCCAGAAGGT**G**CAGGTGCTGATCGCGCTG-3' and reverse 5'-TCTGGGTG**C**AGGAGGAAAAGGGGTGGCCGTAGAGG-3'. The cycling condition used is; (1) one cycle of initial denaturation at 95ºC for 7 minutes, (2) twelve (12) cycles of denaturation at 95ºC for 1 minute, 53.0ºC annealing for 1 minute and 68ºC extension for 3.5 minutes, (3) three cycles of denaturation at 95ºC for 1 minute, 47.0ºC annealing for 1 minute and 68ºC extension for 3.5 minutes, (4) three cycles of denaturation at 95ºC for 1 minute, 70.5ºC annealing for 1 minute and 68ºC extension for 3.5 minutes and (5) final extension at 68.0ºC for 20 minutes.

3.8.11 Plasmid digestion and transformation into XL10-gold ultracompetent cell

To digest the methylated plasmid, 2 µl of Dpn-I enzyme was added to 50 µl of the product of PCR reaction and incubated at 37ºC for 5 minutes. The digested plasmid was then transformed into XL10-gold ultracompetent cells as follows. 45 µl of the XL10-gold ultracompetent cells were aliquoted into pre-chilled 14 ml BD falcon polypropylene round bottomed tube. 2 µl of β-mercaptoethanol was then added and the contents were swirled and then placed on ice for 2 minutes. 2 µl of Dpn-I treated plasmid was then added and the contents swirled to gently mix them. This was placed on ice for 30 minutes. The cells were then exposed to heat shock for 30 seconds at 42ºC. The tube was incubated on ice for 2 minutes and 250 µl of room temperature S.O.C. medium was added. This was incubated at 37ºC for 1 hour and thereafter, 100 µl was spread on LB plates containing

100 µg/ml ampicillin. This was then incubated overnight at 37ºC. Plasmids were extracted as described in section (4.4.9) and sent for sequencing to confirm the mutations (Appendix F-K).

3.8.12 Plasmid transformation and protein expression

Both the wild type and mutants (C10F, K107T, and A180P) recombinant KKSG6 were overexpressed using BL21 (star) (DE3) as follows. About 5-10ng of recombinant plasmid in 1 to 5 µl volume was transformed into one vial each of BL21 (star) (DE3) chemically competent cells and were mixed by gentle stirring. These were then incubated on ice for 30 mins. The cells were then heat shocked at 42ºC for exactly 30 secs and the tubes were immediately transferred to ice. 250 µl of room temperature S.O.C medium was then added. The tubes were tightly capped and incubated at 37ºC for 30 mins with shaking at 200 rpm. The entire transformation reactions were then added into 10 ml of LB broth containing 100 µg/ml ampicillin. These were grown overnight at 37ºC with shaking at 200 rpm. 500 ml of LB containing the above-mentioned antibiotic was then inoculated with the entire 10 ml from the overnight culture. The culture was grown at 37ºC with shaking (200rpm) until the optical density $(OD)_{600}$ reaches about 0.5. 1 mM final concentration Isopropyl β-D-1-thiogalactopyranoside (IPTG) was then added to induce the protein expression and the cells were grown for further three (3) hours. The cells were harvested by centrifugation at 6000rpm for 12 minutes at 4ºC. Lysis buffer containing protease inhibitor (50 µl) and lysozyme (100 µl) was added to the pellets to facilitate the breakdown of the cell wall. The cells were lysed by sonication and centrifuged at 8000 rpm for 60 minutes. The supernatant was collected for GST purification.

Recombinant KKSG9 was overexpressed using Rosseta gami B(DE3) as follows; about 10 ng of recombinant plasmid was transformed into Rosseta-gami B(DE3) chemically competent cells. The transformation reaction was then plated on Luria Bertani

(LB) media plates containing 100 µg/mL ampicillin, 15 µg/mL kanamycin, 34 µg/mL chloramphenicol and 12.5 µg/mL tetracycline. The positive transformant was selected and cultured into 10 mL LB broth containing the combination of the above antibiotics and cultured overnight at 37ºC temperature. 500 mL of LB containing the above-mentioned antibiotics was then inoculated with the entire 10 mL from the overnight culture. The culture was grown at 37ºC with shaking (200 rpm) until the optical density $(OD)_{600}$ reaches about 0.5. 1 mM final concentration of Isopropyl β-D-1-thiogalactopyranoside (IPTG) was then added to induce the protein expression and the cells were grown for further five hours. The cells were harvested by centrifugation at 6000rpm for 12 minutes at 4ºC. Lysis buffer containing 50 µl protease inhibitor (50 µg/ml) and 100 µl lysozyme (10 mg/ml) was added to the pellets to facilitate the breakdown of the cell wall. The cells were lysed by sonication and centrifuged at 8000 rpm for 1 hour. The supernatant was collected for GST purification.

3.8.13 Protein purification

Protein purification was carried out using Amersham Bioscience (GE Healthcare) AKTA FPLC™ connected to a fraction collector. The purification was done using a GSTrap™ HP column (5 ml). The column (5 ml) was first equilibrated with 25 mM sodium phosphate buffer pH 7.4 and 5ml of the supernatant crude lysate was then injected. The flow rate was adjusted to 0.5 ml/min and thereafter the bound protein was eluted using 10 mM reduced glutathione (GSH).

3.8.14 SDS-PAGE electrophoresis

Sodium dodecyl sulfate polyacrylamide gel-electrophoresis (SDS-PAGE) was carried out using Bio-Rad MINI PROTEAN II system following the manufacturer's instructions. A 12% resolving SDS gel and 4% SDS stacking gel were prepared using the formulation

in the Table 4.1 (Laemmli, 1970). The resolving gel was first prepared and overlaid with distilled water. It was allowed to polymerize for about an hour and thereafter, the overlaid distilled water was poured away and replaced with the stacking gel. The 10-welled comb was then placed immediately into the stacking gel and was allowed to polymerize together. After about an hour, the comb was removed and the gel was now ready for loading and running.

Table 3.1: SDS-PAGE gel formulation

Solution	12% Resolving gel (ml)	4% Stacking gel (ml)
30% acrylamide /bis-acrylamide		
1.5M Tris-HCl pH 8.8	2.6	-
0.5M Tris-HCl pH 6.8	-	1.25
Distilled water	3.2	3.0
10% (w/v) SDS	0.1	0.05
10% Ammonium persulphate	0.01	0.005
TEMED	0.01	0.005

The electrophoresis apparatus was assembled following the manufacturer's instructions. Both the crude and purified protein were then diluted (1:2) with the SDS-sample buffer. These were then loaded unto the wells together with Bench mark protein ladder. The electrophoresis was performed using Tris-glycine running buffer with a constant voltage of 120V. It was allowed to run until the marker reaches the bottom end of the gel. The gel was then removed and allowed to stay overnight in commassie brilliant blue staining. The gel was de-stained using 20% methanol and 5% acetic acid in distilled water and viewed under a visible white light, scanned using image scanner and kept.

3.8.15 Bradford assay

Bradford assay was performed in order to prepare a standard curve using bovine serum albumin and also to determine the protein concentration (Bradford, 1976). The standard curve was prepared using various concentrations of albumin mixed with 5 ml of Bradford

reagent. The mixture was shaken and the absorbance was read at 595 nm. The sample protein was also prepared by mixing 100 µl of the sample and 5 ml of Bradford reagent and the absorbance was taken at 595 nm.

3.8.16 Glutathione S-transferase Assay

The glutathione S-transferase assay was carried out at 25 ^{0}C using various available substrates including 1-chloro-2,4-dinitrobenzene (CDNB), 1,2-dichloro-4-nitrobenzene (DCNB), ethacrynic acid (EA), *p*-nitrobenzyl chloride (NBC), hydrogen peroxide (H_2O_2), cumene hydroperoxide (CuOOH), *trans*-2-hexenal, *trans*-2-octenal, *trans*-4-phenylbutene-2-one and *trans*-hepta-2,4-dienal. All assays were carried out using Cary 60 UV-visible spectrophotometer. Progress of conjugating products with the various substrates was monitored over time by the change in absorbance of the respective substrates. Observed reaction velocities were corrected for spontaneous reaction rates where necessary. All initial rates were determined in triplicate in buffers equilibrated at constant temperature.

3.8.16.1 Assay using 1-chloro2,4-dinitrobenzene (CDNB)

The enzyme activity using CDNB as substrate was carried out according to the method described by Habig et al. (1974). The reaction mixture (3 ml) contained 100 mM sodium phosphate buffer (pH 6.5), 1 mM CDNB, 1 mM GSH, and a suitable amount of purified enzyme. The reaction was started by the addition of the substrate and the rate of the reaction was recorded following the increase in absorbance at 340 nm. Molar absorption coefficient, $\varepsilon_m = 9600\ mol^{-1}.cm^{-1}$.

3.8.16.2 Assay using 1,2-dichloro-4-nitrobenzene (DCNB)

The enzyme activity using CDNB as substrate was carried out according to the method described by Motoyama and Dauterman (1974). The reaction mixture (3 ml) contained 100 mM sodium phosphate buffer (pH 7.5), 1 mM CDNB, 5 mM GSH, and a suitable amount of purified enzyme. The reaction was initiated by the addition of purified enzyme and the measurements were recorded at 345 nm for 10 minutes. Molar absorption coefficient, $\varepsilon_m = 8400\ mol^{-1}.cm^{-1}$.

3.8.16.3 Assay using ethacrynic acid (EA) as substrate

This assay was carried out according to the method of Habig and Jakoby (1981). The reaction mixture (3 ml) contained 100 mM sodium phosphate buffer (pH 6.5), 0.2 mM EA, 0.25 mM GSH, and a suitable amount of purified enzyme. The reaction was started by the addition of the substrate and the rate of the reaction was recorded following the increase in absorbance at 270 nm. Molar absorption coefficient, $\varepsilon_m = 5000\ mol^{-1}.cm^{-1}$.

3.8.16.4 Assay using hydrogen peroxide (H_2O_2)

This assay was carried out according to the method of Di Ilio et al. (1986). The assay mixture contained 100 mM Tris-HCl buffer pH 7.2, 1 mM GSH, 2.5 mM NADPH, 6 µg glutathione reductase, final concentration of 0.25 mM for hydrogen hydroperoxide and appropriate amounts of enzymes. The reaction was initiated by the addition of the substrates and the rate of the reaction was recorded following the decrease in absorbance at 340nm. Molar absorption coefficient, $\varepsilon_m = 6220\ mol^{-1}.cm^{-1}$.

3.8.16.5 Assay using cumene hydroperoxide (CuOOH)

This assay was carried out according to the method of Di Ilio et al. (1986). The assay mixture contained 100 mM Tris-HCl buffer pH 7.2, 1 mM GSH, 2.5 mM NADPH, 6 µg

glutathione reductase, final concentrations of 1.2 mM for cumene hydroperoxide and appropriate amounts of enzymes. The reaction was initiated by the addition of the substrates and the rate of the reaction was recorded following the decrease in absorbance at 340 nm. Molar absorption coefficient, ε_m = 6220 $mol^{-1}.cm^{-1}$.

3.8.16.6 Assay using *p*-nitrobenzyl chloride (NBC)

This was done according to the procedure of Habig et al (1974). The reaction mixture (3 ml) contained 100 mM sodium phosphate buffer (pH 6.5), 1 mM NBC, 5 mM GSH, and a suitable amount of purified enzyme. The reaction was started by the addition of the substrate and the rate of the reaction was recorded following the increase in absorbance at 310 nm for 10 minutes. Molar absorption coefficient, ε = 1900 $mol^{-1}.cm^{-1}$.

3.8.16.7 Assay using Hexa-2,4-dienal

This was performed according to the procedure described by Brophy et al. (1989). The reaction mixture (3 ml) contained 100 mM sodium phosphate buffer (pH 6.5), 0.05 mM hexa-2,4-dienal, 2.5 mM GSH, and a suitable amount of purified enzyme. The progress of the reaction was monitored at 280 nm for 10 minutes. Molar absorption coefficient, ε_m = -34200 $mol^{-1}.cm^{-1}$.

3.8.16.8 Assay using *trans*-2-octenal

This was done according to the procedure Brophy et al. (1989). The reaction mixture (3 ml) contained 100 mM sodium phosphate buffer (pH 6.5), 0.025 mM *trans*-2-octenal, 1 mM GSH, and a suitable amount of purified enzyme. The reaction was started by the addition of the substrate and the conjugation reaction was monitored at 225 nm for 10 minutes. Molar absorption coefficient, ε_m = -22000 $mol^{-1}.cm^{-1}$.

3.8.16.9 Assay using *trans*-2-hexenal

This was done according to the procedure Brophy et al. (1989). The reaction mixture (3 ml) contained 100 mM sodium phosphate buffer (pH 6.5), 0.025 mM *trans*-2-hexenal, 1 mM GSH, and a suitable amount of purified enzyme. The reaction was started by the addition of the substrate and the conjugation reaction was monitored at 225 nm for 10 minutes. Molar absorption coefficient, ε_m = -24000 $mol^{-1}.cm^{-1}$.

3.8.16.10 Assay using *trans*-4-phenyl-3-butene-2-one (PBO)

This was done according to the procedure of Habig et al. (1974). The reaction mixture (3 ml) contained 100 mM sodium phosphate buffer (pH 6.5), 0.05 mM PBO, 0.25 mM GSH, and a suitable amount of purified enzyme. The reaction was initiated by the addition of purified enzyme and the conjugation reaction was monitored at 290 nm for 10 minutes. Molar absorption coefficient, ε_m = -24800 $l.mol^{-1}.cm^{-1}$.

3.8.17 Determination of kinetic parameters of KKSG6 using CDNB and GSH as substrates

The kinetic parameters for wild type and mutants KKSG6 were determined using CDNB and GSH as substrates. This was performed by varying the CDNB concentration (0.3-2.1 mM) while keeping the GSH concentration (1.0 mM) constant. For the GSH, it was determined by keeping the concentration of the CDNB (1.0 mM) constant while varying the GSH concentration (0.2-1.8 mM). Initial rates of the reactions were determined and all the measurements were carried out using Cary 60 UV-Visible spectrophotometer. The data was fitted to the Michealis-Menten equation $V= V_{max}[S]/K_m + [S]$ and was analyzed using non-linear regression analysis with GraphPad prism 7 software. Kinetic parameters (K_m and V_{max}) were calculated from the graph while the apparent k_{cat} was calculated using the equation $k_{cat} = V_{max}/[E]_t$.

The kinetic parameters for wild type KKSG6 and mutant (K107T) were determined using EA and GSH as substrates. This was performed by varying the EA concentration (0.02-0.20 mM) while keeping the GSH concentration (1.0 mM) constant. For the GSH, it was determined by keeping the concentration of the EA (1.0 mM) constant while varying the GSH concentration (0.2-1.8). All the measurements were carried out using Cary 60 UV-Visible spectrophotometer. The data were fitted to the Michealis-Menten equation $V= V_{max}[S]/K_m + [S]$ and was analyzed using non-linear regression analysis with GraphPad prism 7 software. Kinetic parameters (K_m and V_{max}) were calculated from the graph while the apparent k_{cat} was calculated using the equation $k_{cat} = V_{max}/[E]_t$.

The kinetic parameters for wild type and mutants KKSG9 were determined using *p*-nitrobenzyl chloride (NBC) and GSH as substrates. This was performed by varying the NBC concentration (0.02-0.2mM) while keeping the GSH concentration constant (1 mM). For the GSH, it was determined by keeping the concentration of NBC constant (1 mM) while varying the GSH concentration (0.4-1.2 mM). All the measurements were carried out using Cary 60 UV-Visible spectrophotometer. The data were fitted to the Michealis-Menten equation $V= V_{max}[S]/K_m + [S]$ and was analyzed using non-linear regression analysis with GraphPad prism 7 software. Kinetic parameters (K_m and V_{max}) were determined from the graph while the apparent k_{cat} was calculated using the equation $k_{cat} = V_{max}/[E]_t$.

3.8.18 Chloride ion detection assay

The activity of purified KKSG6 and KKSG9 toward various organochlorine compounds was measured by its ability to release chloride ions from the substrates. However, chloride ion detection assay described by McGuinness et al. (2007) was used to quantitate the amount of chloride ion released. About 900 µl of purified GST was

incubated with 50 µl of 10 mM of GSH and 50 µl of 10 mM substrates (2-chlorobenzoate, 3-chlorobenzoate, 4-chlorobenzoate, 2,4-dichlorobenzoate, 2,5-dichlorobenzoate 2,6-dichlorobenzoate, DDT, endosulfan, DCA, permethrin, and dieldrin) overnight for 16 hours at 100 rpm and 28 ^{0}C temperature. The reaction was terminated by the addition of 20 µl of 5M H_2SO_4, 200 µl of 13 mM Hg $(SCN)_2$ in 95% ethanol and 200 µl of 0.25 M Fe $(NH_4)(SO_4)_2 \times 12H_2O$ in 9 M HNO_3 was then added to 0.6 ml of the reaction mixture. The absorbance of Fe $(SCN)^{2+}$ produced was measured after 5 mins at 450 nm. The concentration of the chloride ions released was determined from the known concentration of sodium chloride (0.1-1.0 mM) in the standard curve (Appendix C).

3.8.19 Statistical analysis

Analysis of variance (ANOVA) and student's t-test was used to analyze the data using OriginPro 8.5 software. 95% level of significance ($p<0.05$) was used as a criterion to determine whether the variances of the data are statistically significant or not. All the data are reported as mean ± SD of three independent experiments using different enzyme preparations.

3.8.20 Molecular docking studies

In order to understand the binding pattern between KKSG6 and various substrates, a molecular docking study was performed. Molecular docking was performed using autodock 4.2 Software (Goodsell et al., 1996). However, due to the absence of crystal structure of KKSG6, a 3D dimensional structure of KKSG6 which was build using swiss model server was used throughout the studies (Bordoli et al., 2009). The server uses a suitable template from the experimentally determined structure of a related family of protein to build the three-dimensional structure of the target protein. KKSG6 model was built using a crystal structure of BphK (PDB code: 2gdr.1) (Retrieved from

https://www.rcsb.org/pdb/home/home.do). The protein shares 48% sequence similarity with KKSG6. The model showed very high quality as indicated by values of 0.79 and -1.62 on GMQE and QMEAN scoring functions respectively. For KKSG9, the modeled protein was built by a Swiss model server using a crystal structure of maleyl pyruvate isomerase in complex with glutathione (PDB code: 2jl4.1.A) (Retrieved from https://www.rcsb.org/pdb/home/home.do) which shared 21.95% sequence similarity with KKSG9 (Bordoli et al., 2009). The model quality assessment was done using Global QMEAN scoring function (http://swissmodel.expasy.org/qmean/cgi/index.cgi). The model showed very high quality as indicated by values of 0.74 and -1.58 on GMQE and QMEAN scoring functions respectively. Chemsketch software was used to draw the structure of all the ligands which were stored in the form of mol2 file (Mills, 2006). Finally, the protein data bank file (PDB) of all the ligands were constructed using Open babel software. The PDB files of both the ligands and the proteins were used as input file in autodock tools. A blind docking analysis was set up using an autogrid size of 126, 126 and 126 for the x, y and z-axis respectively. During the docking simulation, dihedral angles for all the substrates were treated as flexible. A total of 100 Lamarckian genetic algorithm docking runs were performed for each ligand as implemented in autodock 4.2 program. The following parameters were used in all the docking processes: an initial population of 100 random individuals, a maximum number of 1.5×10^6 energy evaluations, a maximum number of 27000 generations with mutation and crossover rates of 0.02 and 0.08 respectively. Additionally, an optional elitism parameter equals to 1 was also applied. This parameter determines the number of top individuals that will survive into the next generation. A maximum of 30 iterations per local search was allowed. The probability of performing a local search on an individual was 0.06 where the maximum number of consecutive successes or failures before doubling or halving the search step was 4. The Docked conformations clustered within a root mean square deviation of 2Å

were sorted in order of increasing energy. The coordinates of the lowest energy conformations were clustered and visualized using discovery studio software (http://www.accelrys.com).

CHAPTER FOUR: RESULTS

4.1 Predicted molecular weights and isoelectric points of putative GSTs from *Acidovorax* sp. KKS102

The predicted molecular weights and isoelectric points of putative GSTs from *Acidovorax* sp. KKS102 were predicted by an online server of the Expasy ProtParam tool and presented in Table 4.1. For onward studies, all the GSTs in *Acidovorax* sp. KKS102 would be identified as KKSG1-KKSG11 based on their reported position from (5'-3') in the chromosome of the organism.

Table 4.1: Predicted molecular weight and isoelectric points of *Acidovorax* sp. KKS102 GSTs.

Gene name	NCBI Accession number	Position of the gene in the chromosome	ORF (Amino acids)	Predicted molecular weight Mw (kDa)	Predicted isoelectric point (pI)
KKSG1	WP_015012102.1	310527-311171	214	23.38	6.50
KKSG2	WP_015012117.1	325105-325728	207	22.92	6.37
KKSG3	WP_015013129.1	1502409-1503314	301	33.26	6.19
KKSG4	WP_015014269.1	2782353-2782961	202	22.15	6.70
KKSG5	WP_015014376.1	2907537-2908478	313	34.51	6.17
KKSG6	WP_015014999.1	3622149-3622757	202	22.14	6.37
KKSG7	WP_015016004.1	4744892-4745539	215	23.74	6.96
KKSG8	WP_015016200.1	4956613-4957254	213	22.89	5.76
KKSG9	WP_015016207.1	4962905-4963564	219	24.37	6.12
KKSG10	WP_015014176.1	5673017-5673685	222	24.60	6.15
KKSG11	WP_015014226.1	5733533-5734171	212	23.10	5.38

4.2 Phylogenetic analysis of *Acidovorax* sp. KKS102 GSTs

Phylogenetic analysis was performed in order to understand the evolutionary relationship between the putative GSTs in *Acidovorax* sp. KKS102 . The evolutionary history was inferred by the Neighbor-Joining method. The optimal tree with the sum of branch length = 7.54273126 is shown (Figure 4.1). The tree is drawn to scale, with branch lengths in the same units as those of the evolutionary distances used to infer the

phylogenetic tree. The evolutionary distances were computed using the Poisson correction method and are in the units of the number of amino acid substitutions per site. The analysis involved 11 amino acid sequences. All positions containing gaps and missing data were eliminated. There was a total of 178 positions in the final dataset. For reliability testing of the phylogenetic tree, bootstrap values were set at 1000, this indicates the number of times a particular set of sequences are grouped together when trees are generated from resampled alignments. Based on the result of the phylogenetic analysis, the eleven putative GSTs appeared to have originated from various classes with some GSTs clustering together to indicate the possibility of coming from the same class (Figure 4.1). KKSG1 and KKSG3 appeared to have originated from the clade, however, their clustering was only supported by 39% bootstrap value indicating they are not from the same class. KKSG4 originated from the same clade as KKSG1 and KKSG3 with a strong bootstrap value of 85%, indicating that the putative GST might belong to the same class with either one of them. KKSG6 and KKSG2 clade was supported by a strong bootstrap value of 97% indicating the possibility that the two GSTs might belong to the same class. while KKSG8 showed a strong relationship with KKSG10 and KKSG11 with a strong bootstrap value of 95%, the two GSTs (KKSG10 and KKSG11) where only supported by a bootstrap value of 66% indicating the possibility that they may also be in the same class of GST. A strong bootstrap value of 85% suggested that KKSG7 and KKSG9 might belong to the same class of GST. However, KKSG5 clade was supported by a bootstrap value of 69% from a cluster that involves many different GST classes. This suggests that KKSG5 might be a completely different class of GST from all the eleven putative GSTs in *Acidovorax* sp. KKS102.

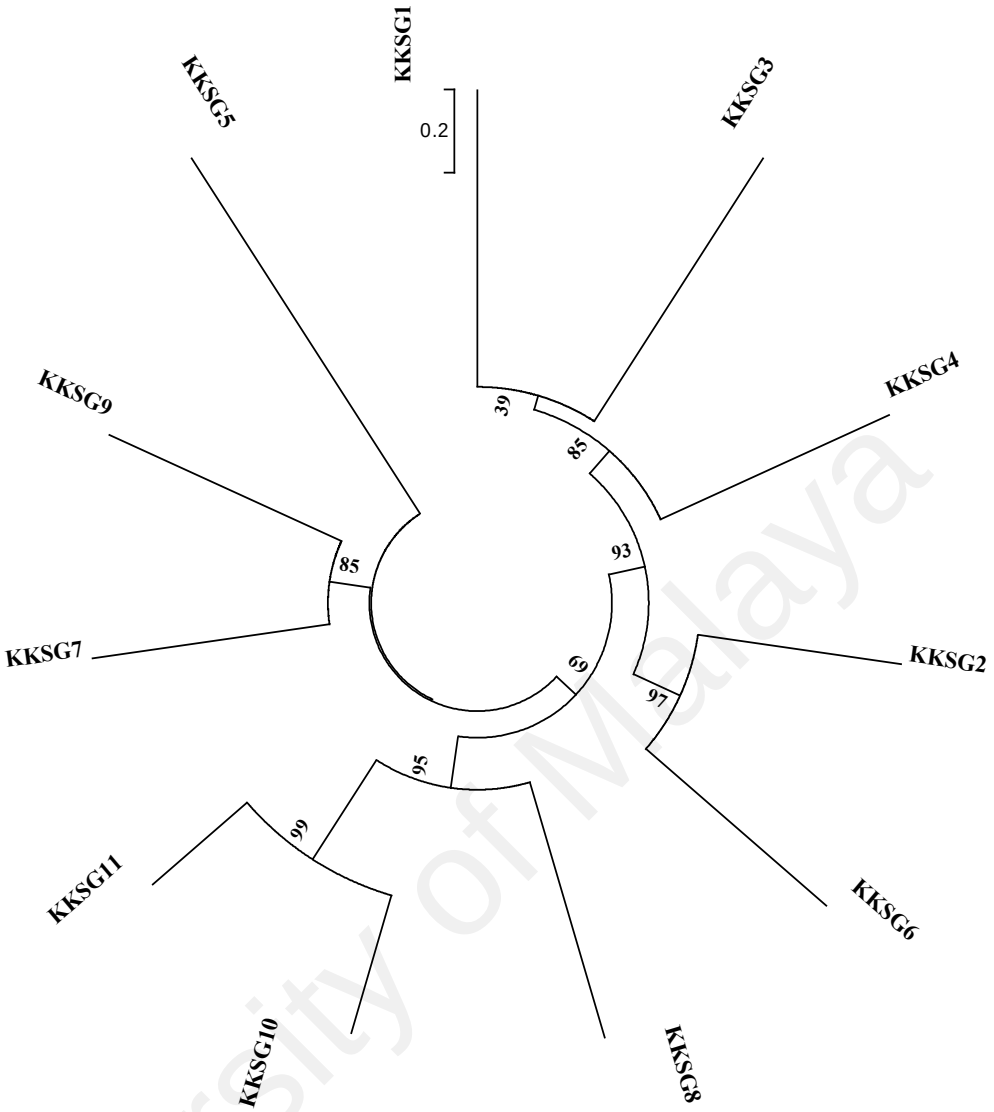

Figure 4.1: Model of the evolutionary relationship of taxa (time-tree) of *Acidovorax* sp. KKS102 GSTs. Numbers at the nodes represent the bootstrap percentages based on 1000 replicates.

4.3 Percent identity matrix and relationship between putative GSTs in *Acidovorax* sp. KKS102 and various GST classes from other organisms

The percentage similarity matrix between the putative GSTs in *Acidovorax* sp. KKS102 was computed by an online server of ClustalW2 (https://www.ebi.ac.uk/Tools/msa/clustalw2/). The data is presented in Table 4.2. Percent identity matrix is one of the criteria used to classify GSTs into their various

classes. Those GSTs that share greater than 40% sequence similarity are grouped into the same class while those with less than 20% are grouped into a different class (Allocati et al., 2009). The data further explain the extent of the relationship between putative GSTs in *Acidovorax* sp. KKS102. Sequence alignment analysis was also carried out in order to analyze the presence of conserved amino acids present in all the eleven putative GSTs. From the result obtained (Figure 4.2), three amino acids were found to be conserved across all the eleven putative GSTs: Leu 69, Pro 104, and aspartic acid 235. Conserved amino acids across different classes of GSTs are more likely structurally important (Brennan et al., 2009). This indicated their probable importance in the catalytic activity of all the putative GSTs in the organism. However, in order to understand the phylogenetic relationship between putative GSTs in *Acidovorax* sp. KKS102 and various GST classes from other organisms, a phylogenetic tree was constructed using all representative GSTs classes from other organisms (Figure 4.3). The analysis showed that all eleven putative GSTs in *Acidovorax* sp. KKS102 have distributed themselves into various related known GST classes.

Table 4.2: Percent identity matrix of *Acidovorax* sp. KKS102 GSTs created by ClustalW2

Enzymes	Percent identity matrix										
	KKSG5	KKSG7	KKSG9	KKSG8	KKSG10	KKSG11	KKSG3	KKSG1	KKSG4	KKSG2	KKSG6
KKSG5	100.00	19.12	17.22	20.20	18.36	20.59	15.32	19.10	19.47	15.46	14.29
KKSG7	19.12	100.00	29.76	20.86	22.87	23.50	18.50	21.69	21.79	26.97	21.11
KKSG9	17.22	29.76	100.00	20.62	23.98	22.51	16.83	20.51	24.19	22.16	22.99
KKSG8	20.20	20.86	20.62	100.00	29.70	34.69	19.70	20.50	27.37	25.53	24.34
KKSG10	18.36	22.87	23.98	29.70	100.00	48.58	21.61	23.59	20.74	22.68	18.65
KKSG11	20.59	23.50	22.51	34.69	48.58	100.00	20.21	24.74	22.83	25.27	23.94
KKSG3	15.32	18.50	16.83	19.70	21.61	20.21	100.00	24.39	26.60	22.34	19.47
KKSG1	19.10	21.69	20.51	20.50	23.59	24.74	24.39	100.00	25.79	34.03	24.74
KKSG4	19.47	21.79	24.19	27.37	20.74	22.83	26.60	25.79	100.00	26.15	28.88
KKSG2	15.46	26.97	22.16	25.53	22.68	25.27	22.34	34.03	26.15	100.00	33.16
KKSG6	14.29	21.11	22.99	24.34	18.65	23.94	19.47	24.74	28.88	33.16	100.00

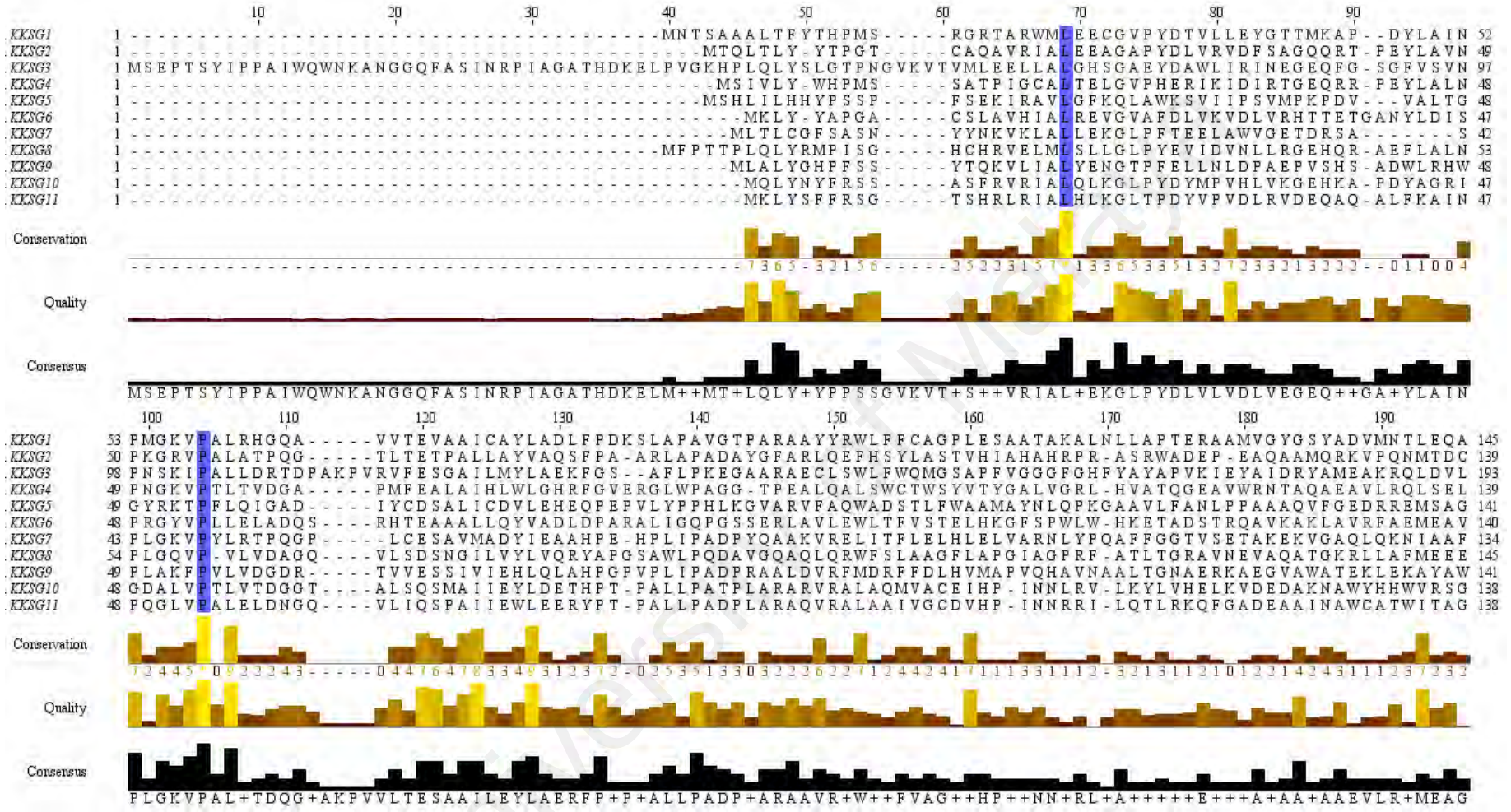

Figure 4.2: Sequence alignment analysis of putative GSTs from *Acidovorax* sp. KKS102. The blue highlighted sequences represent the conserved amino acids in all the eleven putative GSTs. The image was produced using Gel view *(*http://www.ebi.ac.uk/~michele/jalview/contents.htm

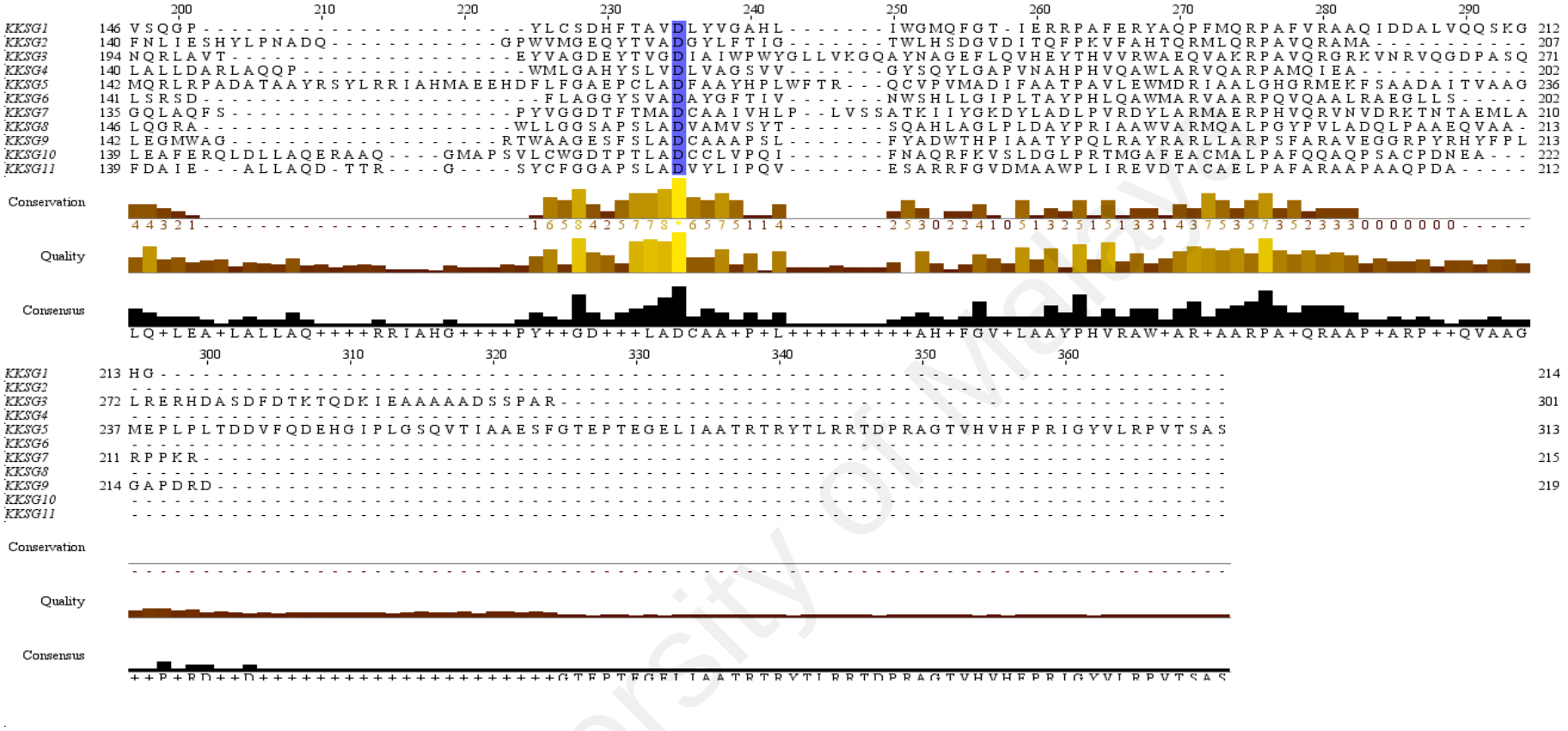

Figure 4.2, Continued

4.4 Identification of BphK homolog from putative GSTs in *Acidovorax* sp. KKS012

Bioinformatic analysis was performed in order to identify a suitable BphK homolog from *Acidovorax* sp. KKS102 for further studies. A search of the public database (NCBI) of GSTs from *Acidovorax* sp. KKS102 showed that the organism contained eleven putative GSTs. In order to examine the genetic relationship between this sequence and all known GST sequences, a phylogenetic tree was constructed using representatives from all GST classes and some identified BphK sequences. The evolutionary history was inferred using the Neighbor-Joining method. The optimal tree with the sum of branch length = 23.65819324 is shown (Figure 4.3). The tree is drawn to scale, with branch lengths in the same units as those of the evolutionary distances used to infer the phylogenetic tree. The evolutionary distances were computed using the Poisson correction method and are in the units of the number of amino acid substitutions per site. The analysis involved 52 amino acid sequences. All positions containing gaps and missing data were eliminated. There was a total of 114 positions in the final dataset. For reliability testing of the phylogenetic tree, bootstrap values were set at 1000, this indicates the number of times a particular set of sequences are grouped together when trees are generated from resampled alignments. The phylogenetic analysis revealed that two GSTs: KKSG6 and KKSG2 are clustered together in the same root with BphKs and beta class GSTs (Figure 4.4). The clustering was strongly supported by bootstrap value of 98%. Further analysis using the percentage sequence similarity (Table 4.3) revealed that KKSG6 shared a greater percentage of sequence similarity; 41.00%, 47.26%, and 45.77% with BphK sequences from *Novosphingobium aromaticivorans, Burkholderia xenovorans* LB400, and *Pseudomonas* sp. CT14, respectively, when compared with KKSG2. (Based on percentage similarity, GSTs that share 40% sequence similarity are included in the same class while those with less than 20-30% are assigned to separate class (Allocati et al., 2009)). Sequence alignment analysis using the KKSG6 and some

BphK sequences showed that the protein (KKSG6) contained some conserved amino acids such as His106, Cys10 as well as the conserved region of 152-158 containing (SVADIYL) (Figure 4.4), which were shown to be essential in the catalytic activity of BphK LB400 (Brennan et al., 2009; Gilmartin et al., 2005; McGuiness et al, 2006). The KKSG6 gene is located at position 3622149-3622757 on the chromosome of *Acidovorax* sp. KKS102 and was selected for further study. It contained an open reading frame of 609 base pairs coding for a polypeptide of 202 amino acids. The protein has a predicted molecular weight (Mw) and isoelectric point (pI) of 22.14 kDa and 6.37 respectively.

Other putative GSTs in *Acidovorax* sp. KKS102 also showed their various distribution across the phylogenetic tree. KKSG1 clade emanate from the chi GSTs, and with a strong bootstrap value of 90%, the GST might likely belong to the chi class. However, for KKSG4, even with a strong bootstrap value of 90%, the GST does not seem to belongs to any class between beta and chi. This suggest the possibility of a new class of GST situated between the chi and beta classes. KKSG3 enjoyed a strong bootstrap value of 99% with nu class representatives, suggesting a close relationship with the nu class GST and may likely belong to that class. KKSG10 and KKSG11 showed a strong bootstrap value of 99% between themselves, suggesting that they might have come from the same class. The two GSTs showed a bootstrap value of 66% with zeta class GSTs and the fact that even the two zeta class GSTs were only able to show a bootstrap value of 66% also between themselves, this suggested that KKSG10 and KKSG11 might likely belongs to zeta class. The putative GST of KKSG8 showed a bootstrap value of 52% with theta class GSTs, a value not strong enough to warrant its classification into this class. KKSG7 and KKSG9 does not align themselves to any particular known cytosolic GST class. This suggest a possibility of new class of GSTs. For KKSG5, the putative GST showed a bootstrap value of only 24% with kappa GSTs. However, since kappa GSTs were found to mitochondrial, this completely exclude the KKSG5 from this class and suggested that

it might likely be a new class of GST. This is also coupled with its unusual molecular weight of 34.51 kDa.

Figure 4.3: Model of the evolutionary relationship of *Acidovorax* sp. KKS102 GSTs. The phylogenetic tree was constructed using all known representative GST classes. Numbers after the underscore are the NCBI accession numbers. Bold arrows represent KKS102 GSTs. NP_852036.1 (*Rattus norvegicus*), NP_057001 (*Homo sapiens*), 4USSA (*Phanerochaete chrysosporium*), NP_195899 (*Arabidopsis thaliana*), ACJ84312(*Medicago truncatula*), NP_080895 (*Mus musculus*), 4YQM_A (*Homo sapiens*), ABF99228 (*Oryza sativa Japonica* Group), P46427 (*Onchocerca volvulus*), NP_000843 (*Homo sapiens*), NP_000840 (*Homo sapiens*), NP_000840 (*Homo sapiens*), NP_000552 (*Homo sapiens*), NP_034487 (*Mus musculus*), NP_665683 (*Homo sapiens*), P46428 (*Anopheles gambiae*), P46088 (*Nototodarus sloanii*), AAN39918 (*Capsicum annuum*), AAO61856 (*Malva pusilla*), AAF64647 (*Drosophila melanogaster*), EDV56071 (*Drosophila erecta*), EDW42478 (*Drosophila sechellia*), CAB03592 (*Anopheles gambiae*), AAA33469 (*Zea mays*), ABQ96852(*Solanum commersonii*), ABV24478 (*Hypophthalmichthys molitrix*), NP_001038525 (*Danio rerio*), BAB39498 (*Homo sapiens*), DAA20393 (*Bos taurus*), WP_001503035 (*Escherichia coli*), WP_004248152 (*Proteu mirabilis*), AAG58126 (*Escherichia coli*), WP_000566471 (*Proteobacteria*), WP_006196313 (*Nodularia spumigena*), WP_009787675 (*Lyngbya* sp. PCC 8106). The bold arrows (♦) indicates the putative GSTs from *Acidovorax* sp. KKS102. Numbers at the nodes represent the bootstrap percentages based on 1000 replicates.

Figure 4.4: A clustalW2 alignment of KKSG6 and BphK sequences. 2DSA is from *Burkholderia xenovorans* LB400, WP0124776224.1 is from *Pseudomonas* sp. CT14, WP010891022.1 is from *Novosphingobium aromaticivorans*. Boxed letters indicate some conserved amino acids known to play a vital role in the catalytic activity of the proteins from previous studies. The image was produced using Gel view (http://www.ebi.ac.uk/~michele/jalview/contents.html).

Table 4.3: Percentage sequence similarity between the KKSG2 and KKSG6 and some BphK sequences. Numbers after the underscore are the NCBI accession numbers of the BphK sequences.

	Percentage sequence similarity				
	KKSG2	**KKSG6**	**BphK_WP010891022**	**BphK_2DSA**	**BphK_WP012477624**
KKSG2	100	32.12	36.79	33.16	31.09
KKSG6	32.12	100.00	**41.00**	**47.26**	**45.77**
BphK_WP010891022	36.79	41.00	100.00	53.73	52.74
BphK_2DSA	33.16	47.26	53.73	100.00	69.46
BphK_WP012477624	31.09	45.77	52.74	69.46	100.00

4.5 DNA extraction

For downstream analysis of GST genes in *Acidovorax* sp. KKS102, the DNA was extracted as described in the methodology section. The gel image of extracted DNA is presented in (Figure 4.5). The image indicated a good and successful DNA extraction as there was no sign of DNA sharing which indicates degradation of the isolated DNA. Analysis of the purity of DNA using 260/280 ratio also showed a value of 1.86 in the nanodrop spectrophotometer indicating high purity for downstream application.

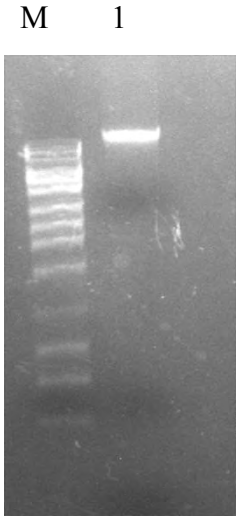

Figure 4.5: Gel image of extracted DNA from *Acidovorax* sp. KKS102. M: Gel ready DNA ladder, Lane 1: Extracted DNA of more than 10kb.

4.6 PCR amplification and cloning of KKSG6

A 609bp of KKSG6 gene was successfully amplified (Figure 4.6) using phusion flash high fidelity polymerase (Thermofisher) and cloned into pET101 D-TOPO vector as described in the methodology section. Various procedures such as colony PCR, PCR using the isolated plasmid and finally DNA-sequencing were performed in order to confirm the clone.

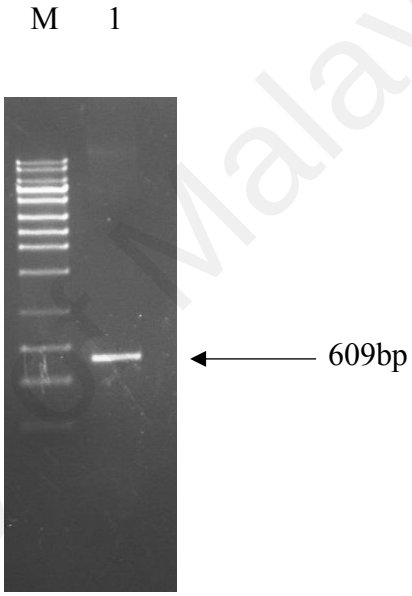

Figure 4.6: Gel image of the PCR amplification of KKSG6. M= Gel ready molecular weight marker, 1= expected gene size containing 609 base pairs.

4.7 Colony PCR

Colony PCR using various set of primers from both the KKSG6 gene and T7 were used to confirm the selection of successful colony and also to make sure that the inserted gene (KKSG6) is in the correct orientation. The extracted plasmid was also employed as a template to confirm a successful selection of the colony using various set of primers from both the KKSG6 gene and T7 bases. Using gene specific forward and reverse primers, the result indicated the expected gene size of 609bp (Figure 4.7). The result obtained using both T7 forward and reverse primers indicated an 875bp (Figure 4.8), that

was the result expected from the analysis of the position of the gene and T7 nucleotide bases in the vector. Colony PCR using gene specific reverse primer and T7 forward primer was found to yield 685bp (Figure 4.9), which was also the expected result from the analysis of their position in the vector. Finally, the result obtained using gene specific forward primer and T7 reverse primer yielded a 783bp (Figure 4.10), which was also the value expected from the analysis of the position of the gene and T7 nucleotide in the vector. Finally, sequencing the extracted plasmid confirmed the presence of the gene in the correct orientation and without any error in the amino acid sequence of the gene (Appendix F).

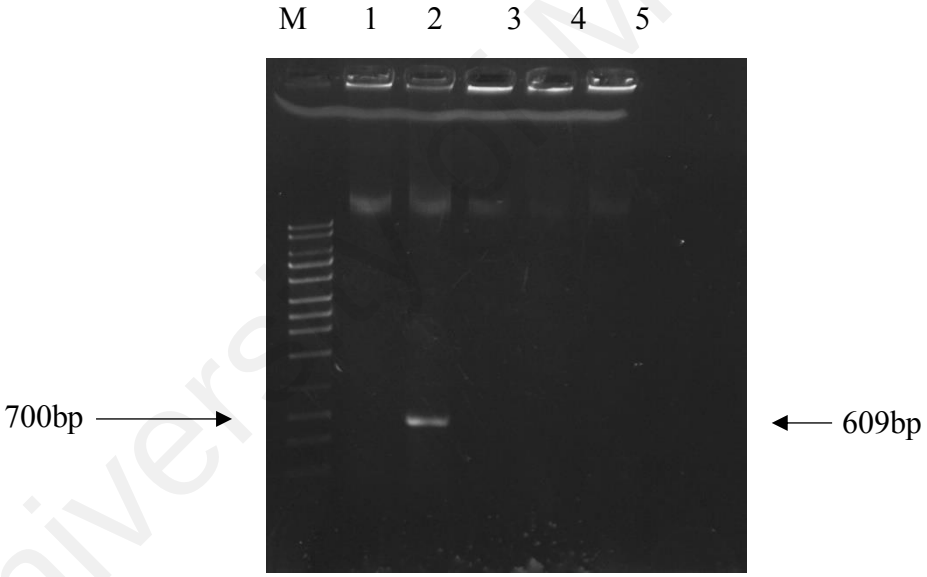

Figure 4.7: Gel image of colony PCR of KKSG6 using the KKSG6 gene specific forward and reverse primers. M= Gel ready molecular weight marker, lanes 1-5= various colonies picked for analysis, 2= colony containing the expected gene size of 609 base pairs.

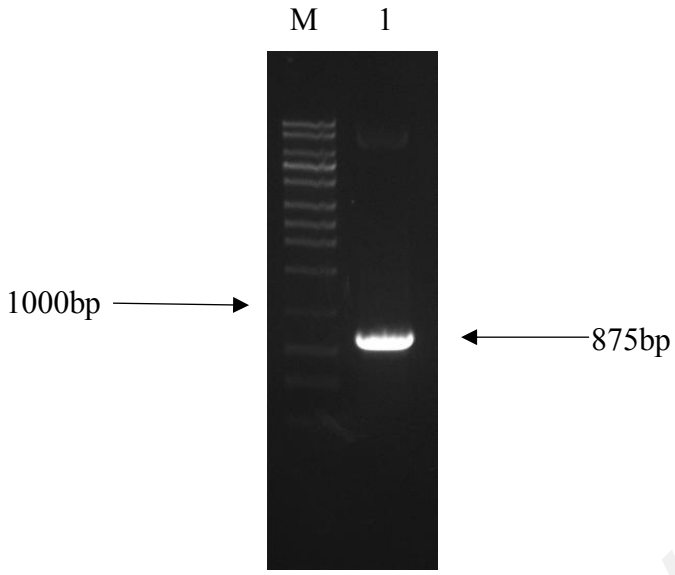

Figure 4.8: Gel image of PCR amplification of KKSG6 from the extracted plasmid using T7 forward and T7 reverse primers. M= Gel ready molecular weight marker, 1= Expected gene size of 875 bp.

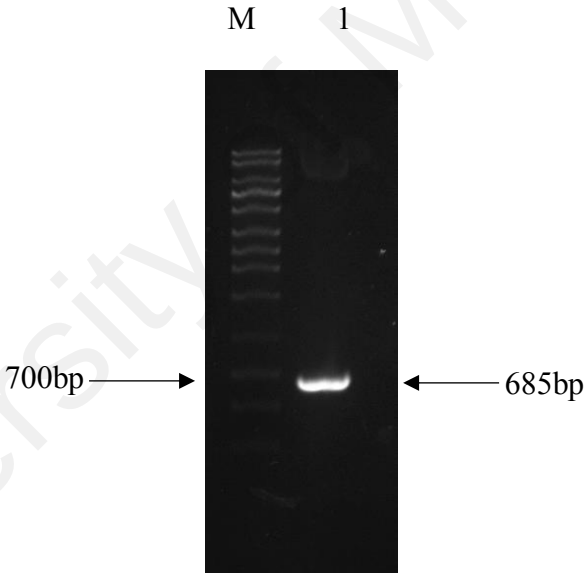

Figure 4.9: Gel image of PCR amplification of KKSG6 from the extracted plasmid using the gene specific reverse primer and T7 forward primer. M= Gel ready molecular weight marker, 1= Expected gene size of 685 bp.

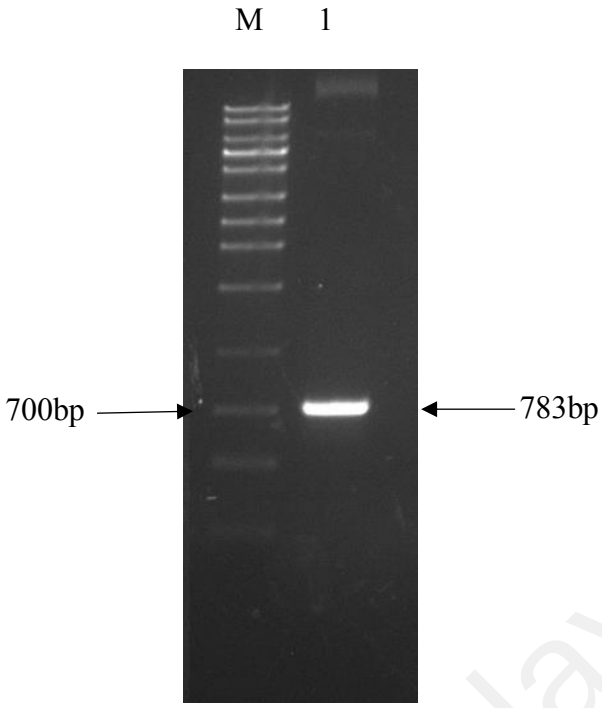

Figure 4.10: Gel image of PCR amplification of KKSG6 from the extracted plasmid using the gene specific forward primer and T7 reverse primer. M= Gel ready molecular weight marker, 1= Expected gene size of 783 bp.

4.8 Molecular docking study of KKSG6 and standard GST substrates and selection of amino acids for site-directed mutagenesis

Molecular docking study was carried out in order to explore the binding pattern and the amino acids involved in the interaction of various substrates with KKSG6. From the molecular docking result, the KKSG6 was found to bind the GSH molecule and the substrates; CDNB, ethacrynic acid and cumene hydroperoxide in the pocket occupied by the residues; A9, C10, L32, Y51, P53, V52, E65, A66, S102, H106, K107, W112 and L113 (Figures 4.11, 4.12 and 4.13). Cluster analysis of docked result in CDNB using root mean square deviation (RMSD) of 2Å revealed 10 different conformations. The lowest binding energy obtained was -6.63 kJ mol^{-1} which occurred in the 52^{nd} run of the cluster containing 11members (Figure 4.11). Cluster analysis of docked result in ethacrynic acid using root mean square deviation (RMSD) of 2Å revealed 9 different conformations. The lowest binding energy obtained was -9.31 kJ mol^{-1} which occurred in the 46^{th} run of the cluster containing 4 members (Figure 4.12). Cluster analysis of docked result in cumene

hydroperoxide using root mean square deviation (RMSD) of 2Å revealed 13 different conformations. The lowest binding energy obtained was -6.91 kJ mol^{-1} which occurred in the 56^{th} run of the most populated cluster containing 28 members (Figure 4.13). The presence of several polar amino acid side chains in both the G-site and H-site of the binding cleft suggest that both hydrogen bonding and hydrophobic interactions could be stabilizing the complexes formed. Various interactive forces including hydrogen bonding and hydrophobic interactions bound the substrates to the G and H-site of KKSG6. In addition to the hydrophobic interactions, at least two hydrogen bonds were predicted between the oxygen atom of CDNB and Lys107 of KKSG6, two hydrogen bonds between Trp 112 and Lys107 and oxygen atoms ethacrynic acid, and two hydrogen bonds between oxygen atom of cumene hydroperoxide and Ser 110 residue and another hydrogen bond between Leu 113 of KKSG6 and the substrate cumene hydroperoxide. Lys107 from the H-site appeared to be more prominent as it forms a direct hydrogen bonding with all the substrates under study. It was thought that the amino acid might be involved in the binding and proper orientation of the substrates. Sequence alignment analysis also revealed that this amino acid is conserved across all the BphK sequences and KKSG6, thus it was selected for site directed mutagenesis studies in order to investigate its functional role in the catalytic activity of KKG6 and the effect of the mutation on the kinetic parameters of the enzyme. The positively charged lysine was converted to hydrophilic threonine residues so as to investigate the effect of the mutation on the functional role of charged amino acid at that position. Molecular docking study of the K107T mutant was also carried out in order to investigate the nature of the interaction between the mutant and ethacrynic acid in particular (Figure 4.14). Moreover, Cys10 is a conserved amino acid in almost all beta class GSTs and was shown to play a role in the binding of the co-substrate (GSH). According to Brennan et al. (2009), mutating cys10 to phenylalanine results in a significant increase in the catalytic activity of GST BphK LB400 towards

CDNB. In order to investigate the behavior of (C10F) mutant in KKSG6 toward standard GST substrates, kinetic parameters, and dechlorination activity, the amino acid was selected for site directed mutagenesis studies. McGuiness et al. (2007) showed that mutating Ala180 to proline in glutathione S-transferase (BphK) of *Burkholderia xenovorans* LB400 results in significant increase in the catalytic activity of the protein towards organochlorine pesticides. Also, in order to investigate the activity of similar mutant (A180P) in KKSG6 toward standard GST substrates, kinetic parameters and dechlorination activity, the amino acid was also mutated.

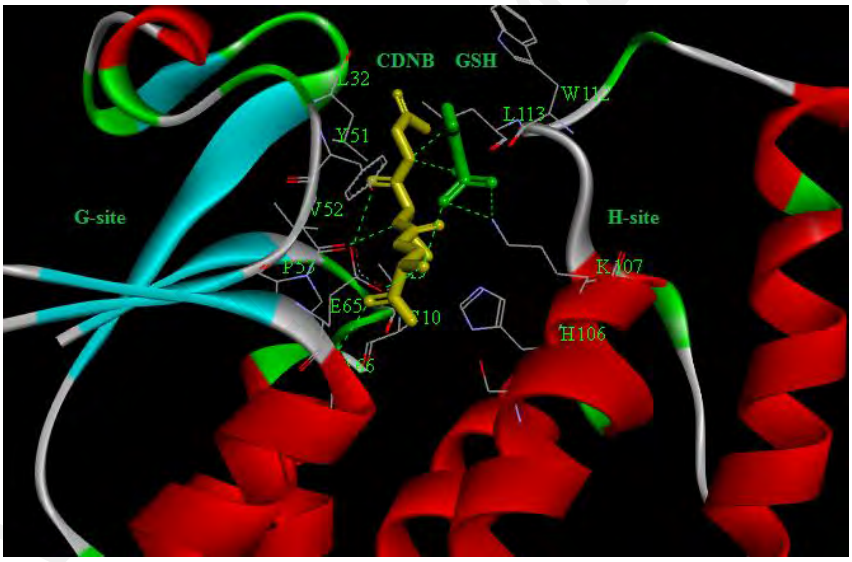

Figure 4.11: Predicted docking orientation of the lowest docking energy conformation of CDNB to the binding pocket of wild type KKSG6. The co-substrate (GSH) is shown in yellow while the CDNB in green ball and stick presentations. The green dash lines represent the hydrogen bondings. The residue side chains represent the amino acids involve in the catalysis.

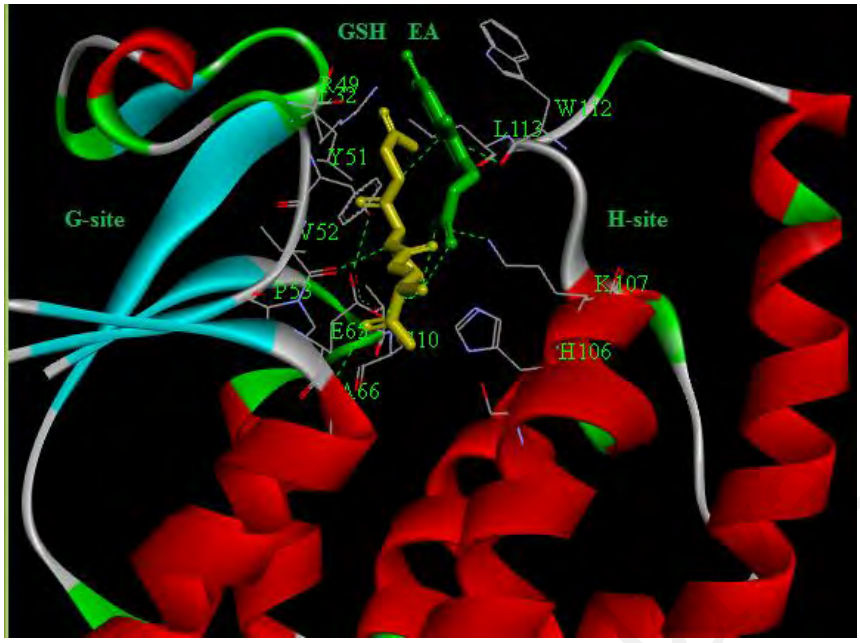

Figure 4.12: Predicted docking orientation of the lowest docking energy conformation of ethacrynic acid to the binding pocket of wild type KKSG6. The co-substrate (GSH) is shown in yellow while the ethacrynic acid in green ball and stick presentations. The green dash lines represent the hydrogen bondings. The residue side chains represent the amino acids involve in the catalysis.

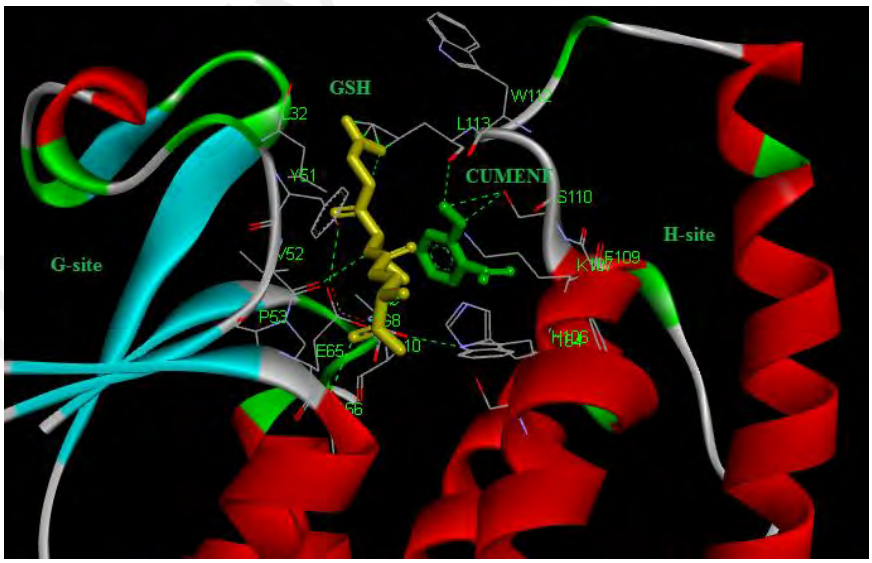

Figure 4.13: Predicted docking orientation of the lowest docking energy conformation of cumene hydroperoxide to the binding pocket of KKSG6. The co-substrate is shown in yellow while the cumene hydroperoxide in green ball and stick presentations. The green dash lines represent the hydrogen bondings. The residue side chains represent the amino acids involve in the catalysis.

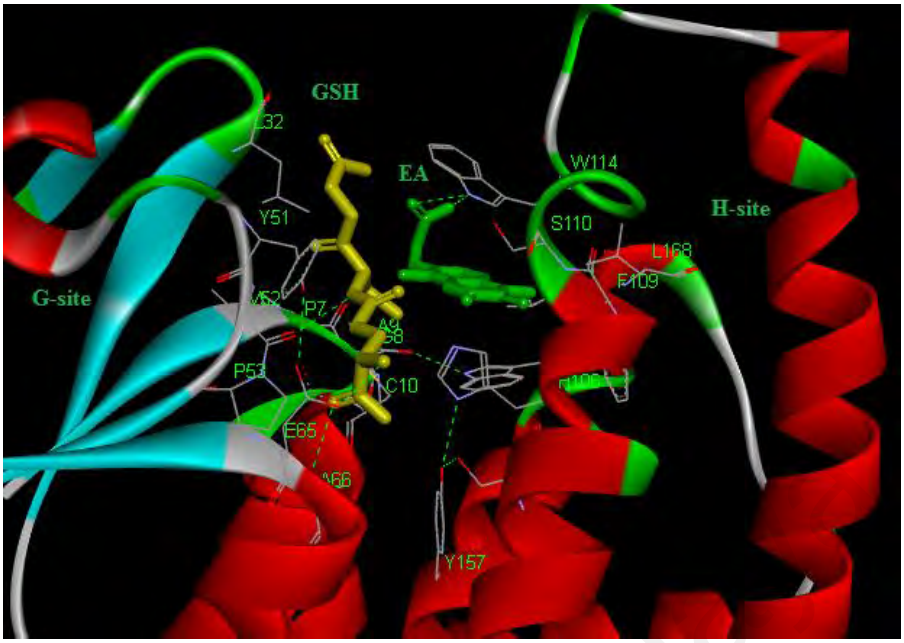

Figure 4.14: Predicted docking orientation of the lowest docking energy conformation of ethacrynic acid to the K107T mutant binding pocket. The co-substrate is shown in yellow while the ethacrynic acid in ball and stick presentations. The green dash lines represent the hydrogen bondings. The residue side chains represent the amino acids involve in the catalysis.

4.9 Protein expression and purification of KKSG6

Both the KKSG6 wild type and mutants were expressed in BL21$^{(star)}$(DE3) competent cells as described in the methodology section. The protein was purified by fast protein liquid chromatography (FPLC) and the purity was judged on SDS-PAGE where a single band was obtained (Figures 4.15 and 4.16).

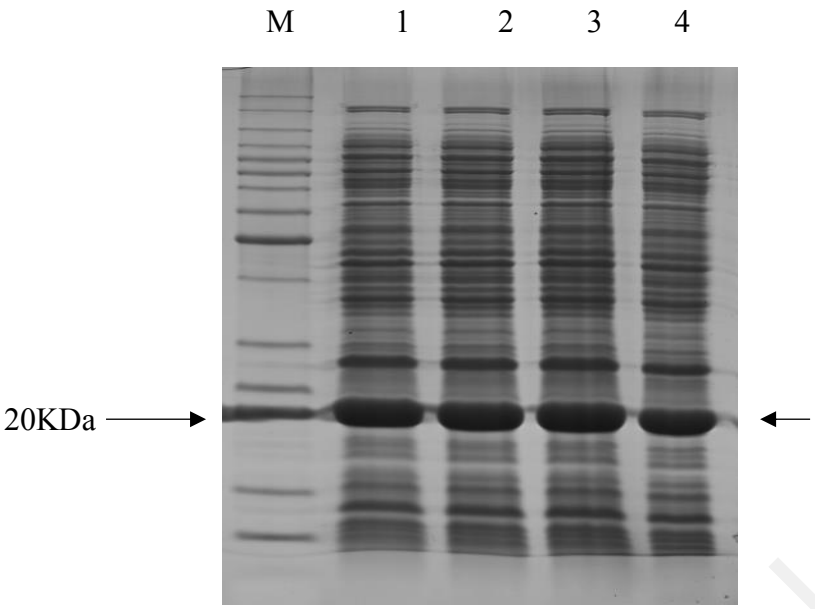

Figure 4.15: SDS-PAGE of (a) Crude protein from the E-coli BL21 (DE3) containing overexpressed wild type and mutant KKSG6. M: Bench mark molecular weight marker. Lane 1: Crude lysate of wild type KKSG6, Lane 2: Crude lysate of C10F, Lane 3: Crude lysate of K107T, Lane 4: Crude lysate of A180P. The arrow indicates the expected protein size (22 kDa) of the overexpressed recombinant wild type and mutants KKSG6.

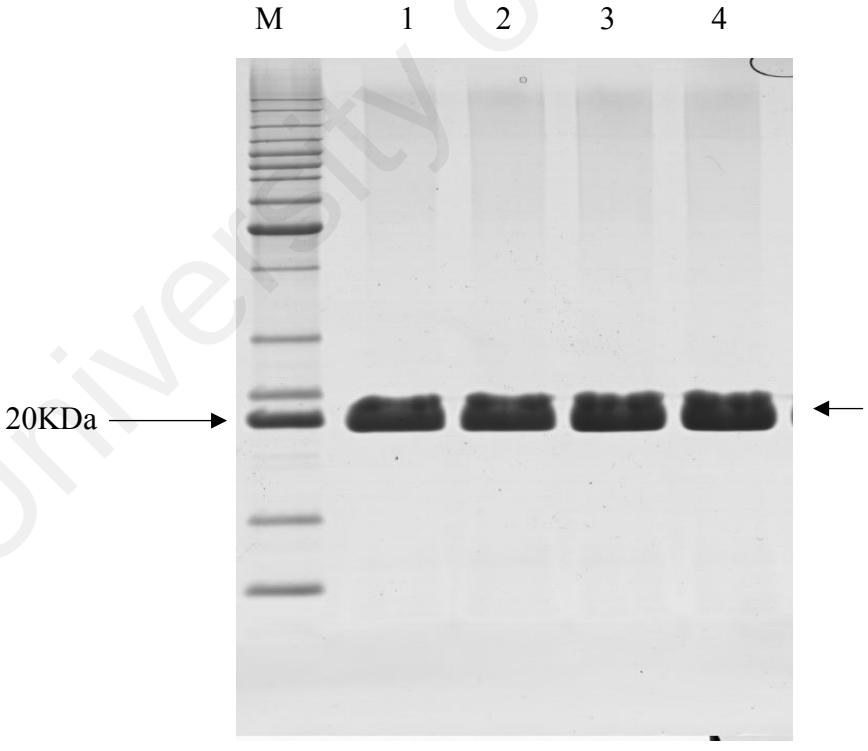

Figure 4.16: SDS-PAGE of Purified recombinant KKSG6 (1) wild type (2) C10F (3) K107T (4) A180P. The arrow indicates the expected protein size (22 kDa) of the purified recombinant wild type and mutant KKSG6.

4.10 Substrate specificity of wild type and mutant KKSG6

In order to determine the substrate specificity of the enzyme, a range of known GST substrates was used. The result of the specific activities of the recombinant wild type and mutant (C10F, K107T, and A180P) KKSG6 enzyme were presented in Table 4.4. KKSG6 displayed GST activity toward CDNB, ethacrynic acid (EA), hydrogen peroxide and cumene hydroperoxide (Table 4.4). Wild type (WT) KKSG6 displayed highest activity toward CDNB 0.78±0.14 μmol/min/mg. C10F and A180P mutants all displayed a respective increase of 1.18-fold and 1.35-fold toward CDNB when compared with the wild type. In contrast, K107T mutant showed a statistically significant 3.47-fold decrease in activity toward CDNB when compared with the wild type. The activity of wild type KKSG6 using ethacrynic acid as substrate was found to be (0.10±0.01 μmol/min/mg). Unlike in CDNB, all the three mutants (C10F, K107T, and A180P) were found to show increased catalytic activity with respect to ethacrynic acid. While C10F and A180P mutants were found to show 1.26-fold and 1.29-fold, increases respectively, the K107T mutant was found to show a statistically significant 2.25-fold increased catalytic activity toward ethacrynic acid compared with the wild type. We tried to investigate the reason for the increased catalytic activity of K107T mutant toward ethacrynic acid by molecular docking. From (Figure 4.15) of the molecular docking result, it appeared that when K107 is mutated to Thr, the ethacrynic acid changed its primary binding site from K107 in the wild type to W114 in the K107T mutant (Figure 4.10). This suggested that while the change in the binding site might preferentially favor ethacrynic acid, at the same time it appeared to have disrupted the proper orientation of other substrates leading to decrease in the activity of the enzyme.

The peroxidase activities of the wild type KKSG6 toward hydrogen peroxide and cumene hydroperoxide were found to be 0.10 ± 0.002 μmol/min/mg and 0.09±0.005

μmol/min/mg respectively. While both C10F and A180P did not show any significant changes in the peroxidase activities against hydrogen peroxide and cumene hydroperoxide, K107T showed statistically significant decreases of 2.72-fold and 2.68-fold, respectively, compared with the wild type.

Table 4.4: Specific activities of wild type KKSG6 and mutants (C10F, K107T, and A180P) toward various substrates. Data are mean ± S.D of at least three independent determinations. ND = not detected.

Substrates	**Specific activities (μmol/min/mg)**			
	WT	**C10F**	**K107T**	**A180P**
1-chloro-2,4-dinitro benzene (CDNB)	0.78±0.1	0.92±0.01	0.225 ±0.06	1.06± 0.12
Ethacrynic acid	0.10±0.01	0.12±0.02	0.218 ±0.05	0.13 ±0.012
Hydrogen peroxide (H_2O_2)	0.09 ± 0.02	0.10±0.04	0.04±0.001	0.09 ±0.006
Cumene hydroperoxide (CuOOH)	0.09±0.005	0.099±0.08	0.03 ±0.003	0.08 ±0.007
p-nitrobenzyl chloride (NBC)	ND	ND	ND	ND
1,2-dichloro-4-nitrobenzene (DCNB)	ND	ND	ND	ND
Trans-2-hexenal	ND	ND	ND	ND
Trans-2-octenal	ND	ND	ND	ND
Hexa-2,4-dienal	ND	ND	ND	ND
Trans-4-phenyl-butane-2-one	ND	ND	ND	ND

4.11 Kinetic properties of KKSG6 using CDNB and GSH as substrates

The results of the kinetic studies of the wild type and mutants KKSG6 using CDNB and GSH as substrates are presented in (Table 4.5). We examined the changes that might occur to the kinetic parameters of KKSG6 when Cys10 is mutated to Phe. Mutation of Cys10 to Phe had resulted in 1.16-fold and 1.51-fold increase in the K_m toward CDNB and GSH respectively, when compared with wild type. The increase in K_m signifies a decrease in the affinity of both the substrates toward KKSG6 and this had resulted in 1.15 and 2.13 and, 2.23 and 3.95 folds, increase in the V_{max} and k_{cat} of the

enzyme toward CDNB and GSH respectively. The catalytic efficiency of the C10F mutant was also found to increase by 1.80-fold and 1.75-fold for CDNB and GSH, respectively, when compared with the wild type. When Lys 107 was mutated to Thr, the K_m for the CDNB was found to slightly increase by 1.08-fold while that of GSH was found to decrease by 1.35-fold. Even though the mutation did not abrogate the activity of the enzyme toward CDNB, however, it does decrease the V_{max} and k_{cat} of both CDNB and GSH by 1.56 and 1.07 and, 1.50 and 1.19 folds respectively. The catalytic efficiency of the K107T mutant toward CDNB and GSH was also found to decrease by 1.65- and 1.34-fold respectively. Alanine 180 even though not strictly conserved in all BphKs, however, mutation of Ala 180 to Pro in KKSG6 had resulted in 1.13- and 1.18-fold increase in the K_m of the protein toward CDNB and GSH respectively, when compared with wild type. The V_{max} and k_{cat} of the protein also increased by 1.21 and 2.03, and 2.02 and 3.83-folds for CDNB and GSH respectively. The mutation was found to affect the catalytic efficiency as there was an increase of 1.69- and 2.13-fold for the CDNB and GSH respectively.

Considering the unexpected increase in specific activity that was observed in the K107T mutant with respect to ethacrynic acid. We tried to examine the kinetic behavior of the enzyme using ethacrynic acid and GSH as substrates and the result is presented in (Table 4.6). The result of the kinetic studies showed that many of the kinetic parameters were affected by the mutation of K107T. The kinetic parameters for ethacrynic acid showed an increase of 1.45, 1.63 and 1.42-fold for K_m, V_{max}, and k_{cat} respectively. However, the catalytic efficiency of the wild type and mutant toward ethacrynic acid did not show any significant change. In GSH, the kinetic parameters showed a general increase of 1.42, 1.81, 2.18, and 1.52-fold in K_m, V_{max}, k_{cat} and k_{cat}/K_m respectively. The changes observed in the kinetic parameters of KKSG6 toward ethacrynic acid further

corroborates with the earlier increase observed in specific activity and the change in the orientation of the substrate that was observed in molecular docking studies.

Table 4.5: Kinetic parameters of wild type and mutants KKSG6 using CDNB and GSH as substrates. Data are mean ± S.D of at least three independent determinations.

Enzyme	CDNB				GSH			
	K_m (mM)	V_{max} (mM. min^{-1})	k_{cat} (min^{-1})	$k_{cat/Km}$ ($min^{-1}.mM^{-1}$)	K_m (mM)	V_{max} (mM.min^{-1})	k_{cat} (min^{-1})	$k_{cat/Km}$ ($min^{-1}.mM^{-1}$)
WT	2.58 ± 0.14	0.12 ± 0.006	46.81 ± 5.6	19.30 ± 3.08	0.92 ± 0.14	0.03 ± 0.005	12.30 ± 3.08	20.35 ± 0.88
C10F	3.00 ± 0.07	0.14 ± 0.004	104.22 ± 8.0	34.75 ± 1.69	1.38 ± 0.18	0.07 ± 0.01	48.58 ± 3.19	35.62 ± 6.80
K107T	2.79 ± 0.14	0.08 ± 0.004	31.17 ± 1.08	11.66 ± 1.59	0.68 ± 0.04	0.03 ± 0.002	10.30 ± 1.53	15.22 ± 3.10
A180P	2.92 ± 0.13	0.15 ± 0.01	94.56 ± 6.81	32.52 ± 1.05	1.08 ± 0.001	0.07 ± 0.01	47.08 ± 1.63	43.39 ± 1.53

Table 4.6: Kinetic constants for the wild type KKSG6 and mutant (K107T) using ethacrynic (EA) acid as substrate

Enzyme	EA				GSH			
	K_m (mM)	V_{max} (mM.min^{-1})	k_{cat} (min^{-1})	$k_{cat/Km}$ ($min^{-1}.mM^{-1}$)	K_m (mM)	V_{max} (mM. min^{-1})	k_{cat} (min^{-1})	$k_{cat/Km}$($min^{-1}.mM^{-1}$)
WT	0.92 ± 0.12	0.03 ± 0.002	20.04 ± 2.1	21.90 ± 2.93	0.72 ±0.11	0.03 ±0.003	10.49 ±2.08	14.20 ±2.05
K107T	1.34 ± 0.09	0.04 ± 0.001	28.42 ± 2.4	21.23± 0.43	1.03 ±0.80	0.05 ±0.005	22.87 ±3.78	21.56 ±3.48

4.12 Molecular docking study of KKSG6 and organochlorine compounds

4.12.1 Monochlorobenzoates

Glutathione S-transferases contained two binding sites; a highly conserved glutathione binding site known as G-site located at the C-terminal and which spans about 1-70 amino acids, and a more variable substrate binding site located at the N-terminal which spans approximately 90-200 amino acids (Brennan et al., 2009). Molecular docking study was performed in order to predict the possibility and the nature of the interaction of KKSG6 and various organochlorine substrates. A blind docking was set up because of the high variability in the G-site of GSTs. Analysis of the docking result with various substrates reveals the presence of several amino acids both in the G and H-site that play roles in the binding of co-substrate (GSH) and other chlorinated substrates. From the molecular docking result, the KKSG6 was found to bind to the GSH molecule and the substrates 2-Chlorobenzoate, 3-Chlorobenzoate, 4- Chlorobenzoate in the pocket occupied by the residues A9, C10, L32, Y51, V52, P53, E65, A66, S102, H106, K107, W112, and L113.

Cluster analysis of the docked result in 2-Chlorobenzoate (Figure 4.17) using root mean square tolerance (RMSD) of 2Å reveal the presence of three different conformations. The lowest minimum binding energy obtained was -5.83 kJ mol^{-1} which occurred in the 14^{th} run of the second most populated cluster containing 46 members. In addition, P111 was also found to be among the amino acids in the binding pocket during the interaction with 2-Chlorobenzoate. In 3-Chlorobenzoate (Figure 4.18), the cluster analysis revealed four different conformations with the lowest minimum binding energy of -6.01 kJ mol^{-1} obtained in the 24^{th} run of the most populated cluster containing 59 members. Cluster analysis in 4-chlorobenzoate revealed the presence of three different conformations (Figure 4.19). The lowest minimum binding energy obtained was -6.43 kJ mol^{-1} which occur in the second most populated cluster containing 48 members. In

addition, the binding pocket in the docked result of KKSG6 with 4-chlorobenzoate also contains P111.

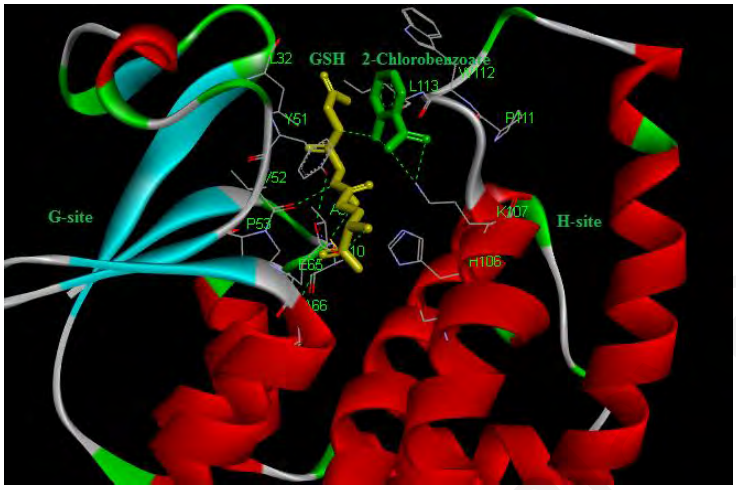

Figure 4.17: Predicted docking orientation of the lowest docking energy conformation of 2-chlorobenzoate to the binding pocket of KKSG6. The co-substrate is shown in yellow while the 2-chlorobenzoate is in green ball and stick presentations. The green dash lines represent the hydrogen bondings. The residue side chains represent the amino acids involve in the catalysis.

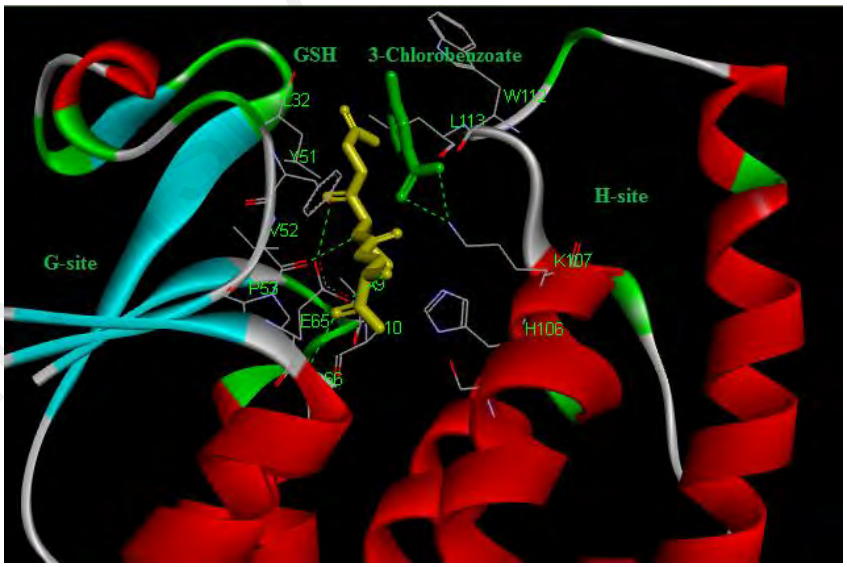

Figure 4.18: Predicted docking orientation of the lowest docking energy conformation of 3-chlorobenzoate to the binding pocket of KKSG6. The co-substrate is shown in yellow while the 3-chlorobenzoate is in green ball and stick presentations. The green dash lines represent the hydrogen bondings. The residue side chains represent the amino acids involve in the catalysis.

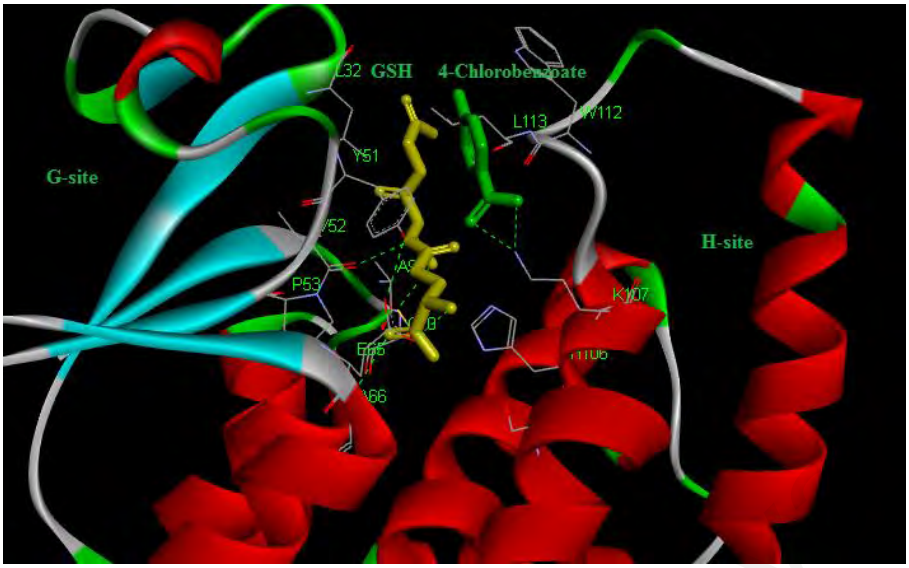

Figure 4.19: Predicted docking orientation of the lowest docking energy conformation of 4-chlorobenzoate to the binding pocket of KKSG6. The co-substrate is shown in yellow while the 4-chlorobenzoate is in green ball and stick presentation. The green dash lines represent the hydrogen bondings. The green dash lines represent the hydrogen bondings. The residue side chains represent the amino acids involve in the catalysis.

4.12.2 Dichlorobenzoates

Cluster analysis of the di-chlorobenzoate derivatives also revealed the same amino acids in the binding pocket as was observed in monochlorobenzoates derivatives (A9, C10, L32, Y51, V52, P53, E65, A66, S102, H106, K107, W112, and L113.). In 2,4-Dichlorobenzoate (Figure 4.20), cluster analysis revealed the presence of three different conformations. The lowest minimum binding energy obtained was -6.25 kJ mol^{-1} which occurred in the 71st run of the least populated cluster containing 12 members. Analysis of the cluster in 2,5-Dichlorobenzoate (Figure 4.21) showed four different conformations. The minimum binding energy obtained was -6.34 kJ mol^{-1} which occurred in the 81st run of the second most populated cluster containing 44 members. 2,6-Dichlorobenzoates (Figure 4.23) was also found to have contained four clusters during the cluster analysis. The minimum binding energy obtained here was -5.87 kJ mol^{-1} which occurred in the 96th

run of the most populated cluster containing 70 members. In addition to the hydrophobic interactions, at least two hydrogen bonds were predicted between the oxygen atom of all the substrates above and K107 of KKSG6. The validity of the interactions was further confirmed in the chloride ion detection assay.

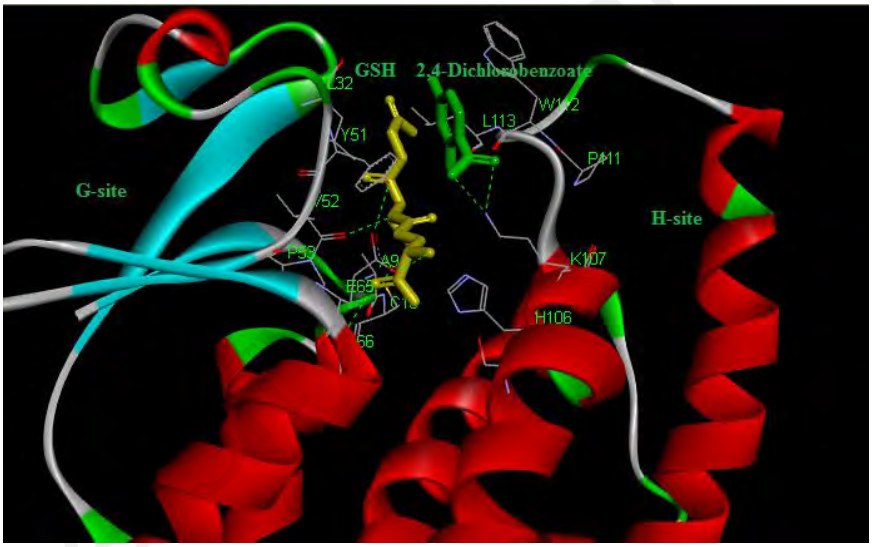

Figure 4.20: Predicted docking orientation of the lowest docking energy conformation of 2,4-dichlorobenzoate to the binding pocket of KKSG6. The co-substrate is shown in yellow ball and stick presentation. The green dash lines represent the hydrogen bondings.

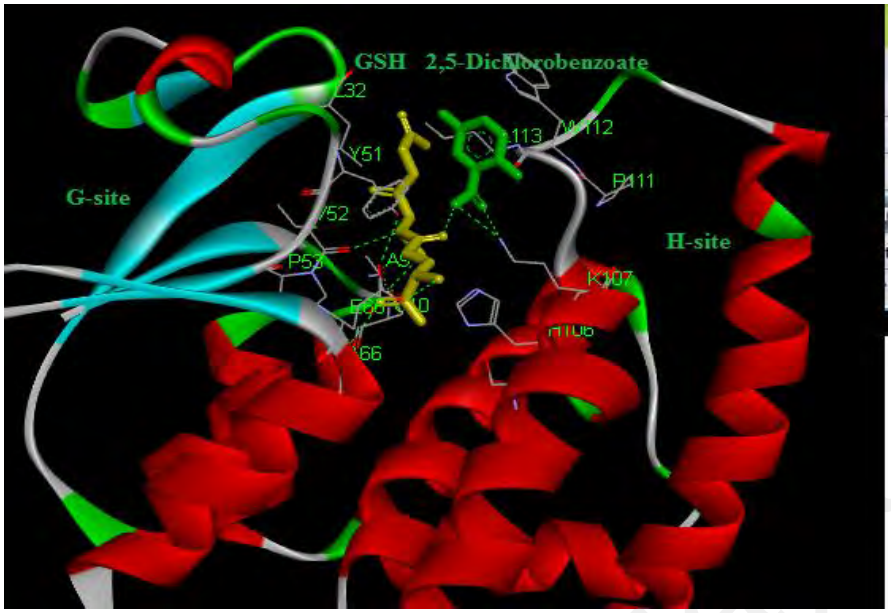

Figure 4.21: Predicted docking orientation of the lowest docking energy conformation of 2,5-dichlorobenzoate to the binding pocket of KKSG6. The co-substrate is shown in yellow while the 2,5-dichlorobenzoate is in green ball and stick presentations. The green dash lines represent the hydrogen bondings. The residue side chains represent the amino acids involve in the catalysis

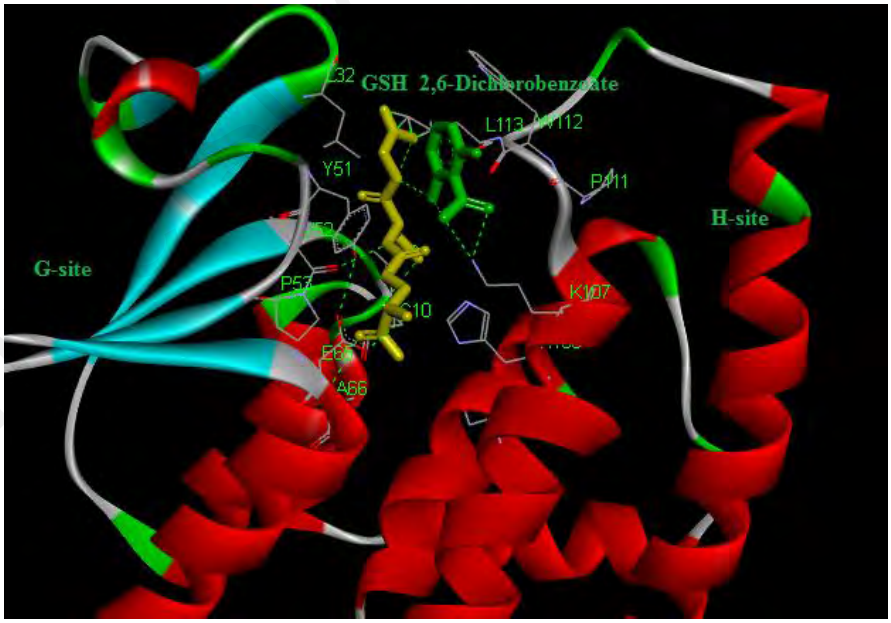

Figure 4.22: Predicted docking orientation of the lowest docking energy conformation of 2,6-chlorobenzoate to the binding pocket of KKSG6. The co-substrate is shown in yellow while the 2,6-chlorobenzoate is in green ball and stick presentations. The green dash lines represent the hydrogen bondings. The residue side chains represent the amino acids involve in the catalysis.

4.12.3 Organochlorine pesticides (DDT, Endosulfan, and Permethrin)

Analysis of the docked conformations in the substrates; DDT, Endosulfan, and permethrin revealed some differences compared to what was observed in mono and di-chlorobenzoate derivatives. Analysis of the docked result in endosulfan (Figure 4.24) showed that amino acids; A9, C10, L32, Y51, V52, P53, E65, A66, S102, H106, and K107 were found to occupy the binding pocket of KKSG6 and the substrate Endosulfan. Cluster analysis of the docked conformation showed that it contained seven different conformations. The lowest minimum binding energy obtained was -9.92 Kj mol^{-1} which occurred in the 36^{th} run of the most populated cluster containing 85 members. However, in both DDT and permethrin (Figures 4.23 and 4.25), respectively, analysis of the docked conformations showed that in addition to the amino acids mentioned above that occupied their binding pockets, F109, W114, W164, L167, and L168 were also found to be present. Cluster analysis of the docked conformations in DDT showed that it contained three different conformations. The lowest minimum binding energy obtained was -8.99 kJ mol^{-1} which occur in the 96^{th} run of the second most populated cluster containing 23 members. In permethrin, cluster analysis revealed the presence of 48 different conformations. The lowest minimum binding energy obtained was -10.08 kJ mol^{-1} which occurred in the most populated cluster containing seven members. However, unlike in chlorobenzoates, the docked conformations in DDT and Permethrin did not show any hydrogen bonding with the surrounding amino acids, rather, the interaction was found to be largely mediated by hydrophobic interactions. In endosulfan, at least three hydrogen bondings were predicted between the co-substrate GSH and the ligand oxygen.

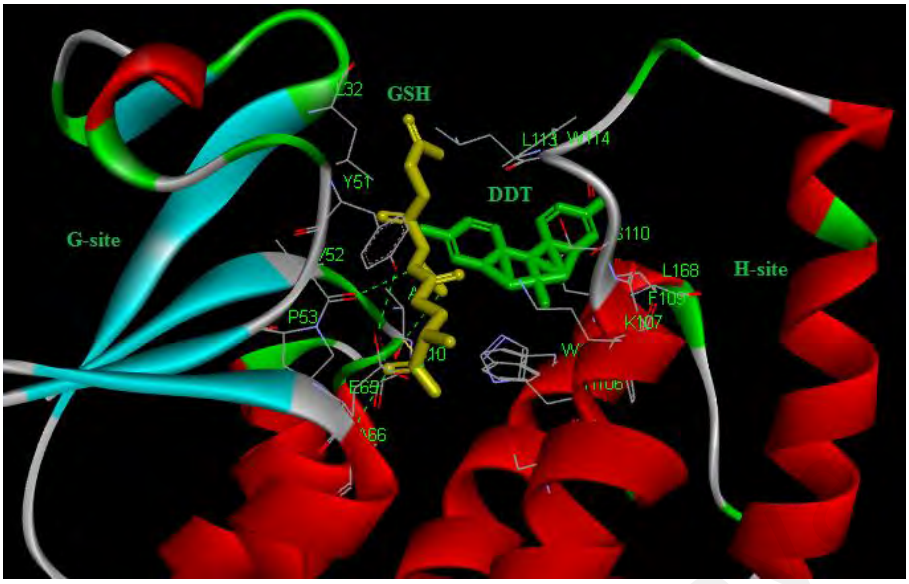

Figure 4.23: Predicted docking orientation of the lowest docking energy conformation of DDT to the binding pocket of KKSG6. The co-substrate is shown in yellow while the DDT is in green ball and stick presentations. The green dash lines represent the hydrogen bondings. The residue side chains represent the amino acids involve in the catalysis.

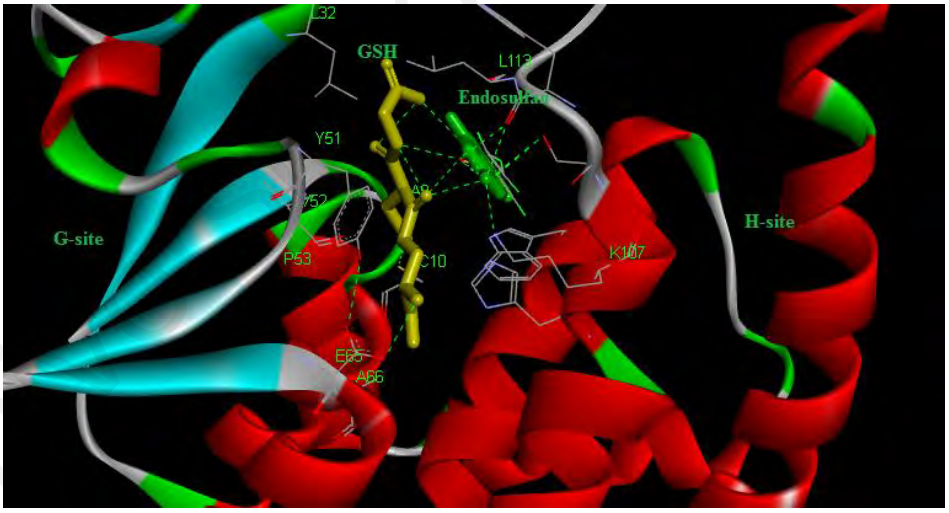

Figure 4.24: Predicted docking orientation of the lowest docking energy conformation of endosulfan to the binding pocket of KKSG6. The co-substrate is shown in yellow while the endosulfan is in green ball and stick presentations. The green dash lines represent the hydrogen bondings. The residue side chains represent the amino acids involve in the catalysis.

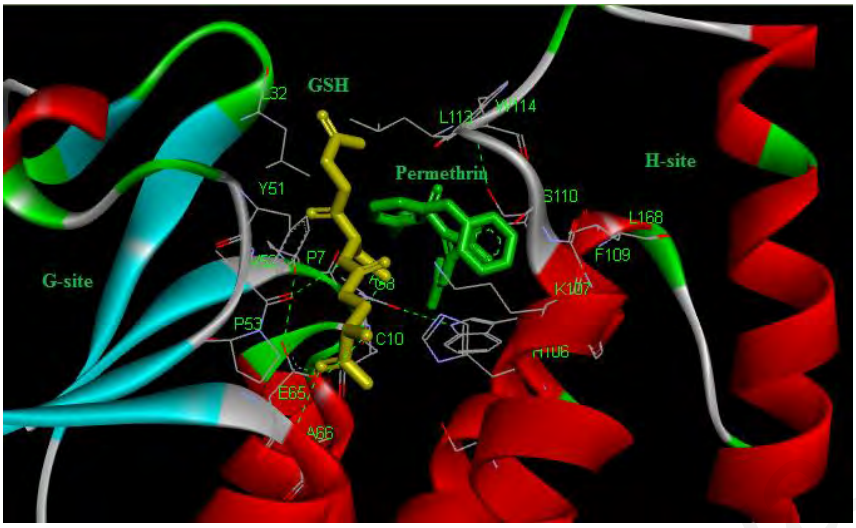

Figure 4.25: Predicted docking orientation of the lowest docking energy conformation of permethrin to the binding pocket of KKSG6. The co-substrate is shown in yellow while the permethrin is in green ball and stick presentation. The green dash lines represent the hydrogen bondings. The residue side chains represent the amino acids involve in the catalysis.

4.13 Dehalogenation function of KKSG6 using mono and di-chlorobenzoates as substrates

Chloride ion detection assay was used to measure the activity of purified wild type and mutants (C10F and K107T, A180P) KKSG6 towards both mono and di-chlorinated benzoate substrates. Moreover, the model substrate for GSTs, CDNB, was included for comparison purposes. The activity of KKSG6 toward CDNB and mono-chlorobenzoates; 2CLB, 3CLB, and 4CLB is shown (Figure 4.26). The activity of KKSG6 towards CDNB as measured by chloride ion detection showed that the wild type had the activity of 532.5 ± 4.51 (μM/mg protein). A statistically significant increase of 1.32-fold in activity was observed in the C10F mutant ($P < 0.0042$) while for the K107T mutant, a statistically significant 1.67-fold decrease was observed ($P < 0.0001$) compared with wild type. For A180P mutant, a statistically significant 1.53-fold increase in the activity toward CDNB was observed ($P < 0.0011$). For 2-chlorobenzoate, the mutants C10F and A180P both displayed a statistically significant 1.15-fold ($P < 0.001$) and 1.47-fold ($P < 0.0001$)

increase in activity while K107T showed a statistically significant 2.12-fold ($P < 0.0001$) decrease in activity compared with wild type. Chloride ion detection assay using 3-chlorobenzoate as substrate showed that all the mutants (C10F, K107T, and A180P) showed a statistically significant 1.49-fold ($P < 0.002$), 2.29-fold ($P < 0.0001$), 1.77-fold ($P < 0.0001$), respectively, increase towards 3-chlorobenzoate when compared with the wild type. In the case of 4-chlorobenzoate, wild type displayed activity of 653.6 ± 14.2 μM/mg protein. However, C10F and A180P mutants displayed 705.1 ± 11.2 and 797.2 ± 21.7 (μM/mg protein) representing a (1.07-fold and 1.22-fold) respectively increase in activity compared with the wild type. Surprisingly, the K107T mutant showed zero activity against 4-chlorobenzoate. We tried to examine the possible reason for the total loss of activity against 4-chlorobenzoate by the K107T mutant through the molecular docking study. The molecular docking studies using the wild type (figure 4.27) and mutant K107T (Figure 4.28) revealed a productive and unproductive (scattered binding) of 4-Chlorobenzoate to the binding site of the wild type and the mutant, respectively. This suggests that with regards to 4-chlorobenzoate substrate, Lysine at position 107 is the preferred amino acid compared to threonine. The scattered binding of the 4-Chlorobenzoate to the K107T mutant explained the total loss in activity of the mutant and further suggest the importance of Lys107 in the binding of the substrates to KKSG6.

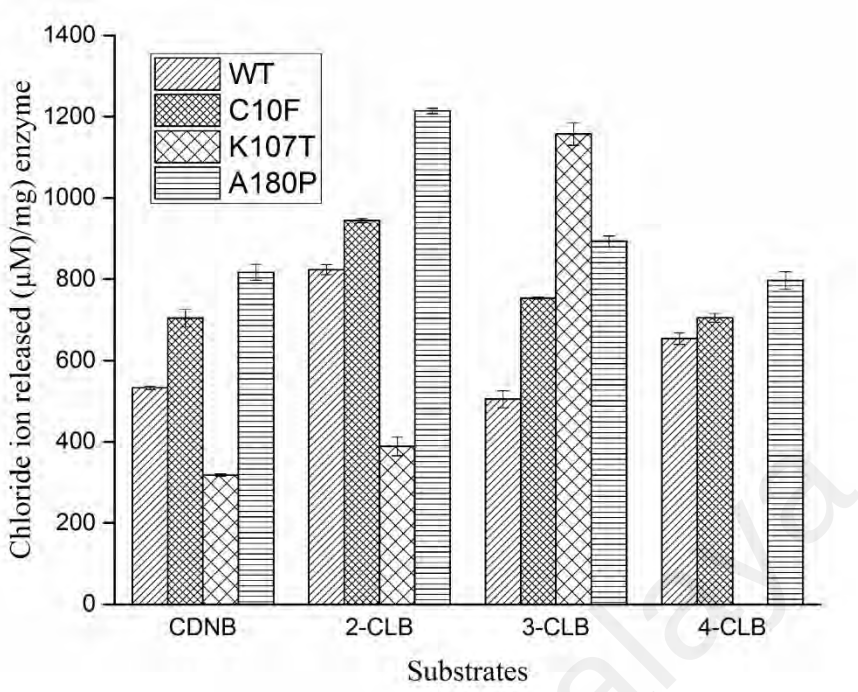

Figure 4.26: Chloride ion detection assay for the substrates: CDNB, (2-CLB) 2-chlorobenzoate, (3-CLB) 3-chlorobenzoate and (4-CLB) 4-chlorobenzoate. The results are mean ± S.D of three independent determinations.

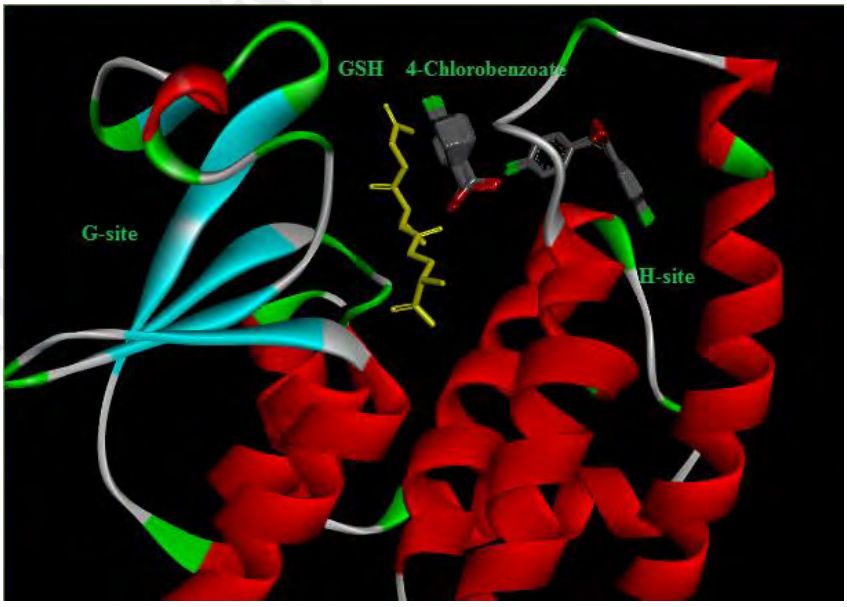

Figure 4.27: Predicted docking orientation of productive binding of 4-chlorobenzoate to the binding pocket of wild type KKSG6. The co-substrate GSH is shown in yellow while the 4-chlorobenzoate is in green ball and stick presentations. The residue side chains represent the amino acids involve in the catalysis.

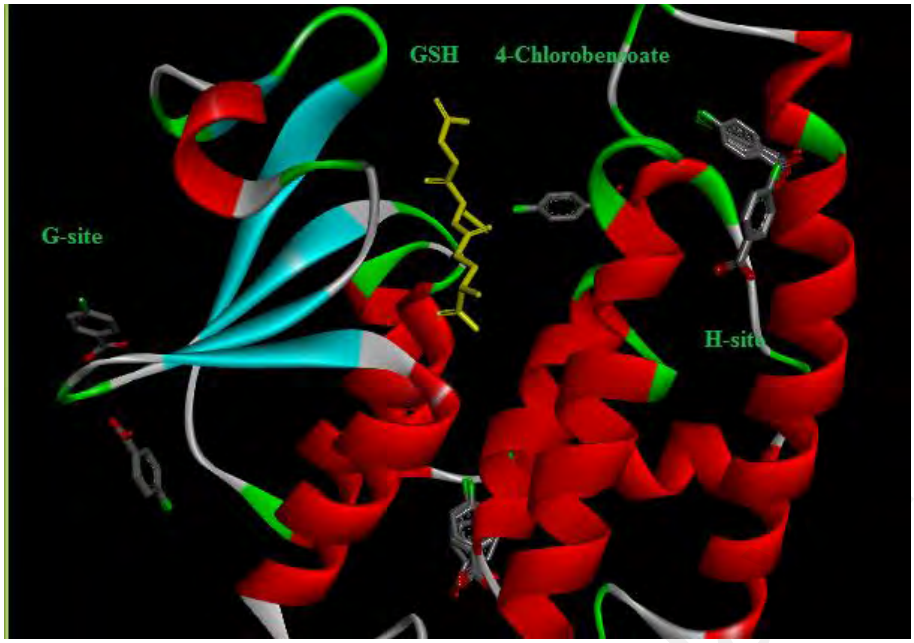

Figure 4.28: Predicted docking orientation of unproductive binding of 4-chlorobenzoate to the binding pocket of K107T mutant. The co-substrate GSH is shown in yellow while the 4-chlorobenzoate is in green ball and stick presentation. The residue side chains represent the amino acids involve in the catalysis.

Di-chlorobenzoate derivatives were found to display low activity compared with the mono-chlorobenzoates counterparts (Figure 4.29). Both the wild type and mutants KKSG6 showed activity with 2, 4-dichlorobenzoate. C10F and K107T mutants showed 1.24-fold and a statistically significant 5.0-fold, respectively, increase in activity compared with wild type. However, in the case of 2, 5 and 2,6-dichlorobenzoates, only K107T mutant showed a little activity of 0.09 ± 0.01 and 0.03 ± 0.003 μM/mg respectively. This showed that the KKSG6 was more specific to the mono chlorinated benzoates compared with the di-chlorobenzoate counterparts. However, the overall dechlorination activity of purified KKSG6 showed that it was a better candidate as compared with BphK of *Burkholderia xenovorans* LB400. BphK LB400 was shown to be able to release chloride ions from the substrates in the unit of nmol/mg of crude protein extract as compared with mmol/mg of purified protein displayed by KKSG6.

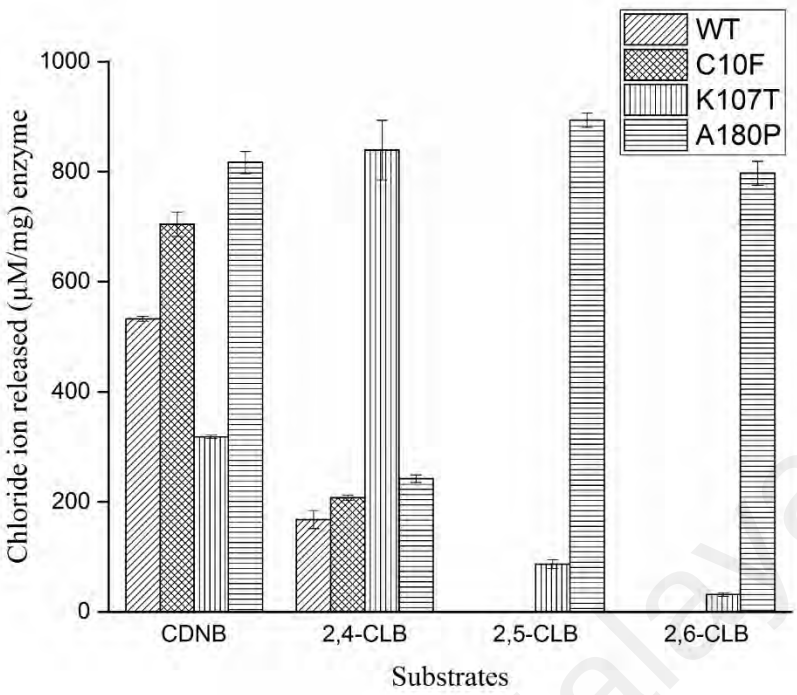

Figure 4.29: Chloride ion detection assay for the substrates CDNB, 2,4-dichlorobenzoate, 2,5-dichlorobenzoate, and 2,6-dichlorobenzoate. The results are mean ± S.D of three independent determinations.

4.14 Dehalogenation function of KKSG6 using organochlorine pesticides as substrates

To further confirm the interaction of wild type and mutants KKSG6 with organochlorine pesticides (DDT, endosulfan, and permethrin), a chloride ion detection assay was carried out. The GST activity of the wild type KKSG6 as measured by chloride ion detection assay using DDT as a substrate is 81.6 ± 8.5 μM/mg of the purified protein (Figure 4.30). A statistically significant 1.85-fold reduction in the activity was observed in K107T mutant ($P < 0.003$) when compared with the wild type. However, in the case of C10F and A180P mutants, there was no statistically observable change in the activity of these mutants with DDT. In the case of endosulfan, the wild type KKSG6 showed 91.7 ± 12.0 μM/mg protein of chloride ions released (Figure 4.31). Unlike in DDT, the K107T mutant showed a statistically significant 1.46-fold ($P < 0.002$) increase in activity toward endosulfan as compared with the wild type. However, while C10F did not show any

statistically significant increase in catalytic activity, Ala180P mutant showed a statistically significant 1.32-fold ($P < 0.001$) increase in the catalytic activity of the enzyme. Permethrin even though structurally contained less number of chlorine atoms as compared with DDT and endosulfan, however, the compound showed several folds higher activity when compared with DDT and endosulfan (Figure 4.32). The activity of wild type KKSG6 toward permethrin as measured by chloride ion detection assay is 363.01 ± 15.22 μM/mg protein. K107T mutant showed a significant 2.11-fold ($P < 0.001$) decrease in activity while C10F and A180P mutants showed a statistically significant 1.51-fold ($P < 0.0001$) and 1.20 ($P < 0.001$) decreases respectively, increase in the dechlorination activity of the protein when compared with the wild type.

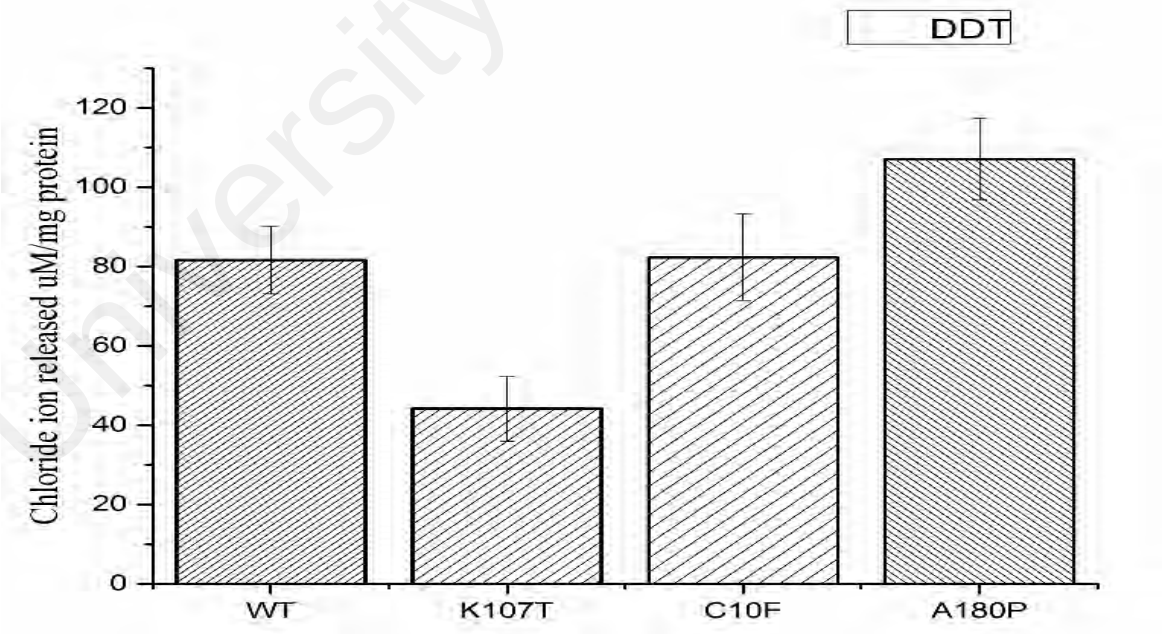

Figure 4.30: Chloride ion detection assay for the substrate DDT. The results are mean ± S.D of three independent determinations.

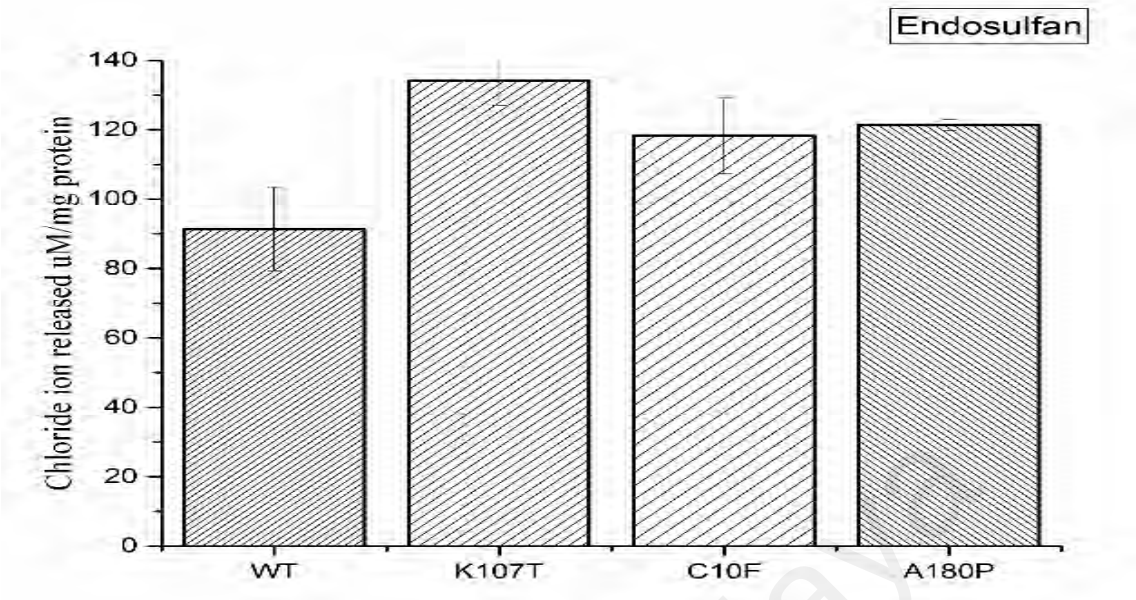

Figure 4.31: Chloride ion detection assay for the substrate Endosulfan. The results are mean ± S.D of three independent determinations.

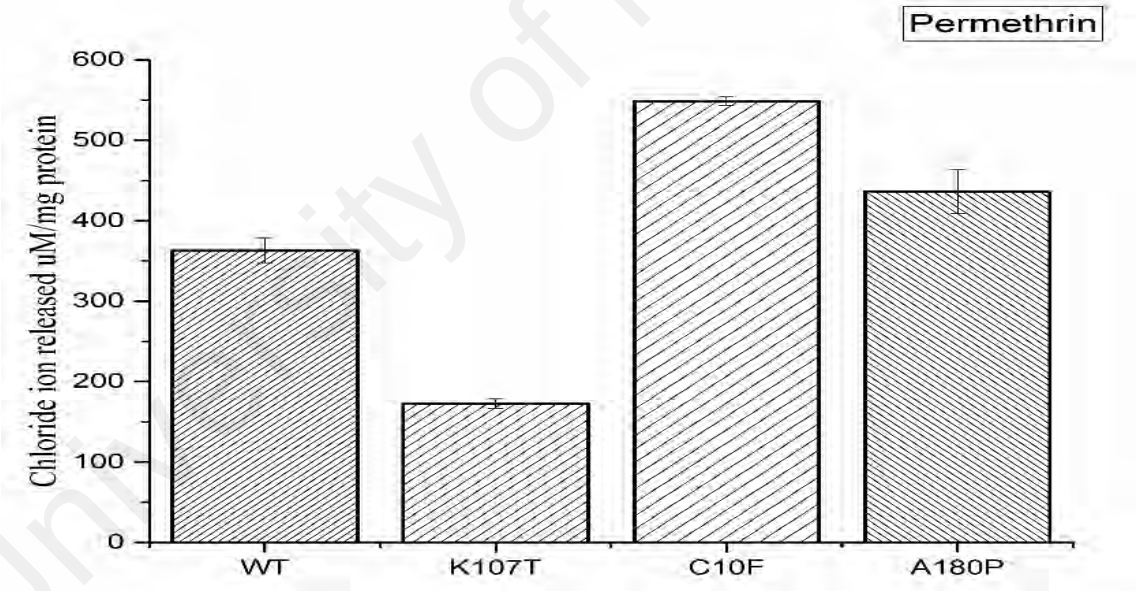

Figure 4.32: Chloride ion detection assay for the substrate permethrin. The results are mean ± S.D of three independent determinations.

4.15 In-Silico analysis of zeta-like glutathione s-transferase from *Acidovorax* sp. KKS102 (KKSG9)

In-silico analysis of GSTs from *Acidovorax* sp. KKS102 revealed the presence of at least eleven putative GSTs. Phylogenetic analysis using representatives from all GST

classes showed that putative sequences (KKSG9 and KKSG7) showed a strong bootstrap value of 94% indicating the possibility of the two being from the same class, however, the two GSTs did not align themselves to any particular class of known GST (Figure 4.3). This suggest that the two GSTs might likely belongs to a new class. However, in order to ascertain the relationship between the known GST classes and KKSG9, another phylogenetic tree was constructed using all known GST classes and only the KKSG9 among the GSTs in *Acidovorax* sp. KKS102 (Figure 4.33). With a bootstrap value of only 46% and still the KKSG9 does not align itself to any particular GST class, this suggest a possibility of new class of GST. Further analysis using sequence alignment showed that KKSG9 contained a motif closely related to that of zeta class GSTs (Figure 4.34). Using NCBI protein blast, the first five hits were found to be dominated by similar genes from *Acidovorax* sp. strains (Figure 4.35). Further sequence alignment analysis of the amino acids from the first five hits of NCBI protein blast and KKSG9 showed that the *Acidovorax* sp. from the first five hits contained a motif that was identical to the one observed in KKSG9 (Figure 4.36). The protein was designated as KKSG9 based on its position (5'-3') in relation to other putative GSTs in the genome and was also selected for further study. KKSG9 displayed low sequence similarity with the representatives of all GSTs, showing the highest similarity of 23.30% with eukaryotic zeta GST from *Capsium annuum*. The protein has an open reading frame of 657 base pairs coding for 219 amino acid residues with predicted molecular weight and isoelectric point (pI) of 24.4 kDa and 6.12 respectively.

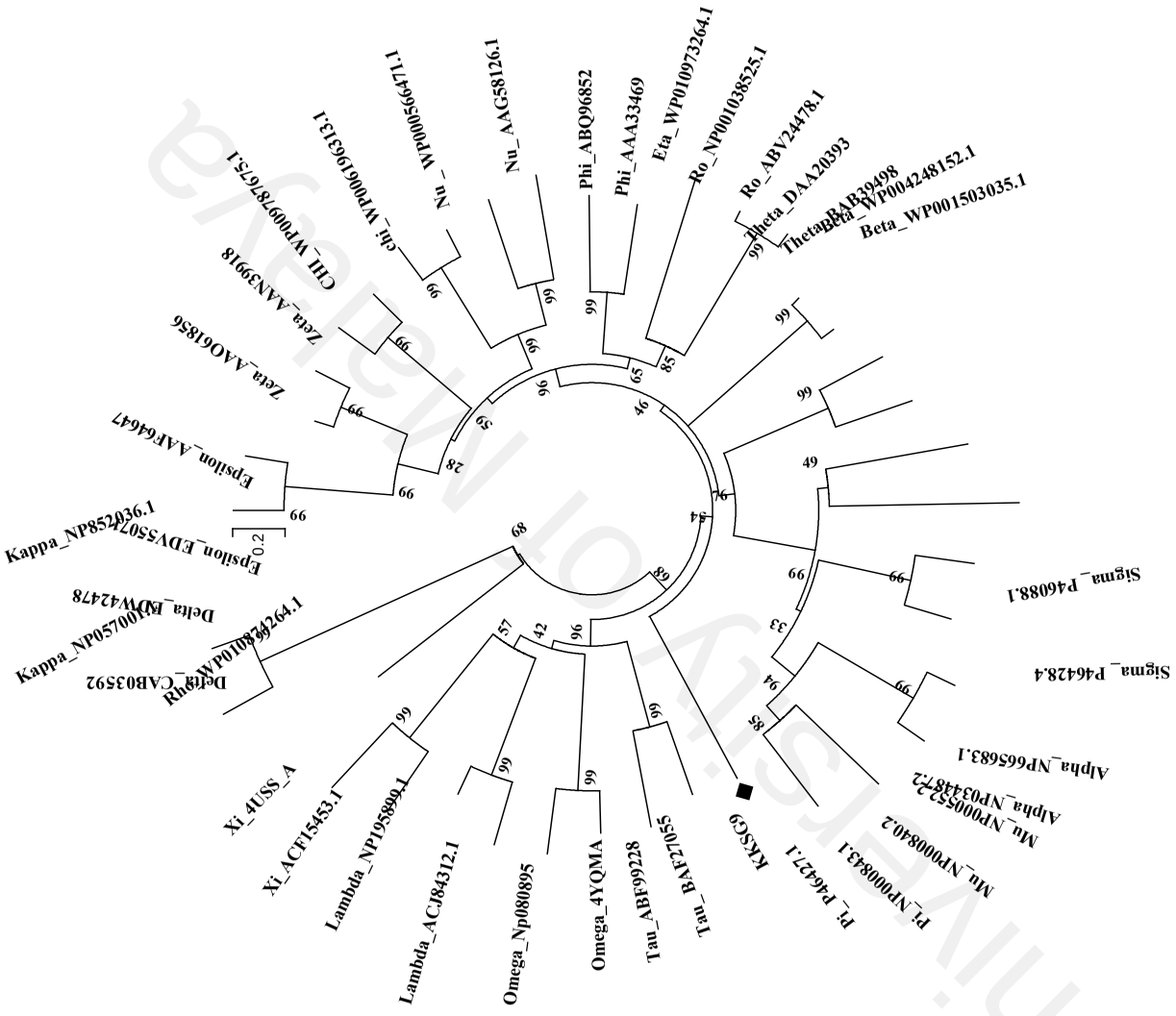

Figure 4.33: Model of the evolutionary relationship of *Acidovorax* sp. KKS102 GSTs. The phylogenetic tree was constructed using the representative from all GST classes. Numbers after the underscore are the NCBI accession numbers. Bold arrows represent KKSG9. NP_852036.1 (*Rattus norvegicus*), NP_057001 (*Homo sapiens*), 4USSA (*Phanerochaete chrysosporium*), NP_195899 (*Arabidopsis thaliana*), ACJ84312(*Medicago truncatula*), NP_080895 (*Mus musculus*), 4YQM_A (*Homo sapiens*), ABF99228 (*Oryza sativa Japonica* Group), P46427 (*Onchocerca volvulus*), NP_000843 (*Homo sapiens*), NP_000840 (*Homo sapiens*), NP_000840 (*Homo sapiens*), NP_000552 (*Homo sapiens*), NP_034487 (*Mus musculus*), NP_665683 (*Homo sapiens*), P46428 (*Anopheles gambiae*), P46088 (*Nototodarus sloanii*), AAN39918 (*Capsicum annuum*), AAO61856 (*Malva pusilla*), AAF64647 (*Drosophila melanogaster*), EDV56071 (*Drosophila erecta*), EDW42478 (*Drosophila sechellia*), CAB03592 (*Anopheles gambiae*), AAA33469 (*Zea mays*), ABQ96852(*Solanum commersonii*), ABV24478 (*Hypophthalmichthys molitrix*), NP_001038525 (*Danio rerio*), BAB39498 (*Homo sapiens*), DAA20393 (*Bos taurus*), WP_001503035 (*Escherichia coli*), WP_004248152 (*Proteu mirabilis*), AAG58126 (*Escherichia coli*), WP_000566471 (*Proteobacteria*), WP_006196313 (*Nodularia spumigena*), WP_009787675 (*Lyngbya* sp. PCC 8106). Bold arrow indicated KKSG9 with its clade emanating from the zeta class GSTs.

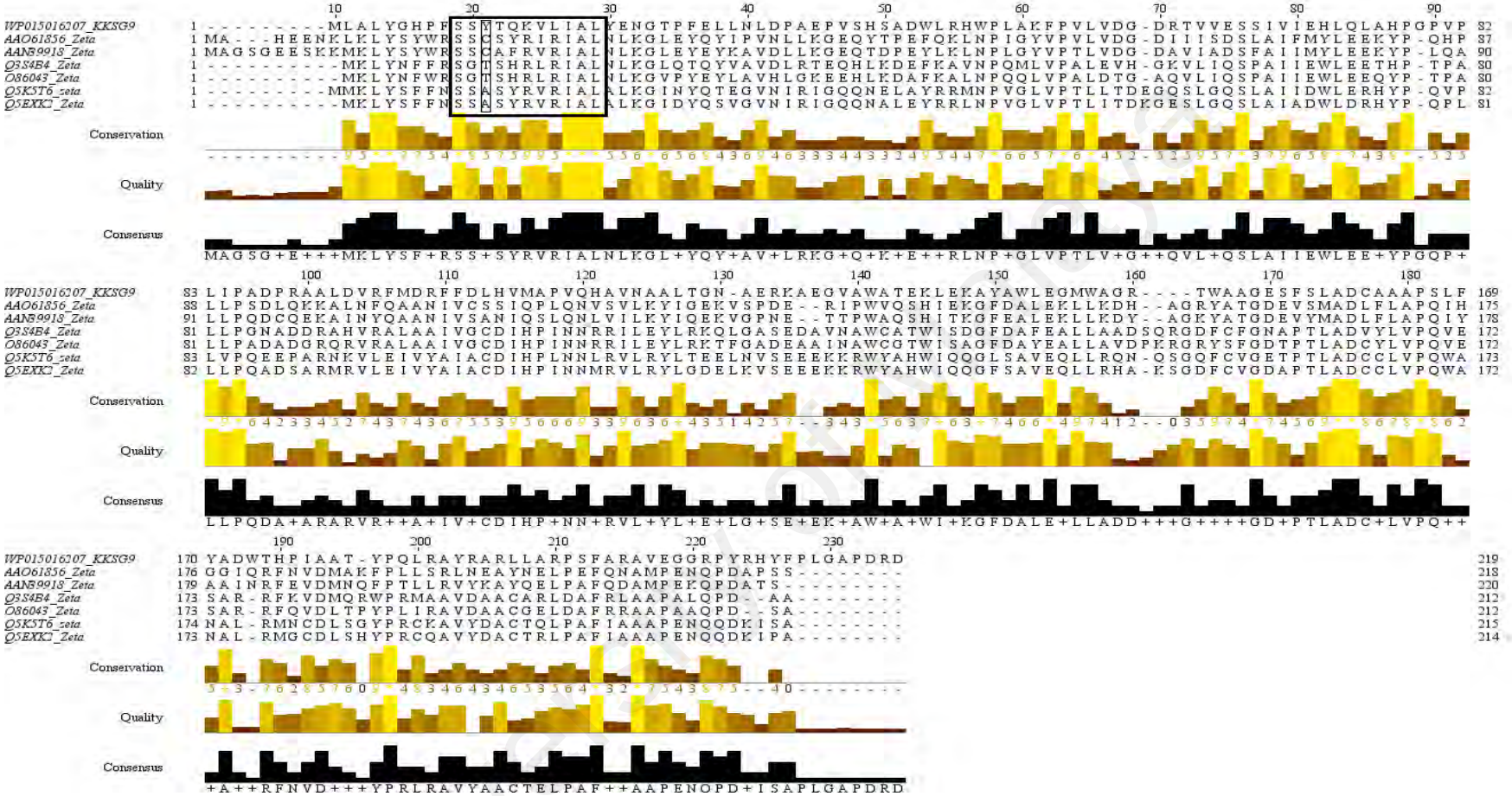

Figure 4.34: Multiple sequence alignment of KKSG9 with representatives from zeta class; WP015016207 is KKSG9 from *Acidovorax* sp. KKS102, AAO61856 is from the eukaryotic *Malva pusilla*, AAN39918 is from eukaryotic *Capsicum annuum*, Q3S4B4 is from *Polaromonas naphthalenivorans* CJ2, O86043 is from *Ralstonia* sp., Q5K5T6 is from *Escherichia coli* and Q5EXK2 is from *Klebsiella pneumonia*. The boxed letters indicated the motif observed in KKSG9 and other zeta class GSTs. The small box inside the motif indicated the variation in amino acid between prokaryotic (dominated by Cys) and eukaryotic (dominated by Ala or Thr) zeta class GSTs.

Sequences producing significant alignments:

Select: All None Selected:0

Alignments Download GenPept Graphics Distance tree of results Multiple alignment

Description	Max score	Total score	Query cover	E value	Ident	Accession
glutathione S-transferase [Acidovorax sp. KKS102]	444	444	100%	6e-158	100%	WP_015016207.1
glutathione S-transferase [Acidovorax sp. SCN 65-28]	442	442	100%	5e-157	99%	ODS79911.1
glutathione S-transferase [Acidovorax delafieldii]	442	442	100%	5e-157	99%	WP_060984870.1
glutathione S-transferase [Acidovorax sp. Root568]	433	433	100%	1e-153	98%	WP_056742938.1
glutathione S-transferase [Acidovorax sp. Root402]	433	433	100%	1e-153	98%	WP_056067934.1
glutathione S-transferase [Acidovorax sp. Root70]	432	432	100%	3e-153	97%	WP_056643847.1
glutathione S-transferase [Burkholderiales bacterium RIFCSPHIGHO2_01_FULL_64_960]	382	382	100%	5e-133	84%	OGA63779.1
glutathione S-transferase [Burkholderiales bacterium GWA2_64_37]	381	381	100%	6e-133	84%	OGA87593.1
glutathione S-transferase [Acidovorax sp. SD340]	380	380	100%	1e-132	84%	WP_055397775.1
glutathione S-transferase [Burkholderiales bacterium RIFCSPHIGHO2_02_FULL_64_19]	380	380	100%	2e-132	84%	OGB07435.1
glutathione S-transferase [Acidovorax sp. SCN 65-108]	377	377	100%	2e-131	84%	ODS62154.1
MULTISPECIES: glutathione S-transferase [Acidovorax]	369	369	100%	3e-128	82%	WP_056411658.1
glutathione S-transferase [Acidovorax sp. RAC01]	341	341	99%	3e-117	81%	WP_069104062.1
glutathione S-transferase [Massilia putida]	335	335	99%	6e-115	78%	WP_075794363.1
glutathione S-transferase [Archangium violaceum]	334	334	99%	2e-114	75%	WP_043390575.1

Figure 4.35: Blast analysis of KKSG9 using NCBI protein blast. The first five hits of the blast analysis were dominated by various strains of *Acidovorax* sp.

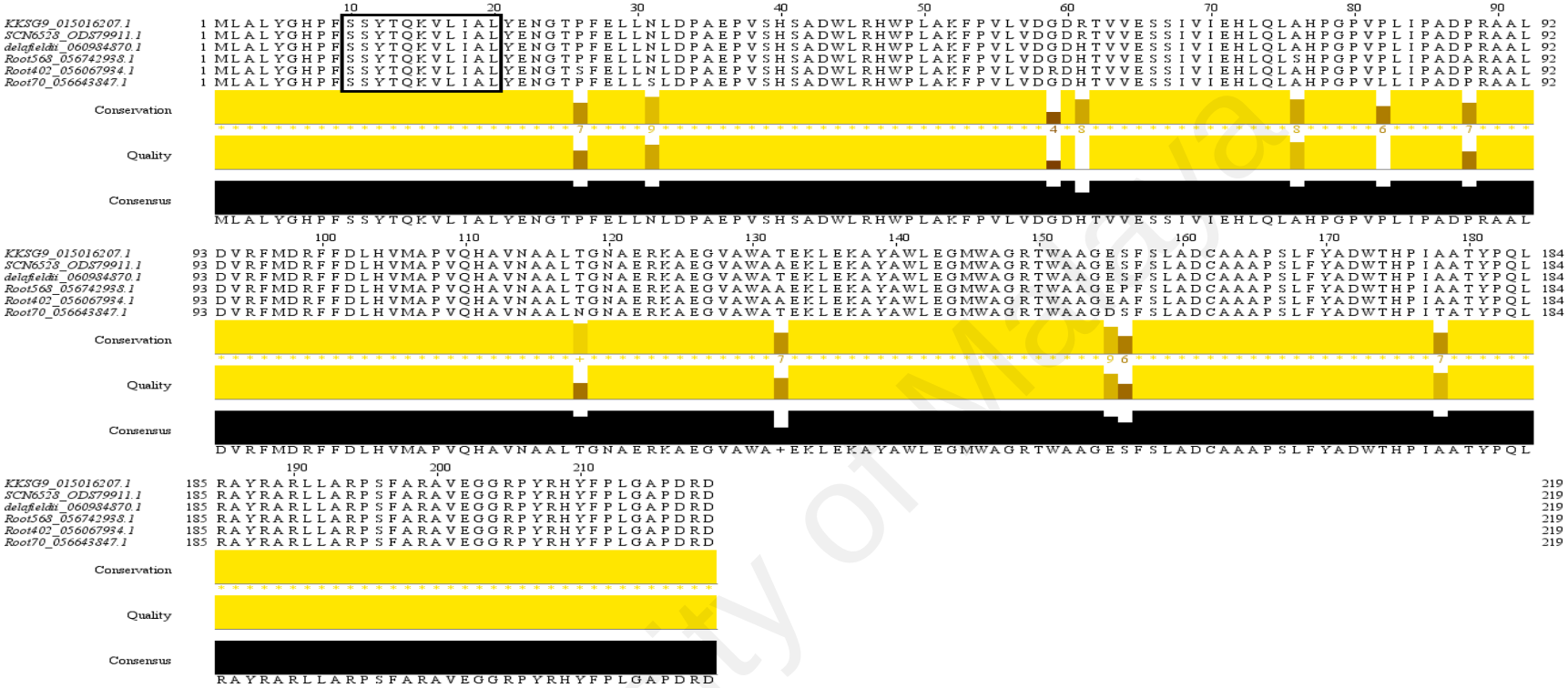

Figure 4.36: Multiple sequence alignment of KKSG9 with the first five hits from blast analysis. Numbers after the underscore are NCBI accession numbers while the first letter indicate the species number of the *Acidovorax* family. The box letters indicate a perfect match of the motif between KKSG9 and putative GSTs from the other *Acidovorax* sp.

4.16 PCR amplification and cloning of KKSG9

A 657 bp of KKSG9 gene was successfully amplified using phusion flash high fidelity polymerase (Thermo-Fisher) and cloned into pET 101 D-TOPO vector as described in the methodology section. The amplicon with the expected 657 base pairs is shown in (Figure 4.37).

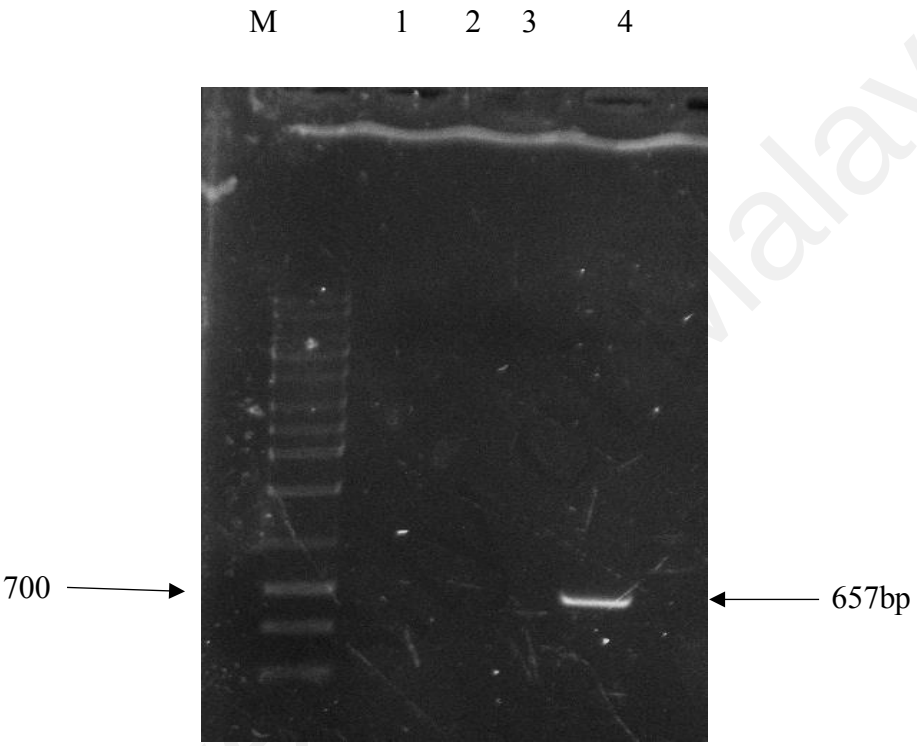

Figure 4.37: Amplified KKSG9 gene from *Acidovorax* sp. KKS102. M: Gel ready molecular weight marker 4: Expected gene size of 657 base pairs

4.17 Colony PCR

Various sets of primers from both the KKSG9 gene and T7 were used to confirm the selection of successful colony and also to make sure that the inserted gene (KKSG9) is in the correct orientation. The extracted plasmid was also employed as a template to confirm a successful selection of the colony using various set of primers from both the KKSG9 gene and T7 nucleotide bases. Amplification with gene specific forward and reverse primers indicated the expected gene size of 657 bp band (Figure 4.38). However, using both T7 forward and reverse primers, the amplification indicated the expected gene size

of 923 bp band, lane 1 of Figure 4.40. Colony PCR using gene specific reverse primer and T7 forward primer was found to yield 831 bp band, lane 2 of Figure 4.39, which was the expected result from the analysis of their position in the vector. Finally, amplification using gene specific forward primer and T7 reverse primer yielded a 751 bp band, lane 3 of Figure 4.39, which was the value expected from the analysis of the position of the gene and T7 nucleotide in the vector. Sequencing the extracted plasmid confirmed the presence of the gene in the correct orientation and without any error in the amino acid sequence of the gene (Appendix J).

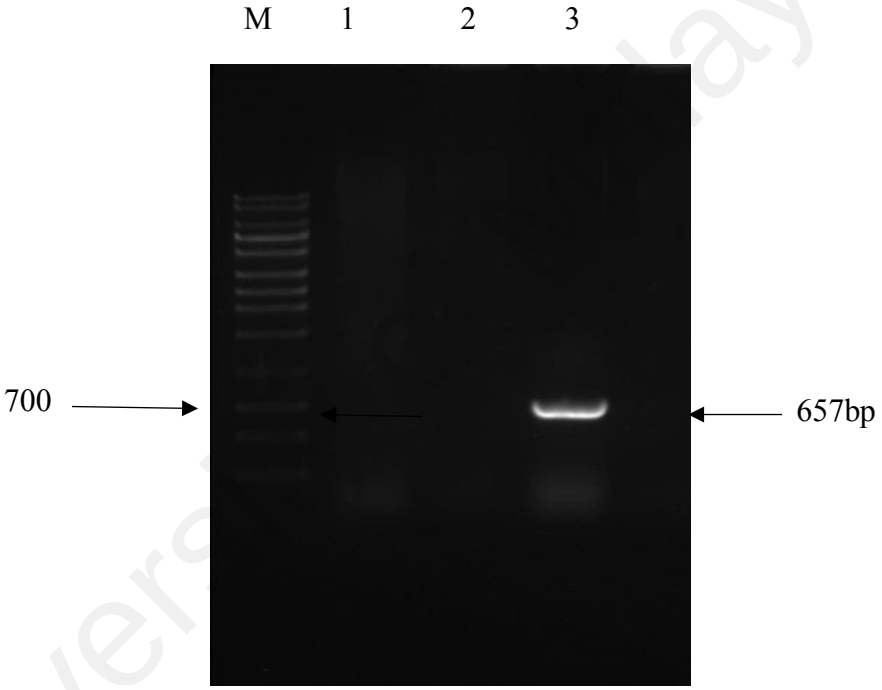

Figure 4.38: Gel image of colony PCR of KKSG9 using the KKSG9 gene specific forward and reverse primers. M= Gel ready molecular weight marker, lanes 1-3= colonies picked for analysis, 3= Positive colony with the expected gene size of 657 base pairs.

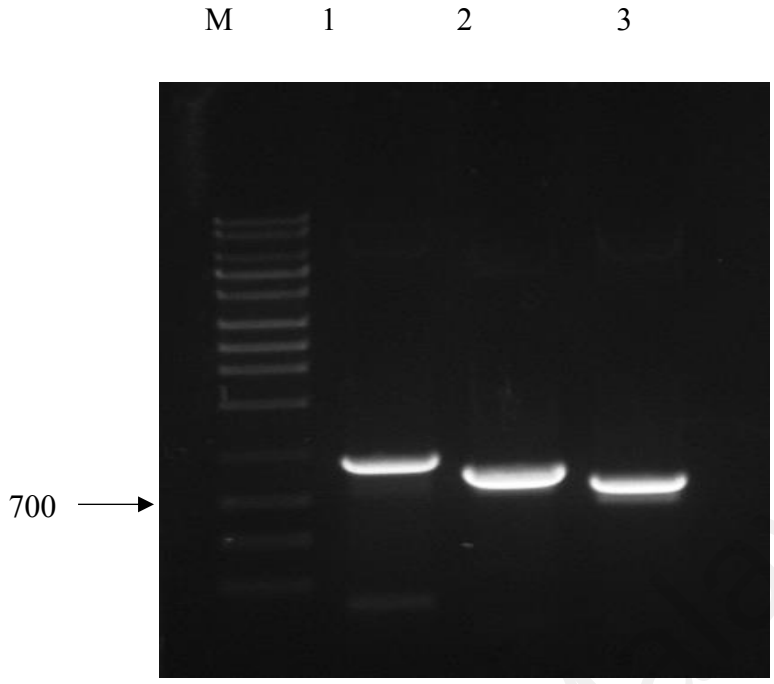

Figure 4.39: Gel image of colony PCR of KKSG9 using (1) T7 forward and reverse primers (923 bp) (2) T7 reverse and gene specific forward (831 bp) (3) T7 forward and gene specific reverse (751 bp). M: Molecular weight marker.

4.18 Protein expression and purification

Both the wild type and mutant KKSG9 were expressed using Rosseta gami B(DE3) competent cells as described in the methodology section. The protein was purified using fast protein liquid chromatography (FPLC) and the purity was judged by SDS-PAGE where a single band was obtained (Figure 4.40).

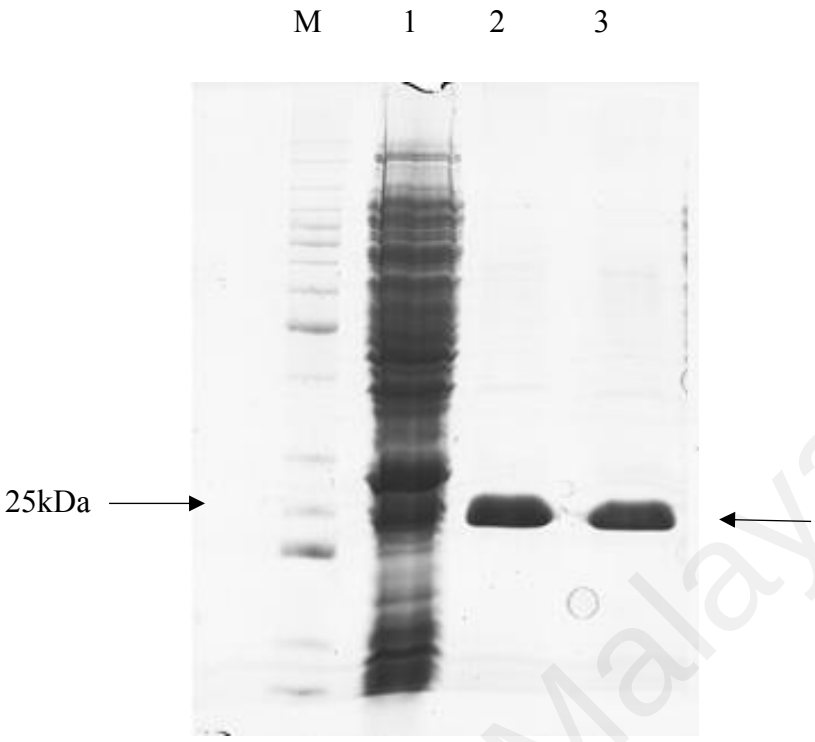

Figure 4.40: SDS-PAGE of purified KKSG9. M: Bench mark molecular weight marker, Lane 1: Crude KKSG9, Lane 2: Purified wild-type KKSG9, Lane 3: Purified Y12C mutant from the GSTrap column. The arrow indicates the expected size of the protein (24.4 kDa) from the recombinant wild type and mutant (Y12C) KKSG9.

4.19 Substrate specificity of wild type and mutant KKSG9

The results of substrate specificity screening of wild type and mutant KKSG9 are presented in (Table 4.7). The enzyme showed very wide substrate specificity by reacting with 1-chloro-2,4-dinitro benzene (CDNB), *Para*-nitro benzyl chloride (NBC), ethacrynic acid, hydrogen peroxide, and cumene hydroperoxide. NBC showed a very high activity when compared with all other substrates while CDNB showed the lowest activity. The specific activity of (Y12C) mutant was generally lower on all the substrates compared to wild type KKSG9. CDNB showed the largest difference of 1.75-fold, while the activity with NBC was 1.33-fold lower in the Y12C mutant. The peroxidase activity towards hydrogen peroxide and cumene hydroperoxide also showed 1.43- and 1.56-fold decrease respectively while activity with ethacrynic acid showed a 1.51-fold decrease.

Table 4.7: Specific activities of wild type and mutant (Y12C) KKSG9 toward various substrates. Data are mean ± S.D of at least three independent determinations. ND = not detected.

Substrates	Specific activities (µmol/min/mg)	
	WT	Y12C
1-chloro-2,4-dinitro benzene (CDNB)	0.016 ± 0.002	0.009 ± 0.0005
p-nitro benzyl chloride (NBC)	1.063 ± 0.04	0.78 ± 0.021
Hydrogen peroxide	0.043 ± 0.008	0.03 ± 0.002
Cumene hydroperoxide	0.14 ± 0.01	0.09 ± 0.003
Ethacrynic acid	0.30 ± 0.04	0.20 ± 0.001
1,2-dichloro-4-nitrobenzene (DCNB)	ND	ND
Trans-2-hexenal	ND	ND
Trans-2-octenal	ND	ND
2,4-Hexadienal	ND	ND
Trans-4-phenyl-butane-2-one	ND	ND

4.20 Kinetic study of wild type and Y12C mutant KKSG9 using NBC as substrate

In order to investigate the behavior of the enzyme, the kinetic parameters were also determined using NBC and GSH as substrates (Table 4.8). Kinetic analysis using NBC and GSH as substrates further revealed that binding of the substrate NBC was affected by the mutation of Tyr12 to Cys as there was 2.23-fold decrease in the K_m value of the mutant (Table 4.8) when compared with the wild type. This was also reflected in the catalytic efficiency and V_{max} of Y12C which decreases by 1.48-fold and 4.07-fold respectively. However, K_m of GSH was not much affected as there was no significant change between the wild type and the mutant values.

4.21 Molecular docking study of KKSG9 and organochlorine pesticides

From the molecular docking result, the KKSG9 was found to bind to the GSH molecule and the substrates dieldrin and permethrin in the pocket occupied by the residues Ser10, Ser11, Tyr12, His40, Lys52, Pro52, Phe53, Glu65, Ser66, Gln110, His111, and Ala112. Cluster analysis of docked result in permethrin using root men square deviation (RMSD) of 2Å revealed 46 different conformations. The lowest binding energy obtained

was -10.55 kJ mol^{-1} which occurred in which occurred in the 7^{th} run of the most populated cluster containing 12 members (Figure 4.41). In dieldrin, the cluster analysis revealed 4 different conformations. The lowest binding energy was -8.83 kJ mol^{-1} which occurred in the 13^{th} run of the most populated cluster containing 37 members (Figure 4.42). The presence of several polar amino acid side chains in both the G-site and H-site of the binding cleft suggest that both hydrogen bonding and hydrophobic interactions could be stabilizing the complexes formed. In addition to the hydrophobic interactions, at least two hydrogen bonds were predicted between the oxygen atom of permethrin and Asn114 and His111 of KKSG9 and one hydrogen bonding was also predicted between the chloride atom of dieldrin and His111 of KKSG9. The validity of the interaction was further confirmed in the chloride ion detection assay.

Table 4.8: Kinetic parameters of wild type and mutant (Y12C) KKSG9 using CDNB and GSH as substrates. Data are mean ± S.D of at least three independent determinations.

Enzyme	NBC				GSH			
	K_m (µM)	V_{max} (µM.min^{-1})	k_{cat} (min^{-1})	k_{cat}/K_m (µM^{-1} min^{-1}) × 10^{-3}	K_m (µM)	V_{max} (µM.min^{-1})	k_{cat} (min^{-1})	k_{cat}/K_m(µM^{-1} min^{-1}) × 10^{-3}
WT	1727.2 ± 222.1	36.1 ± 7.1	16.3 ± 2.2	9.5 ± 0.05	532.4 ± 44.9	8.5 ± 0.7	5.1 ± 0.2	9.7 ± 0.4
Y12C	773.4 ± 46.4	8.9 ± 0.7	5.0 ± 0.8	6.4 ± 0.6	466.1 ± 8.4	5.6 ± 0.2	1.3 ± 0.01	2.9 ± 0.05

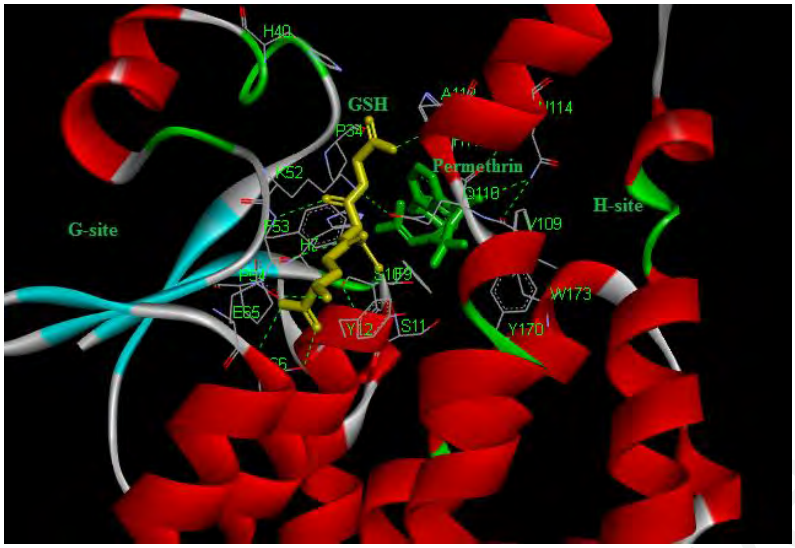

Figure 4.41: Predicted docking orientation of the lowest docking energy conformation of permethrin to the binding pocket of KKSG9. The co-substrate (GSH) is shown in yellow while the permethrin is in green ball and stick presentations. The green dash lines represent the hydrogen bondings. The residues side chains represent the amino acids involve in the catalysis.

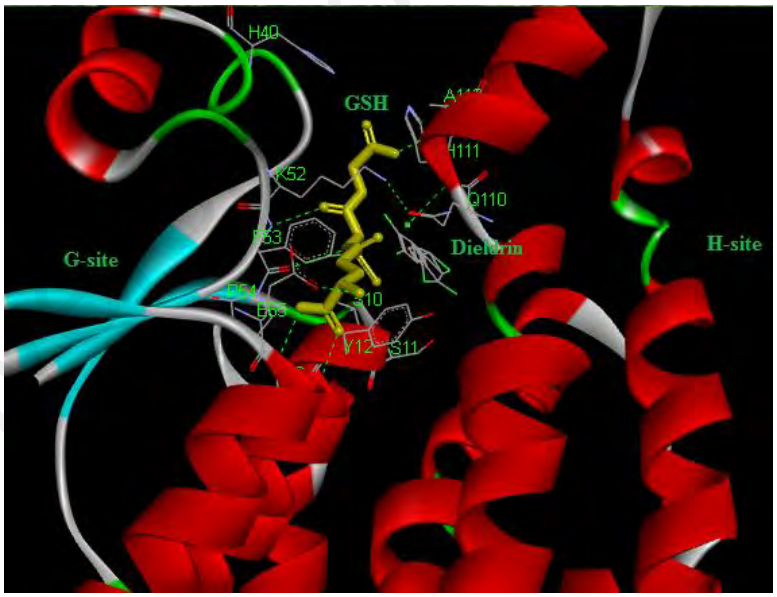

Figure 4.42: Predicted docking orientation of the lowest docking energy conformation of dieldrin to the binding pocket of KKSG9. The co-substrate (GSH) is shown in yellow while the dieldrin is in grey ball and stick presentations. The green dash lines represent the hydrogen bondings. The residues side chains represent the amino acids involve in the catalysis.

4.22 Dechlorination of DCA, Permethrin and Dieldrin by wild type and mutant (Y12C) KKSG9

The activity of the wild type and mutant enzyme was further determined with dichloroacetate (DCA), permethrin, and dieldrin as substrates and the results are presented in Figure 4.43. The enzyme displayed activity towards all these substrates as measured by chloride ion detection assay. The wild type enzyme displayed the highest activity of 94.7 ± 8.5 µmol/mg of the purified protein against permethrin, this is followed by dieldrin with 73.7 ± 7.9 and DCA showed the lowest activity of 41.6 ± 6.8 µmol/mg. In contrast, the mutant (Y12C) showed a decrease in its activity with all the substrates. This could also be attributed to the stabilization of the protein structure by the Tyr12 residue in the wild type when compared with the Cys residue as reflected in the specific activity of the enzyme.

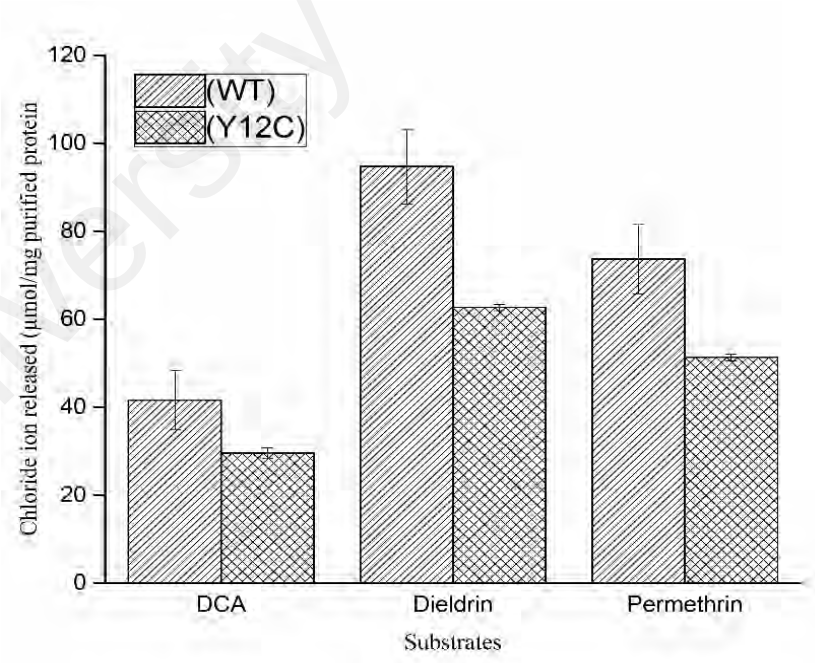

Figure 4.43: Chloride ion detection assay for the substrates Dichloroacetate (DCA) permethrin and dieldrin. The results are mean ± S.D of three independent determinations.

CHAPTER FIVE: DISCUSSION

5.1 Bioinformatic analysis of glutathione S-transferases from *Acidovorax* sp. KKS102

Bioinformatic analysis has provided a new era for easy identification, analysis, and organization of data (Luscombe et al., 2001). Recently, analysis of the complete genome of many bacteria has shown the existence of several putative GSTs in bacteria (Allocati et al., 2009; Vuilleumier, 1997). The complete genome sequence does not only represent a complete set of genes and their precise location in a chromosome but also gene similarity relationships within the genome and across species (Kanehisa & Bork, 2003). This was made possible through comparative sequence analysis and making functional inferences using evolutionary history of related sequences (Vuilleumier & Pagni, 2002). In this regard, several new classes of bacterial GSTs are coming into the light with novel function. GSTs possess a unique property by their ability to bind to many substrates. This is possible because of the variability in their substrate binding sites. The variability eventually aids in the recognition of large repertoire of substrates for biotransformation and hence their detoxification in the environment (Nagata et al., 1999; Zablotowicz et al., 1995). They offered a promising biotechnological application with regards to bioremediation of recalcitrant chemicals such as pesticides, herbicides, and heavy metals (Chen & Wilson,1997; Zablotowicz et al., 1995). The fact that most bacterial GSTs exhibit low activity towards standard GST substrates compared to their counterpart in plants and animals, however, the sheer number of bacterial cells will undoubtedly give them the upper hand to be employed for bioremediation purposes (Wood, 2008). At the same time, many of these bacterial species were isolated in an already polluted site, which means they have already became adapted to the environment and as such, they can be

easily used for bioremediation purposes or be easily engineered for a specific activity toward a targeted pollutant (Samanta et al., 2002).

With the current influx of biological data, computational analysis has become an indispensable tool for biological investigations (Bao et al., 2014; Gomez-Cabrero et al., 2014). With the tremendous increase in the genome sequence of many organisms and structural information of many proteins becoming available, the field of bioinformatics is increasingly becoming a valuable resource (Land et al., 2015; Loman & Pallen, 2015). The field provides several avenues for comparing and grouping a biological data based on meaningful similarities as well as analyzing one set of a data so as to infer and understand observations in another set of data (Huang et al., 2008). These help in organizing and understanding large-scale biological information, at the same time, it helps examine one individual system in detail and then compare them with other related systems in order to understand the similarities between the systems and differences that makes each system unique on its own (Luscombe et al., 2001; Pedersen et al., 2000).

The current explosive development in gene sequencing technique and the ease at which it is being carried out nowadays spurred a lot of interest into the full genomic sequencing of many organisms (Luscombe et al., 2001; Vuilleumier, 1997). Bioinformatic analysis is a valuable tool for analyzing and effectively organizing such a biological data (Kearse et al., 2012; Luscombe et al., 2001; Skolnick & Fetrow, 2000). The full genomic data scale normally provides diverse information such as, metabolic pathways, regulatory networks, and even protein-protein interaction (Akutsu et al., 2000; De Jong et al., 2003; Franzot & Carugo, 2003). With the availability of complete genome sequence of many bacterial species, this tool is of valuable importance for analysis and subsequent interpretation of biological data (Baxevanis & Ouellette, 2004). As one of the criteria for classifying GSTs relied on the percentage sequence similarity, newly identified GSTs can

be easily classified by utilizing information from previously characterized GSTs. The structure of a protein can be modeled as well using information from the previously characterized proteins (Šali & Blundell, 1993). The structural data could help in studying the relationship between different protein fold and their function (Hegyi & Gerstein, 1999; Martin et al., 1998). Other valuable information such as analyzing conserved amino acids for subsequent study of their importance in catalysis can be done through this process. In general, it is a tool that can be used for effective organization and analysis of biological data in a much easier way than expected.

The result of the genome sequencing studies carried out by Ohtsubo et al., (2012) revealed the presence of eleven (11) putative GSTs in *Acidovorax* sp. KKS102. For easy identification of the putative GSTs in *Acidovorax* sp. KKS102, we decided to designate them as KKSG1-KKSG11 based on the position of their nucleotide sequence (5'-3') in the DNA of the organism (Table 4.1). In order to understand the relationship between the various amino acids in the putative GSTs, phylogenetic analysis, and sequence alignment studies were carried out (Figure 4.1 and Figure 4.2). The sequence alignment study revealed the presence of some conserved amino acids in all the eleven GSTs indicating their probable importance in the catalytic activity of the enzyme. Previous studies have highlighted Pro 53 and Asp 155 from *Proteus mirabilis* GST B1-1 as strictly conserved amino acids based on comparing the sequence with other GST class found in Swiss-Prot protein sequence data bank (Allocati et al., 1999). Other amino acids that were shown to be conserved in the previous studies are; proline at position 104 and aspartic acid at position 235. However, in the present study, additional amino acid, leucine at position 69 was also discovered to be conserved among all the eleven putative GSTs in *Acidovorax* sp. KKS102.

Pro 53 was found to be a conserved amino acid not only in GSTs but even from the thioredoxin superfamily of proteins from which the GSTs were thought to have evolved (Rossjohn et al., 1998). X-ray crystallography study has shown that the amino acid played a significant role in maintaining a functional active site probably in all GST classes (Dirr et al., 1994). It exerts an unusual *cis*-configuration which ensured that the main chain atoms of the proceeding amino acid residues are able to form an anti-parallel β-sheet interaction with the main chain atom of the cysteinyl moiety of the substrate (Dirr et al., 1994; Wilce & Parker, 1994). The functional role of this amino acid was investigated in *Proteus mirabilis* GST B1-1 (Allocati et al., 1999). The result showed that even though the residue does not play a direct role in the catalysis of the enzyme, however, it does participate in maintain a proper conformation and play a significant role in antibiotic binding displayed by the enzyme (Allocati et al., 1999). However, considering the fact that not all GST classes might be involved in antibiotic binding, this might suggest other possible roles played by this residue in catalysis.

All known GSTs and GST-related proteins were shown to contain a motif called capping box at the beginning of the α-helix in their structures (Aceto et al., 1997; Dasgupta & Bell, 1993; Harper & Rose, 1993). The capping box contains a locally conserved motif "Ser/Thr-Xaa-Asp" which was shown to play a structural and functional role in the proteins with Aspartate residue as the conserved amino acid in the motif (Aceto et al., 1997; Harper & Rose, 1993). The conserved Aspartate residue was found to play a significant role in the protein folding and thermostability (Gilmartin et al., 2003). However, there are variable results obtained from site-directed mutagenesis of the conserved Aspartate residue in different GST classes. Lower thermostability was observed in human GSTP1-1when the aspartate was converted to alanine while in GST YaYa , there was a total loss in the catalytic activity of the protein (Kong et al., 1993; Wang et al., 1992). In *Burkholderia xenovorans* BphK GST, Asp155 which corresponds

to the aspartate residue in this sequence was shown to impact stability on to the protein structure (Gilmartin et al., 2005) Mutating the amino acid Asp155Tyr in *Burkholderia xenovorans* LB400 BphK was shown to decreases the thermo-stability of the enzyme without affecting its activity with CDNB (Gilmartin et al., 2005). From the sequence alignment study, all the putative GSTs in *Acidovorax* sp. KKS102 were also found to contain the amino acids predicted in the capping box (Figure 4.2). From the various reference studies indicated above, it became clear that the Aspartate residue has a very significant role both in the structure as well as catalysis by GSTs. Furthermore, the variable results obtained from different studies might be as a result of using different amino acids during the site-directed mutagenesis. Nevertheless, the results suggested the importance of this residue in the structure and function of GST and GST-related proteins.

Previous studies did not indicate the presence of conserved leucine residue in various GST classes as was observed in *Acidovorax* sp. KK102. Furthermore, sequence alignment studies using other GST classes showed that the residue is not conserved across all the GST classes as was observed with Asp and Pro. However, considering the structural and catalytic roles played by leucine residues in some other proteins it is possible that this amino acid might play a significant role in both structural and catalytic role of these GSTs. Leucine was found to be the amino acid with the highest propensity of forming alpha-helical structures in many proteins analyzed (Chou & Fasman, 1973). Leucine-rich repeats found in some proteins were also shown to be responsible for providing a versatile structural framework for the formation of protein-protein interaction (Kobe & Kajava, 2001). This suggests that leucine residues in proteins play a vital role both in the structure, catalysis, and interaction with other proteins.

To understand the evolutionary relationship between the putative GSTs in *Acidovorax* sp. KKS102, a phylogenetic tree was constructed using all the eleven GSTs (Figure 3.1).

The result of the phylogenetic analysis indicated that the GSTs distributed themselves into seven different groups. KKSG5 appeared to be more ancient than all the remaining GSTs because of its relative divergence time which is greater than that of all other GSTs, the KKSG5 forms a separate clade. KKSG9 and KKSG7 formed a separate clade very close to two maleyl acetoacetate isomerases (KKSG10 and KKSG11). Maleyl acetoacetate isomerases: KKSG10 and KKSG11 (an alternative name for the zeta class GSTS), formed a separate group while KKSG8 formed another separate group originating from KKSG10 and KKSG11. KKSG2 and KKSG6 form another separate group while KKSG4 originated from a group formed by KKSG1 and KKSG3. However, to fully understand their distribution, classification, and relationship with already characterized GST classes, another phylogenetic tree was constructed using various known GST class representatives from other organisms.

The result of the phylogenetic analysis using representatives from all known GST classes and *Acidovorax* sp. KKS102 GSTs is presented in (Figure 3.3). From the phylogenetic tree, KKSG5 appeared to have originated from mitochondrial kappa class GST and also very close to the newly discovered rho class GST. However, Kappa class GST is mitochondrial specific GST and using percentage sequence similarity, KKSG5 did not satisfy the 40% bench mark to enable its classification into that class. Furthermore, Both KKSG5 and the rho GST shared less than 20% sequence similarity with the kappa GSTs. The percentage similarity between KKSG5 and rho is slightly greater, reaching up to 25%. However, despite that, still, it is not enough to place KKSG5 into the rho class. Therefore, other criteria have to be implored to correctly classify KKSG5 or it might be a novel class of GST that has not been assigned to any class. KKSG10 and KKSG11 are closely related GSTs known as maleyl acetoacetate isomerase. From the phylogenetic tree (figure 3.3), they are closely related to zeta class GTS and also from the sequence alignment studies with other characterized zeta class GSTs, they have satisfied the criteria

of having greater than 40% sequence similarity to enable their classification into zeta class.

KKSG2, KKSG4, and KKSG6 all have their clades originated from beta class GST. However, the result of sequence alignment studies together with the percentage identity matrix with known beta class GSTs revealed that only KKSG6 possessed enough percentage similarity to enable its classification into beta class. However, even though KKSG2 lacks the required percentage similarity to enable its classification into beta class but the presence of cysteine residue which aligned itself with the cysteine residue of KKSG6 at the glutathione binding site might provide some evidence to enable its classification into beta class GSTs. Beta class GSTs have strong activity with CDNB and there is the presence of cysteine residue at the glutathione binding site (Allocati et al, 2009). However, KKSG4 might be a new variant GST with unknown characteristics.

KKSG9 and KKSG7 originated from a clade that is non-specific and appeared to position themselves between the rho and xi class GSTs. This probably pointed to the fact that GST9 and GST7 might likely be a new class of GSTs with unique properties.

KKSG1 originated from the chi class GST clade. Sequence alignment study and percentage identity matrix also showed that KKSG1 shared at least 30% sequence similarity with the chi class GSTs. Though not enough similarity to out rightly places KKSG1 into chi class, however, the 30% sequence similarity showed that it might be a close relative of the chi GST. KKSG3 shows a very close similarity with the newly discovered nu-class GST as it possessed about 66% sequence similarity with the nu-GST. Using this evidence, KKSG3 can be assumed to belong to nu-class. However, other evidences such as biochemical characterization and structural similarity are necessary to fully confirm its placement into nu-class GSTs, so also others.

The percentage similarity matrix across the eleven GSTs in *Acidovorax* sp. KKS102 (Table 4.2) did indicate that only KKSG10 and KKSG11 possessed enough percentage identity (48.58%) to be assigned into the same class. This is not surprising because right from the genome sequencing study, the two GSTs were already assigned as maleylacetoacetate isomerases. Others failed to show enough percentage identity to enable classification of two or more GSTs from *Acidovorax* sp. KKS102 into the same class.

5.2 Cloning, purification, and characterization of KKSG6

From the bioinformatic analysis of *Acidovorax* sp. KKS102 GSTs, KKSG6 was found to be a suitable homolog of BphK for further studies. The gene was subsequently amplified, cloned into pET 101 D-TOPO vector, expressed, and purified. Several studies have shown that the catalytic mechanism of various classes of GSTs is mediated by their ability to lower the pK_a of the thiol group in the co-substrate GSH thereby enhancing the nucleophilic attack on the diverse classes of electrophilic substrates (Allocati et al., 2009; Board et al., 1997; Dourado et al., 2008; Sheehan et al., 2001). This function was found to be mediated by specific amino acid residues in specific GST classes. In beta and omega class GSTs, this role was shown to be mediated by the conserved Cys residue (Allocati et al., 2000; Allocati et al., 2009). Serine residue was found to be responsible for the activation in other GST classes such as; Tau, Theta, Zeta, Delta, Epsilon and Phi classes (Board et al., 1997; Bocedi et al., 2013). Other classes such as Alpha, Pi, Mu, and Sigma utilizes tyrosine residue in the activation process (Bocedi et al., 2013; Sherratt & Hayes, 2001). Several studies have shown that bacterial beta class GST utilizes a conserved Cys10 residue in the binding and activation of the co-substrate GSH (Allocati et al., 2000; Wang et al., 2009). In KKSG6 and other BphK sequence analyzed (Figure 4.5), Cys10 is a conserved amino acid. The general increase in the catalytic activity observed in

KKSG6 (C10F) towards all substrates was thought to be as a result of the increase in the stability of the protein brought upon by the aromatic ring of phenylalanine. The aromatic ring of phenylalanine was shown to form a stack with other aromatic side chains in some proteins and this further stabilizes the protein and increases its catalytic efficiency (Brennan et al., 2009). Furthermore, Brennan et al. (2009) showed that mutating Cys10 to Phe had resulted in significant increase in the catalytic activity of BphK LB400 toward the substrate CDNB. Even though cysteine is a hydrophobic amino acid but it can form a disulfide linkage with the thiol group of GSH thereby preventing a rapid release of the product. In KKSG6, this was further manifested by the increase in V_{max}, k_{cat} and catalytic efficiency of the mutant (C10F). It seems like the polarity of the amino acid at that position normally determines the affinity of the GSH and the substrate to the protein. A similar result was reported by Wang et al. (2009) in which mutation of Cys 10 to Ser in E. *coli* beta class glutathione S-transferase results in significant decrease in the K_m of E-*coli* GST toward CDNB and subsequent decrease in k_{cat}. The result presented here suggested an enhanced release of the product mediated by the decrease in the affinity of the GSH in the Phe-mutant.

Lysine 107 is a conserved amino acid in KKSG6 and BphKs and was shown to play a role in the stabilization of GSH residue in beta class GST in *Proteus mirabilis* GSTB1-1(Allocati et al., 2000). However, molecular docking studies of KKSG6 with various substrates predicted the existence of hydrogen bond between Lys 107 and the substrates; CDNB, ethacrynic acid and cumene hydroperoxide. This demonstrates a probable role played by this residue in the binding of the substrates in addition to the stabilization of GSH. Surprisingly, while both the CDNB and peroxidase activities of K107T indicated a decrease in their specific activities, KKSG6 showed a significant increase in activity with ethacrynic acid. When this phenomenon was investigated by molecular docking studies, the ethacrynic acid was found to change its primary binding site from K107 in the wild-

type to W112 in the K107T mutant (Figure 4.15). Surprisingly, the minimum binding energy of the mutant was found to decrease from -9.31 kJ mol^{-1} observed in the wild-type to -7.24 kJ mol^{-1} in the mutant. The decrease in minimum binding energy signifies lesser affinity when compared with the wild-type and the catalytic activity is expected to decrease. This clearly showed that *in-silico* analysis using molecular docking studies has to be treated with caution and could only be confirmed after performing the real experiment. However, on investigating the phenomenon using kinetic studies and employing the ethacrynic acid and GSH as substrates. There was an increase in the parameters such as K_m, V_{max}, and k_{cat} for both the ethacrynic acid and GSH. This suggests that the increase in specific activity observed in K107T mutant toward ethacrynic acid is as a result of the change in the behavior of the enzyme toward this particular substrate. While the change in the behavior might preferentially favor ethacrynic acid, at the same time it might have disrupted the proper orientation of CDNB leading to decrease in the catalytic activity of the enzyme toward CDNB and the peroxidase activities as well. Lysine is a basic amino acid with long side chain while threonine is a polar amino acid with a short side chain. The fact that Lys 107 might contribute to the stabilization of the GSH as well as substrate binding suggests that changing the amino acid to threonine may probably interfere with the catalytic efficiency of the enzyme. A preferential binding of the co-substrate GSH to the H-site was observed when Cys10 is mutated to Ala in *Ochrobactrum anthropi* GST (Allocati et al., 2008). This has confirmed the possibility of GST substrates utilizing other potential binding sites when a preferred amino acid is mutated. The result presented here suggests a potential utilization of other binding sites in the K107T mutant by the substrate ethacrynic acid which eventually increases the catalytic activity of KKSG6 toward ethacrynic acid and at the same time, decreases the catalytic activity of the protein toward other substrates. The result also further suggested the importance of the residue Lys107 in mediating substrate specificity in KKSG6.

Alanine 180 though not a strictly conserved amino acid in KKSG6 and BphKs as seen from the sequence alignment result (Figure 4.5). The general increase in the catalytic activity of A180P mutant in KKSG6 was thought to be as a result of dramatic alteration in the 3D structure of KKSG6 brought upon by mutation of alanine to proline. Proline is an amino acid known to produce a kink in the protein structure thereby altering the conformation of the protein while alanine is a hydrophobic amino acid mostly situated deep in the hydrophobic core of proteins. (McGuiness et al., 2007). Mutation of Ala 180 to Pro in *Burkholderia xenovorans* LB400 was shown to increase the dechlorination activity of BphK LB400 toward some organochlorine pesticide substrates (McGuinness et al., 2007). The result obtained in this research further affirmed the increase in catalytic activity of A180P mutant, however, the increased was only observed toward some substrates as the peroxidase activities did not indicate any significant changes. The result further suggests a dramatic alteration in the 3D structure of KKSG6 brought upon by mutation of alanine to proline and subsequent increase in the catalytic activity of the protein toward some substrates.

5.3 Dechlorination of mono and di-chlorobenzoate derivatives by KKSG6

Among the major challenges during the bacterial biodegradation of PCBs are the PCBs themselves and its metabolic products. PCBs themselves are lipophilic and are therefore expected to accumulate in the bacterial cell membranes causing a significant decrease in the cell viability (Passatore et al., 2014; Harrad, 2010). Furthermore, some metabolic products of PCB biodegradation such as chlorobenzoates appeared to be even more toxic than the PCBs themselves causing a further decrease in the cell viability and eventual decrease in the efficiency of bioremediation processes (Adebusoye, 2017; Robertson & Hansen, 2015; Hu et al., 2014). Some metabolites such as chlorocatechol were found to inhibit dioxygenase enzymes and therefore affecting the biodegradation process

(Adebusoye, 2017). Therefore, in order to establish an optimized bioremediation process of PCBs, it is important to overcome the dead-end metabolites.

There were various attempts to genetically improve the biodegradation capability of KKS102 including the insertion of a constitutive promoter that enhances the overexpression of the bph genes (Ohtsubo et al., 2003). Furthermore, the symbiotic relationship of KKS102 with *Pseudomonas fluorescence* KKL101 was extensively studied (Kikuchi et al., 1995; Kimbara et al., 1988). The latter utilizes by-product of PCB degradation, benzoates, of the former as its source of carbon. However, studies have shown that KKL101 cannot be able to utilize chlorobenzoates and therefore occurred as dead-end metabolites in the biodegradation process (Kikuchi et al., 1995). With the availability of information on the complete genome sequence of *Acidovorax* sp. KKS102 and the presence of many putative GSTs, studying the dehalogenation function of identified BphK homolog (KKSG6) from *Acidovorax* sp. KKS102 might open a door for its eventual utilization to genetically engineer a strain with better degradation capability or use the enzyme in bioremediation of organochlorine pollutants.

The wider substrate specificity displayed by KKSG6 will be of paramount importance in dealing with the toxic metabolites generated during PCB biodegradation. Furthermore, the peroxidase action displayed by KKSG6 will neutralize the reactive oxygen species (from the activity of dioxygenases), which were found to affect the biodegradation process (Ponce et al., 2011). The dechlorination activity against various classes of monochlorobenzoates observed in KKSG6 will release benzoic acid which can eventually be degraded by *Pseudomonas fluorescence* KKL101, thereby enhancing the complete biodegradation of PCBs. The increase in catalytic activity observed in C10P and A180P mutants with regard to some substrates could also accelerate the biodegradation process with regards to those substrates. Furthermore, the mutant K107T showed differences in

its activity toward various substrates and coupled with the fact that molecular docking studies suggested that it might likely play an important role in the catalytic process, this amino acid might be important in designing a specific enzyme that could be directed against a specific substrate.

5.4 Dechlorination of organochlorine pesticides by KKSG6

The use of pesticides either in agriculture or in the control diseases causing vectors in humans is a universal phenomenon (Nishant & Upadhyay, 2016). However, agriculture contributed largely to a lot of pesticides being used on daily basis (Kumar et al., 2013; Nishant & Upadhyay, 2016). This development has much of its negative consequences on the environment. Air, water, and land have become so much polluted to the extent that 40% of the deaths worldwide are attributed to the effect of pollution (Glick, 2015; J. Kumar et al., 2014; Oliveira et al., 2016; Suk et al., 2016). To mention but a few, some pesticides such as 1,1,1-trichloro-2,2-bis-(p-chlorophenyl ethane) (DDT), dieldrin and polychlorinated biphenyls have already proven to be recalcitrant as such they can stay in the environment for a very long time and gradually accumulate in food chain even decades after their application to soil (Aislabie et al., 2006; Jiang et al., 2009; Jurelevicius et al., 2016). Others such as simazine and atrazine are biodegradable at a slow rate and they may be leached from the soil to the ground water causing a problem to the drinking water supplies (Kannan et al., 1994). Metal working industries, mining, disposal of ash residues from coal combustion and vehicular traffics have also resulted in the release of heavy metals posing a great threat to human health and environment as well (Clemens, 2006). Even though some of these chemicals were banned a long time ago, however, they are still present in the already polluted sites and this has continued to be of great danger to human health, animals, and the environment as well (Carvalho, 2017).

There are strong evidences which linked exposure to DDT with liver cancer, testicular cancer, breast cancer, and immunosuppression (Cocco et al., 2005; Kelce et al., 1995; McGlynn et al., 2006; McGlynn et al., 2008). Endosulfan is one of the persistent and also enlisted organochlorine pesticides by the United State environmental agency (USEPA). It is an endocrine-disrupting chemical with the tendency to induce hyperthyroidism. (Fang et al., 2016) Permethrin is considered to be less toxic among the organochlorine pesticides, however, increasing evidence is beginning to emerge for its various toxicities including immunotoxicity, cardiotoxicity and its effect on the digestive system (Fang et al., 2016). Another persistent organochlorine pesticide is 4, 4'-dichlorodiphenyltrichloroethane (DDT), DDT is attributed to various health implications such as cancer, neurodegenerative and immunological disorders. The re-introduction of the use of DDT for control of malarial parasite vector in 2006, after it has been banned by the world health organization is a cause for concern on further pollution of the environment by this chemical (Mansouri et al., 2016).

Dehalogenation of organochlorine pesticides by diverse classes of enzymes is considered to be one of the primary mechanism of detoxification (Correa-Torres et al., 2016; Kurashvili et al., 2016; Portier et al., 1990). Dehalogenation either render the pesticide more soluble thereby reducing its hydrophobic nature or less toxic thereby reducing its tendency to cause toxicity in humans, animals, and environment at large (Chen et al., 2015; Jaiswal et al., 2017; Aislabie et al., 2006). Furthermore, the phenomenon was shown to provide a protective effect to the plants thereby enhances root growth and overall yield of the plant (McGuinness et al., 2007). The result of dehalogenation function of KKSG6 indicated a promising application of this enzyme in the bioremediation of these classes of organochlorine pollutants. Permethrin appeared to be a better substrate in the dehalogenation function of KKSG6 when compared with DDT and endosulfan. This may be attributed to the low minimum binding energy in the docked

conformation of permethrin (-10.70 kJ mol^{-1}) when compared with DDT (-8.99 kJ mol^{-1}) and endosulfan (-9.92 kJ mol^{-1}). The low minimum binding energy signifies better binding interaction of permethrin to KKSG6 when compared with DDT and endosulfan. Furthermore, the molecular docking conformation of permethrin revealed the presence of only hydrophobic interaction binding permethrin with KKSG6 unlike in endosulfan, whereby both hydrogen bonding and hydrophobic interactions were predicted to have played a role in its binding. The presence of hydrogen bonding in the interaction of KKSG6 and endosulfan suggests an increased affinity of this substrate to the enzyme which might prevent the rapid release of the substrate. Even though the binding of DDT with KKSG6 was also found to be mainly mediated by hydrophobic interactions, however, the high hydrophobic nature of DDT when compared with endosulfan might have contributed to the low dehalogenation function of KKSG6 when compared with permethrin. While the increase in activity observed in C10F and A180P mutants could be used to accelerate the biodegradation process, the substrate-dependent changes observed in K107T mutant also suggest a probable function of the protein in determining substrate specificity in this enzyme. This suggests that those amino acids could be used to genetically engineer an enzyme with superior degradation capability or directed against a specific substrate.

5.5 Bioinformatic analysis of KKSG9

The N-terminal domain of zeta class GSTs is characterized by the presence of a signature motif; SSCX(W/H) RVRIAL and RSSASYRVRIAL (Figure 4.34) for eukaryotic and prokaryotic sequences respectively (Board et al., 1997; Marsh et al., 2008). The result of sequence alignment studies of various GST-classes showed that the first serine residue in these motifs is highly conserved and is analogous to the catalytic serine found in theta, Phi and delta classes (Board et al., 1997). It is responsible for

glutathione (GSH) binding during co-activation to form a thiolate ion. Two distinct groups of zeta class GSTs were observed based on the analysis of more than 200 similar sequences (Marsh et al., 2008). The first group is found in eukaryotic sequences and they contained the first serine and a cysteine residue in the motif partnered by glutamine at the N-terminal domain that function in the stabilization of the GSH. This group is usually found in MAAI and tetrachlorohydroquinone dehalogenases (TCHQ-DH). The second group is usually found in prokaryotes and they contained serine but in place of cysteine, a polar side chain usually (Ser, Thr or Ala) is present partnered by histidine 104 at the N-terminal domain. Even though this second group was found to lie within the clusters of a gene involved in tyrosine metabolism, however, lack of cysteine residue suggests that they are not required for MAAI activity (Thom et al., 2001). This group was found to be predominantly MPIs with alanine contributing to >50% of the residue at that position (Marsh et al., 2008; Yamamoto et al., 2009). In this second group, the residues RS----RVRIAL were also shown to be >85% conserved with the first arginine functions in substrate recognition (Marsh et al., 2008). However, in KKSG9 the motif observed using sequence alignment analysis is FSSYTQKVLIAL (Figure 4.35).

Sequence alignment studies using other zeta class GSTs also showed that the first serine residue in the KKSG9 motif is equivalent to the essential catalytic serine found in other zeta class GSTs (Figure 4.34). However, the commonly found Ser, Thr or Ala in prokaryotic sequences is replaced by Tyr residue. In addition, the motif in KKSG9 completely lacks arginine residues including the first arginine which functions in substrate recognition. However, the sequence contained the expected histidine 104 that function in the stabilization of GSH.

Blast analysis of KKSG9 revealed an interesting scenario, whereby uncharacterized proteins from different strains of *Acidovorax* sp. dominated the first five hits and shared

between 97-99% sequences similarities with KKSG9 (Figure 4.35). In addition, the motif FSSYTQKVLIAL present in KKSG9 was 100% conserved in such strains (Figure 4.36). Several other strains of bacteria also showed up to 70% sequence similarity with KKSG9 and a well-conserved motif that was observed in KKSG9. This suggests the possibility of a new variant of zeta-like GST that could have been distributed to other strains through the conjugal transfer of genes. This mechanism of gene transfer was found to play a role in the evolution of novel enzymes that can degrade the ever-increasing novel compounds such as pesticides (McGowan et al., 1998)

5.6 Specific activity and kinetic parameters of KKSG9

KKSG9 displayed a typical behavior of zeta class GSTs as reported by Board et al., (1997), as it binds to the GST-affinity column slowly before it was eluted using 10mM GSH. Substrate specificity of the enzyme was determined using a range of known GST substrates. The enzyme displayed wide substrate specificity compared to most zeta class GSTs by reacting with (CDNB), (NBC), (EA), hydrogen peroxide (H_2O_2) and cumene hydroperoxide (CuOOH) (Table 4.7). This is consistent with what was observed in most zeta class GSTs especially with regards to low catalytic activity with CDNB and presence of peroxidase activity with some organic hydroperoxides (Board et al., 1997). From the sequence alignment analysis (Figure 4.34), the equivalent residue at position 12 was found to be alanine. We examined the differences that may occur in the catalytic activity of the protein when Tyr12 is mutated to the originally known cysteine residue. While mammalian zeta class GST largely maintained cysteine residue at that position, bacterial zeta class GSTs contained either Cys, Ser, Thr or Ala with Ala containing > 50% of the residue. In *Rastolnia* sp. strain U2, the equivalent position was found to be occupied by threonine. Site-directed mutagenesis of Thr11Ala was shown to cause an unexpected decrease in the K_m of GSH (Fang et al., 2011). In KKSG9, mutating the tyrosine to

cysteine residue was found to affect the catalytic activity of the protein toward all the substrates (CDNB, NBC, EA, H_2O_2, and CuOOH), and the kinetic parameters of NBC were also found to be affected. However, the kinetic parameters of GSH remained largely unchanged. This is probably because while the wild-type containing the tyrosine residue could provide a hydrogen bonding with the nitrogen or thiol group of the cysteinyl moiety, the mutant containing the cysteine residue could as well provide disulfide linkage with the thiol group of the cysteinyl moiety. The improved catalytic activity of the wild-type, when compared with the mutant might be as a result of the presence of the aromatic ring in the tyrosine residue. The aromatic ring was shown to form a stack with other aromatic amino acids in some proteins thereby stabilizing the protein and improve its catalytic activity (Brennan et al., 2009). The tyrosine residue (Tyr12) in KKSG9 is lying close to a phenylalanine residue (Phe9) which could form a stack with the aromatic ring of Tyr12 and thereby further enhances the stabilization of the protein. These findings suggested that the variation in the equivalent residues at that position in other bacterial zeta class GSTs and the presence of tyrosine in KKSG9 might represent an evolutionary step for improvement in the catalytic activity of the protein. Furthermore, the finding also corroborates with the suggestion by Fang et al. (2011), that this residue may be important in the rational design of an effective and competitive enzyme in zeta class GSTs.

5.7 Binding interaction and dechlorination activity of KKSG9 towards some organochlorine compounds

Molecular docking study was carried out in order to explore the binding pattern and the amino acids involved in the interaction of permethrin and dieldrin with KKSG9. The N-terminal part of glutathione S-transferases contained the amino acids responsible for the binding of co-substrate GSH while the C-terminal part contained the substrate binding site. The C-terminal part is more variable as compared with the N-terminal part as it

contains the binding site for a wide range of substrates that react with GSTs (Allocati et al., 2009). Molecular docking analysis of KKSG9 with dieldrin and permethrin revealed the possibility of interaction and therefore catalysis by KKSG9 against these substrates. However, surprisingly while the minimum binding energy of permethrin is lower compared with dieldrin, the dechlorination activity of KKSG9 against dieldrin was found to be higher when compared with that of permethrin. This also showed that minimum binding energy in molecular docking interactions does not always reflect the true catalytic activity of the enzyme against a particular substrate.

Within the past decades, there is a growing interest in the study of glutathione S-transferase in bacteria. This is because of their potential to be used as bioremediation agents for many classes of pollutants which is more economical when compared with physicochemical methods (Agullo et al., 2017; El-Sheek & Mahmoud, 2017). While other dehalogenases are specific for certain substrates, GSTs appeared to be broad in its substrate specificity which gives the enzyme a greater advantage to be employed for several bioremediation purposes (Seeger & Pieper, 2010). This makes GST in bacteria one of the suitable targets to be used for bioremediation of diverse form of pollutants. Another advantage of GST in bioremediation is the fact that it can react with a diverse range of electrophilic substrates, unlike other enzymes which are specific to a certain substrate (Agullo et al., 2017; Azubuike et al., 2016).

One of the characteristics of zeta class glutathione S-transferases is dehalogenation reaction. Various forms of a zeta class GSTs exist which catalyzes various dehalogenation reaction on a diverse class of substrates leading to their detoxification (Yamamoto et al., 2009). Dichloroacetate is one of the water contaminants that is believed to be carcinogenic, while permethrin is considered to be less-toxic among the organochlorine pesticides, however, increasing evidence is beginning to emerge for its various toxicities

including immunotoxicity, cardiotoxicity and its effect on the digestive system (Wang et al., 2016; Dai et al., 2014). Dieldrin is an extremely persistence organochlorine pesticides whose toxicity after long-term exposure was shown to be more detrimental to humans and animals than the target insects (Zaffar et al., 2016). Organochloride pollutants were shown to be more recalcitrant as the number of chlorine atoms attached to the parent compound is increased. Dehalogenation of these compounds was shown to decrease their recalcitrance and eventually helps in their rapid biodegradation (Carvalho, 2017; Chakraborty & Das, 2016; Catallo & Portier, 1992). The ability of KKSG9 to display activity toward these compounds showed that it will be valuable in the bioremediation of these organochlorine compounds. Dehalogenation served as the primary mechanism for detoxification of various organochlorine compounds making them vulnerable to attack by other degradative enzymes (Chakraborty & Das, 2016; Nagata et al., 2016; Vedler et al., 2009).

CHAPTER SIX: CONCLUSION

6.1 Conclusion

Two glutathione S-transferases designated as KKSG6 and KKSG9 were cloned, expressed, and biochemically characterized from a biphenyl/polychlorobiphenyl degrading organism *Acidovorax* sp. KKS102. KKSG6 was selected because of the significant sequence similarity between the GST and some BphK sequences. BphKs are GSTs that are located within the *bph* operon, this operon contained series of genes that code for enzymes responsible for biphenyl/PCB biodegradation in biphenyl degrading organisms. The idea was to identify a homolog that could be employed in the biodegradation of metabolites that were released during PCB biodegradation, since in *Acidovorax* sp. KKS102, the bph operon lacks the corresponding BphK gene. Lack of BphK enzyme would leave the metabolites such as chlorobenzoates un-degraded, so that they could be potentially toxic to the degrading organism or transformed into even more toxic metabolite (protoanemonin) by other microbial flora. The identified homolog showed wide substrate specificity using standard GST substrates, unlike what was observed in BphK of *Burkholderia xenovorans* LB 400 which reacted only with CDNB. KKSG6 also showed peroxidase activities; a vital component which deals with the reactive oxygen species produced as a result of the activity of dioxygenase enzyme.

KKSG6 was also found to dechlorinate PCB metabolites, such as 2-chlorobenzoate, 3-chlorobenzoate, 4-chlorobenzoate, and 2,4-dichlorobenzoates. Site-directed mutagenesis on some selected amino acids highlighted their importance in the catalytic activity of the protein. While C10F and A180P mutants were found to display an increase in the catalytic activity of the protein, K107T was found to show variable results. This suggests that C10F and A180P mutants could be useful in the acceleration of biodegradation process. The variable result obtained in K107T mutant signifies the importance of the amino acid in

determining substrate specificity in KKSG6. The amino acid could be useful in the engineering of a specific enzyme directed against a specific substrate. Furthermore, the mutant K107T showed a little activity with 2,5-dichlorobenzoate and 2,6-dichlorobenzoate, unlike the wild-type enzyme. This further signifies the importance of the amino acid in determining substrate specificity in KKSG6.

Determination of kinetic parameters using CDNB and GSH as substrates showed that GSH displayed a lower K_m for the enzyme when compared with the CDNB. The kinetic parameters of C10F and A180P mutants both showed an increase in V_{max} with a corresponding increase in turn over number and catalytic efficiency of the enzyme. The kinetic parameters of the mutant (K107T) using ethacrynic acid and GSH as substrates showed an increase in k_{cat}, K_m, and V_{max} and catalytic efficiency for both the ethacrynic acid and GSH when compared with the wild-type. Molecular docking studies between KKSG6 and some organochlorine pesticides (DDT, endosulfan, and permethrin) further revealed a potential binding interaction. The enzyme was also found to show dechlorination function against these organochlorine pesticides. This indicates the versatility of function displayed by KKSG6 as it can also be used in the bioremediation of organochlorine pesticides.

KKSG9 was also cloned, expressed, purified and characterized. The protein was chosen because of its unusual phylogenetic relationship. Phylogenetic analysis showed that the enzyme lies very close to maleylacetoacetate isomerases (zeta class GSTs) and contained a signature motif which closely resembles that of zeta class GSTs. However, sequence alignment studies and percentage sequence similarity showed that the enzyme has very low sequence similarity with representatives from the zeta class GSTs despite the fact that zeta GSTs were known for maintaining high sequence similarity among its members. Determination of specific activity of the enzyme using standard GST substrates

showed that it has very wide substrate specificity compared to most zeta class GSTs. The motif in KKSG9 was also found to contain Tyr 12, which replaces the commonly found Ala, Thr Cys or Ser at that position. Site-directed mutagenesis was carried out on the Tyr 12 residue which was converted to cysteine. The mutant displayed low catalytic activity toward all the substrates when compared with the wild-type.

Kinetic study using NBC and GSH as substrates further revealed that all the kinetic parameters for both NBC and ethacrynic acid were affected by the mutation. The kinetic parameters of the mutant (K_m, V_{max}, k_{cat} and k_{cat}/K_m) were all affected by the mutation of Tyr to Cys. This suggests that the presence of Tyr residue at that position might be an evolutionary trend toward improving the catalytic activity of the enzyme.

The enzyme was also found to display dichloroacetate dechlorinating function, a known function displayed by zeta class GSTs. Molecular docking studies of KKSG9 with some organochlorine pesticides (dieldrin and permethrin) further revealed a potential binding interaction between the enzyme and the substrates. Further analysis of the dechlorinating function of this enzyme against this substrate showed that it possessed dechlorinating activity with the wild-type displaying more activity when compared with the mutant. This also suggests that the enzyme could have a potential application in the bioremediation of organochlorine pollutants.

6.2 Future work

Future work on this research should involve inserting the KKSG6 within the *bph* operon of *Acidovorax* sp. KKS102 in order to see how possible KKSG6 can help improve the bioremediation capability of polychlorobiphenyls by the organism. Furthermore, studies on the stability of the mutants C10F and A180P could also help in ascertaining their possible recruitment toward rapid bioremediation of the PCB metabolites.

Additional site-directed mutagenesis study on Lys107 will probably reveal some additional roles played by this residue in the catalysis by KKSG6 as the residues seems to play a great role in mediating substrate specificity in the enzyme. Considering the dechlorinating function displayed by KKSG6 against some organochlorine pesticides, future studies should as well consider inserting the genes into a rhizospheric bacteria to ascertain the possibility of employing the enzymes in growth promoting bacteria so as to help in protecting plants against the effect of organochlorine pesticides. Other organochlorine compounds may as well be tested to see if they are also substrates for this enzyme.

The low sequence similarity displayed by KKSG9 against all known cytosolic GST classes suggested that it may likely be a new class of GST or a new variant of zeta class with improved catalytic activity. The dichloroacetate dechlorinating activity displayed by the enzyme could as well be exploited in using the enzyme for bioremediation of dichloroacetate. Furthermore, since the enzyme also displayed dechlorinating activities against dieldrin and permethrin, field work for possible bioremediation of these pollutants by the enzyme should be considered. The versatility of substrate specificity against standard GST substrates displayed by KKSG9 could as well be extended to determine the activity of the enzyme against other organochlorine pollutants. This might open other potential functions of the enzyme not covered in this research.

REFERENCES

Abraham, W.-R., Nogales, B., Golyshin, P. N., Pieper, D. H., & Timmis, K. N. (2002). Polychlorinated biphenyl-degrading microbial communities in soils and sediments. *Current Opinion in Microbiology, 5*(3), 246-253.

Aceto, A., Dragani, B., Melino, S., Allocati, N., Masulli, M., Di Ilio, C., & Petruzzelli, R. (1997). Identification of an N-capping box that affects the α6-helix propensity in glutathione S-transferase superfamily proteins: A role for an invariant aspartic residue. *Biochemical Journal, 322*(1), 229-234.

Adebusoye, S. A. (2017). Biological degradation of 4-chlorobenzoic acid by a PCB-metabolizing bacterium through a pathway not involving (chloro) catechol. *Biodegradation, 28*(1), 37-51.

Agulló, L., Pieper, D. H., & Seeger, M. (2017). *Genetics and biochemistry of biphenyl and PCB biodegradation: Aerobic utilization of hydrocarbons, oils & lipids*. Berlin: Springer.

Aislabie, J., Saul, D. J., & Foght, J. M. (2006). Bioremediation of hydrocarbon-contaminated polar soils. *Extremophiles, 10*(3), 171-179.

Akutsu, T., Miyano, S., & Kuhara, S. (2000). Inferring qualitative relations in genetic networks and metabolic pathways. *Bioinformatics, 16*(8), 727-734.

Al-Majed, A. A., Adebayo, A. R., & Hossain, M. E. (2012). A novel sustainable oil spill control technology. *Environmental Engineering & Management Journal*, *28*, 333-353.

Albro, P., & McKinney, J. (1981). The relationship between polarizability of polychlorinated biphenyls and their induction of mixed function oxidase activity. *Chemico-Biological Interactions, 34*(3), 373-378.

Alias, Z., & Clark, A. G. (2010). Adult *Drosophila melanogaster* glutathione S-transferases: Effects of acute treatment with methyl parathion. *Pesticide Biochemistry & Physiology, 98*(1), 94-98.

Allocati, N., Casalone, E., Masulli, M., Ceccarelli, I., Carletti, E., Parker, M. W., & Di Ilio, C. (1999). Functional analysis of the evolutionarily conserved proline 53 residue in *Proteus mirabilis* glutathione transferase B1-1. *FEBS letters, 445*(2), 347-350.

Allocati, N., Casalone, E., Masulli, M., Polekhina, G., Rossjohn, J., Parker, M. W., & Carmine, D. (2000). Evaluation of the role of two conserved active-site residues in beta class glutathione S-transferases. *Biochemical Journal, 351*(2), 341-346.

Allocati, N., Federici, L., Masulli, M., & Di Ilio, C. (2009). Glutathione transferases in bacteria. *FEBS Journal, 276*(1), 58-75.

Allocati, N., Federici, L., Masulli, M., Favaloro, B., & Di Ilio, C. (2008). Cysteine 10 is critical for the activity of *Ochrobactrum anthropi* glutathione transferase and its mutation to alanine causes the preferential binding of glutathione to the H-site. *Proteins: Structure, Function, & Bioinformatics, 71*(1), 16-23.

Ames, B. N., Profet, M., & Gold, L. S. (1990). Nature's chemicals and synthetic chemicals: comparative toxicology. *PNAS, 87*(19), 7782-7786.

Anandarajah, K., Kiefer, P. M., Donohoe, B. S., & Copley, S. D. (2000). Recruitment of a double bond isomerase to serve as a reductive dehalogenase during biodegradation of pentachlorophenol. *Biochemistry, 39*(18), 5303-5311.

Andersson, C., Mosialou, E., Weinander, R., & Morgenstern, R. (1994). Enzymology of microsomal glutathione S-transferase. *Advances in Pharmacology, 27*, 19.

Arca, P., Hardisson, C., & Suarez, J. (1990). Purification of a glutathione S-transferase that mediates fosfomycin resistance in bacteria. *Antimicrobial Agents & Chemotherapy, 34*(5), 844-848.

Arca, P., Rico, M., Brana, A., Villar, C., Hardisson, C., & Suarez, J. (1988). Formation of an adduct between fosfomycin and glutathione: A new mechanism of antibiotic resistance in bacteria. *Antimicrobial Agents & Chemotherapy, 32*(10), 1552-1556.

Armstrong, R. N. (1997). Structure, catalytic mechanism, and evolution of the glutathione transferases. *Chemical Research in Toxicology, 10*(1), 2-18.

Armstrong, R. N. (2000). Mechanistic diversity in a metalloenzyme superfamily. *Biochemistry, 39*(45), 13625-13632.

Ashworth, K., Wild, O., & Hewitt, C. (2010). Sensitivity of isoprene emissions estimated using MEGAN to the time resolution of input climate data. *Atmospheric Chemistry & Physics, 10*(3), 1193-1201.

Atkinson, H. J., & Babbitt, P. C. (2009). Glutathione transferases are structural and functional outliers in the thioredoxin fold. *Biochemistry, 48*(46), 11108-11116.

Azubuike, C. C., Chikere, C. B., & Okpokwasili, G. C. (2016). Bioremediation techniques–classification based on site of application: Principles, advantages, limitations and prospects. *World Journal of Microbiology & Biotechnology, 32*(11), 180-190.

Bader, R., & Leisinger, T. (1994). Isolation and characterization of the *Methylophilus* sp. strain DM11 gene encoding dichloromethane dehalogenase/glutathione S-transferase. *Journal of Bacteriology, 176*(12), 3466-3473.

Baez, S., Segura-Aguilar, J., Widersten, M., Johansson, A., & Mannervik, B. (1997). Glutathione transferases catalyse the detoxication of oxidized metabolites (o-quinones) of catecholamines and may serve as an antioxidant system preventing degenerative cellular processes. *Biochemical Journal, 324*, 25-28.

Bao, R., Huang, L., Andrade, J., Tan, W., Kibbe, W. A., Jiang, H., & Feng, G. (2014). Review of current methods, applications, and data management for the bioinformatics analysis of whole exome sequencing. *Cancer Informatics, 13*(2), 67-75.

Barakat, A. O., Khairy, M., & Aukaily, I. (2013). Persistent organochlorine pesticide and PCB residues in surface sediments of Lake Qarun, a protected area of Egypt. *Chemosphere, 90*(9), 2467-2476.

Bartels, F., Backhaus, S., Moore, E. R., Timmis, K. N., & Hofer, B. (1999). Occurrence and expression of glutathione-S-transferase-encoding bphK genes in *Burkholderia* sp. strain LB400 and other biphenyl-utilizing bacteria. *Microbiology, 145*(10), 2821-2834.

Baxevanis, A. D., & Ouellette, B. F. (2004). *Bioinformatics: A practical guide to the analysis of genes & proteins*. John Wiley & Sons.

Bello, M. L., Battistoni, A., Mazzetti, A. P., Board, P. G., Muramatsu, M., Federici, G., & Ricci, G. (1995). Site-directed Mutagenesis of Human Glutathione Transferase P1-1 spectral, kinetic, and structural properties of cys-47 and lys-54 mutants. *Journal of Biological Chemistry, 270*(3), 1249-1253.

Benson, A. M., Talalay, P., Keen, J. H., & Jakoby, W. B. (1977). Relationship between the soluble glutathione-dependent delta 5-3-ketosteroid isomerase and the glutathione S-transferases of the liver. *Proceeding of the National Academy of Science, 74*(1), 158-162.

Bhowmik, S., Horsman, G. P., Bolin, J. T., & Eltis, L. D. (2007). The molecular basis for inhibition of bphd, a carbon-carbon bond hydrolase involved in polychlorinated biphenyls degradation, large 3-substituents prevent tautomerization. *Journal of Biological Chemistry, 282*(50), 36377-36385.

Blasco, R., Mallavarapu, M., Wittich, R., Timmis, K. N., & Pieper, D. H. (1997). Evidence that formation of protoanemonin from metabolites of 4-chlorobiphenyl degradation negatively affects the survival of 4-chlorobiphenyl-cometabolizing microorganisms. *Applied & Environmental Microbiology, 63*(2), 427-434.

Blasco, R., Wittich, R.-M., Mallavarapu, M., Timmis, K. N., & Pieper, D. H. (1995). From xenobiotic to antibiotic, formation of protoanemonin from 4-chlorocatechol by enzymes of the 3-oxoadipate pathway. *Journal of Biological Chemistry, 270*(49), 29229-29235.

Blocki, F., Logan, M., Baoli, C., & Wackett, L. (1994). Reaction of rat liver glutathione S-transferases and bacterial dichloromethane dehalogenase with dihalomethanes. *Journal of Biological Chemistry, 269*(12), 8826-8830.

Board, G. P., Baker, T. R., Chelvanayagam, G., & Jermiin, S. L. (1997). Zeta, a novel class of glutathione transferases in a range of species from plants to humans. *Biochemical Journal, 328*(3), 929-935.

Bocedi, A., Fabrini, R., Farrotti, A., Stella, L., Ketterman, A. J., Pedersen, J. Z., & Eltis, L. D. (2013). The impact of nitric oxide toxicity on the evolution of the glutathione transferase superfamily, A proposal for an evolutionary driving force. *Journal of Biological Chemistry, 288*(34), 24936-24947.

Booth, J., Boyland, E., & Sims. (1961). An enzyme from rat liver catalysing conjugations with glutathione. *Biochemical Journal, 79*(3), 516-522.

Bordoli, L., Kiefer, F., Arnold, K., Benkert, P., Battey, J., & Schwede, T. (2009). Protein structure homology modeling using SWISS-MODEL workspace. *Nature Protocols, 4*(1), 1-13.

Borja, J., Taleon, D. M., Auresenia, J., & Gallardo, S. (2005). Polychlorinated biphenyls and their biodegradation. *Process Biochemistry, 40*(6), 1999-2013.

Bradford, M. M. (1976). A rapid and sensitive method for the quantitation of microgram quantities of protein utilizing the principle of protein-dye binding. *Analytical Biochemistry, 72*(1-2), 248-254.

Brennan, E., McGuinness, M., & Dowling, D. N. (2009). Bioinformatic analysis and in vitro site-directed mutagenesis of conserved amino acids in BphK LB400, a specific bacterial glutathione transferase. *International Biodeterioration & Biodegradation, 63*(7), 928-932.

Brophy, P. M., Southan, C., & Barrett, J. (1989). Glutathione transferases in the tapeworm *Moniezia expansa*. *Biochemical Journal, 262*(3), 939-946.

Cabrerizo, A., Dachs, J., Barceló, D., & Jones, K. C. (2012). Influence of organic matter content and human activities on the occurrence of organic pollutants in Antarctic soils, lichens, grass, and mosses. *Environmental Science & Technology, 46*(3), 1396-1405.

Caccuri, A. M., Antonini, G., Allocati, N., Di Ilio, C., De Maria, F., Innocenti, F., & Turella, P. (2002). GSTB1-1 from *Proteus mirabilis*, a snapshot of an enzyme in the evolutionary pathway from a redox enzyme to a conjugating enzyme. *Journal of Biological Chemistry, 277*(21), 18777-18784.

Cámara, B., Herrera, C., González, M., Couve, E., Hofer, B., & Seeger, M. (2004). From PCBs to highly toxic metabolites by the biphenyl pathway. *Environmental Microbiology, 6*(8), 842-850.

Camarero, S., Martínez, M. J., & Martínez, A. T. (2014). Understanding lignin biodegradation for the improved utilization of plant biomass in modern biorefineries. *Biofuels, Bioproducts & Biorefining, 8*(5), 615-625.

Cao, L., Gao, Y., Wu, G., Li, M., Xu, J., He, J., . . . Hong, Q. (2013). Cloning of three 2, 3-dihydroxybiphenyl-1, 2-dioxygenase genes from *Achromobacter* sp. BP3 and the analysis of their roles in the biodegradation of biphenyl. *Journal of Hazardous Materials, 261*, 246-252.

Cao, M., Bernat, B. A., Wang, Z., Armstrong, R. N., & Helmann, J. D. (2001). FosB, a cysteine-dependent fosfomycin resistance protein under the control of ςW, an extracytoplasmic-function ς factor in *Bacillus subtilis*. *Journal of Bacteriology, 183*(7), 2380-2383.

Carvalho, F. P. (2017). Pesticides, environment, and food safety. *Food & Energy Security, 6*(2), 48-60.

Catallo, W., & Portier, R. (1992). Use of indigenous and adapted microbial assemblages in the removal of organic chemicals from soils and sediments. *Water Science & Technology, 25*(3), 229-237.

Chakraborty, J., & Das, S. (2016). Molecular perspectives and recent advances in microbial remediation of persistent organic pollutants. *Environmental Science & Pollution Research, 23*(17), 16883-16903.

Chanal, A., Chapon, V., Benzerara, K., Barakat, M., Christen, R., Achouak, W., & Heulin, T. (2006). The desert of Tataouine: an extreme environment that hosts a wide diversity of microorganisms and radiotolerant bacteria. *Environmental Microbiology, 8*(3), 514-525.

Chee, C.-S., Tan, I. K.-P., & Alias, Z. (2014). Characterization of affinity-purified isoforms of *Acinetobacter calcoaceticus* Y1 glutathione transferases. *The Scientific World Journal, 10 (4), 215-221.*

Chelvanayagam, G., Parker, M., & Board, P. (2001). Fly fishing for GSTs: A unified nomenclature for mammalian and insect glutathione transferases. *Chemico-Biological Interactions, 133*(1-3), 256-260.

Chemicals, U. (1999). *Guidelines for the identification of PCBs and materials containing PCBs*: UNEP Chemicals.

Chen, H., Gao, B., Wang, S., & Fang, J. (2015). Microbial degradation of hexachlorocyclohexane (HCH) pesticides. *Advances in Biodegradation & Bioremediation of Industrial Waste*, *181* (4), 222-234.

Chen, S., & Wilson, D. B. (1997). Genetic engineering of bacteria and their potential for Hg 2+ bioremediation. *Biodegradation, 8*(2), 97-103.

Chou, P. Y., & Fasman, G. D. (1973). Structural and functional role of leucine residues in proteins. *Journal of Molecular Biology, 74*(3), 263-281.

Chrysostomou, C., Quandt, E. M., Marshall, N. M., Stone, E., & Georgiou, G. (2015). An alternate pathway of arsenate resistance in E. *coli* mediated by the glutathione s-transferase GSTB. *ACS Chemical Biology, 10*(3), 875-882.

Clemens, S. (2006). Toxic metal accumulation, responses to exposure and mechanisms of tolerance in plants. *Biochimie, 88*(11), 1707-1719.

Cocco, P., Fadda, D., Billai, B., D'Atri, M., Melis, M., & Blair, A. (2005). Cancer mortality among men occupationally exposed to dichlorodiphenyltrichloroethane. *Cancer Research, 65*(20), 9588-9594.

Cogliano, V. J. (1998). Assessing the cancer risk from environmental PCBs. *Environmental Health Perspectives, 106*(6), 317-325.

Combes, B., & Stakelum, G. S. (1961). A liver enzyme that conjugates sulfobromophthalein sodium with glutathione. *The Journal of Clinical Investigation, 40*(6), 981-988.

Cook, A. M. (1987). Biodegradation of s-triazine xenobiotics. *FEMS Microbiology Reviews, 46*(2), 93-116.

Cookson Jr, J. T. (1995). *Bioremediation engineering: Design & application*. Columbus, Ohio: McGraw-Hill, Inc.

Copley, S. D. (1998). Microbial dehalogenases: Enzymes recruited to convert xenobiotic substrates. *Current Opinion in Chemical Biology, 2*(5), 613-617.

Copley, S. D. (2000). Evolution of a metabolic pathway for degradation of a toxic xenobiotic: the patchwork approach. *Trends in Biochemical Sciences, 25*(6), 261-265.

Correa-Torres, S., Kopytko, M., & Avila, S. (2016). *Efficiency of modified chemical remediation techniques for soil contaminated by organochlorine pesticides.* Paper presented at the IOP Conference Series: Materials Science and Engineering.

Dai, S., Vaillancourt, F. H., Maaroufi, H., Drouin, N. M., Neau, D. B., Snieckus, V., & Eltis, L. D. (2002). Identification and analysis of a bottleneck in PCB biodegradation. *Nature Structural & Molecular Biology, 9*(12), 934-939.

Dai, Y., Xiong, X., Huang, G., Liu, J., Sheng, S., Wang, H., & Qin, W. (2014). Dichloroacetate enhances adriamycin-induced hepatoma cell toxicity *in vitro* and *in vivo* by increasing reactive oxygen species levels. *PLoS ONE, 9*(4), 929-962.

Dainelli, B., Paludi, D., Dragani, B., Cocco, R., Principe, D. R., Petrucci, M., Aceto, A. (2002). A novel glutathione transferase from *Haemophilus influenzae* which has high affinity towards antibiotics. *The International Journal of Biochemistry & Cell Biology, 34*(8), 916-920.

Das, S. (2014). *Microbial biodegradation and bioremediation.* Elsevier.

Dasgupta, S., & Bell, J. A. (1993). Design of helix ends. *Chemical Biology & Drug Design, 41*(5), 499-511.

Dash, H. R., Mangwani, N., Chakraborty, J., Kumari, S., & Das, S. (2013). Marine bacteria: Potential candidates for enhanced bioremediation. *Applied Microbiology & Biotechnology, 97*(2), 561-568.

De Jong, H., Geiselmann, J., Hernandez, C., & Page, M. (2003). Genetic Network Analyzer: qualitative simulation of genetic regulatory networks. *Bioinformatics, 19*(3), 336-344.

De Souza, M. L., Seffernick, J., Martinez, B., Sadowsky, M. J., & Wackett, L. P. (1998). The atrazine catabolism genes atzABC are widespread and highly conserved. *Journal of Bacteriology, 180*(7), 1951-1954.

Delawary, M., Ohtsubo, Y., & Ohta, A. (2003). The dual functions of biphenyl-degrading ability of *Pseudomonas* sp. KKS102: energy acquisition and substrate detoxification. *Bioscience, Biotechnology, & Biochemistry, 67*(9), 1970-1975.

Di Ilio, C., Sacchetta, P., Bello, M. L., Caccuri, A. M., & Federici, G. (1986). Selenium independent glutathione peroxidase activity associated with cationic forms of glutathione transferase in human heart. *Journal of Molecular & Cellular Cardiology, 18*(9), 983-991.

Dirr, H., Reinemer, P., & Huber, R. (1994). X-ray crystal structures of cytosolic glutathione S-transferases. *The FEBS Journal, 220*(3), 645-661.

Dixon, D. P., Davis, B. G., & Edwards, R. (2002). Functional divergence in the glutathione transferase superfamily in plants identification of two classes with putative functions in redox homeostasis in *Arabidopsis thaliana*. *Journal of Biological Chemistry, 277*(34), 30859-30869.

Dobbins, D. C. (1995). Biodegradation of pollutants. *Encyclopedia of Environmental Biology: AE, 1*, 169.

Dourado, D. F., Fernandes, P. A., Mannervik, B., & Ramos, M. J. (2008). Glutathione transferase: new model for glutathione activation. *Chemistry-A European Journal, 14*(31), 9591-9598.

Eaton, R. W. (1994). Organization and evolution of naphthalene catabolic pathways: sequence of the DNA encoding 2-hydroxychromene-2-carboxylate isomerase and trans-o-hydroxybenzylidenepyruvate hydratase-aldolase from the NAH7 plasmid. *Journal of Bacteriology, 176*(24), 7757-7762.

Edema, C., Idu, T., & Edema, M. (2013). Remediation of soil contaminated with polycyclic aromatic hydrocarbons from crude oil. *African Journal of Biotechnology, 10*(7), 1146-1149.

Edwards, K. J., Schrenk, M. O., Hamers, R., & Banfield, J. F. (1998). Microbial oxidation of pyrite: Experiments using microorganisms from an extreme acidic environment. *American Mineralogist, 83*(11), 1444-1453.

Edwards, R., Dixon, D. P., & Walbot, V. (2000). Plant glutathione S-transferases: Enzymes with multiple functions in sickness and in health. *Trends in Plant Science, 5*(5), 193-198.

El-Sheekh, M. M., & Mahmoud, Y. A. (2017). Technological approach of bioremediation using microbial tools: Bacteria, fungi, and algae. *Handbook of Research on Inventive Bioremediation Techniques*. IGI Global. Hershey, Pennsylvania, USA. Pp. 134-154.

Erhardt, J., & Dirr, H. (1995). Native dimer stabilizes the subunit tertiary structure of porcine class pi glutathione S-transferase. *European Journal of Biochemistry, 230*(2), 614-620.

Etienne, J., Gerbaud, G., Fleurette, J., & Courvalin, P. (1991). Characterization of *staphylococcal* plasmids hybridizing with the fosfomycin resistance gene fosB. *FEMS Microbiology Letters, 84*(1), 119-122.

Falagas, M. E., Giannopoulou, K. P., Kokolakis, G. N., & Rafailidis, P. I. (2008). Fosfomycin: Use beyond urinary tract and gastrointestinal infections. *Clinical Infectious Diseases, 46*(7), 1069-1077.

Falandysz, J., Brudnowska, B., Kawano, M., & Wakimoto, T. (2001). Polychlorinated biphenyls and organochlorine pesticides in soils from the southern part of Poland. *Archives of Environmental Contamination & Toxicology, 40*(2), 173-178.

Fang, T., Li, D.-F., & Zhou, N.-Y. (2011). Identification and clarification of the role of key active site residues in bacterial glutathione S-transferase zeta/maleylpyruvate isomerase. *Biochemical and Biophysical Research Communications, 410*(3), 452-456.

Fang, Y., Nie, Z., Die, Q., Tian, Y., Liu, F., He, J., & Huang, Q. (2016). Spatial distribution, transport dynamics, and health risks of endosulfan at a contaminated site. *Environmental Pollution, 216*, 538-547.

Faroon, O. M., Keith, L. S., Smith-Simon, C., & De Rosa, C. T. (2003). Polychlorinated biphenyls: Human health aspects. *Concise international chemical assessment document*. *http://apps.who.int/iris/handle/10665/42640.*

Favaloro, B., Tamburro, A., Angelucci, S., Antonella, D., Melino, S., Carmine, D., & Rotilio, D. (1998). Molecular cloning, expression and site-directed mutagenesis of glutathione S-transferase from *Ochrobactrum anthropi*. *Biochemical Journal, 335*(3), 573-579.

Favaloro, B., Tamburro, A., Trofino, M. A., Bologna, L., Rotilio, D., & Heipieper, H. J. (2000). Modulation of the glutathione S-transferase in *Ochrobactrum anthropi*: function of xenobiotic substrates and other forms of stress. *Biochemical Journal, 346*(2), 553-559.

Felsenstein, J. (1985). Confidence limits on phylogenies: An approach using the bootstrap. *Evolution, 39*(4), 783-791.

Feng, H., Cochran, J. K., Lwiza, H., Brownawell, B. J., & Hirschberg, D. J. (1998). Distribution of heavy metal and PCB contaminants in the sediments of an urban estuary: the Hudson River. *Marine Environmental Research, 45*(1), 69-88.

Fiedler, H. (2002). *Persistent organic pollutants*. Springer.

Fillgrove, K. L., Pakhomova, S., Newcomer, M. E., & Armstrong, R. N. (2003). Mechanistic diversity of fosfomycin resistance in pathogenic microorganisms. *Journal of the American Chemical Society, 125*(51), 15730-15731.

Fillgrove, K. L., Pakhomova, S., Schaab, M. R., Newcomer, M. E., & Armstrong, R. N. (2007). Structure and mechanism of the genomically encoded fosfomycin resistance protein, FosX, from *Listeria monocytogenes*. *Biochemistry, 46*(27), 8110-8120.

Finkel, T., & Holbrook, N. J. (2000). Oxidants, oxidative stress and the biology of ageing. *Nature, 408*(6809), 239-247.

Fortin, P. D., Horsman, G. P., Yang, H. M., & Eltis, L. D. (2006). A glutathione S-transferase catalyzes the dehalogenation of inhibitory metabolites of polychlorinated biphenyls. *Journal of Bacteriology, 188*(12), 4424-4430.

Franzot, G., & Carugo, O. (2003). Computational approaches to protein-protein interaction. *Journal of Structural & Functional Genomics, 4*(4), 245-255.

Frova, C. (2006). Glutathione transferases in the genomics era: new insights and perspectives. *Biomolecular Engineering, 23*(4), 149-169.

Fukuda, M., Yasukochi, Y., Kikuchi, Y., Nagata, Y., Kimbara, K., Horiuchi, H., . . . Yano, K. (1994). Identification of the bphA and bphB genes of *Pseudomonas* sp. strain KKS102 involved in degradation of biphenyl and polychlorinated biphenyls. *Biochemical and Biophysical Research Communications, 202*(2), 850-856.

Furukawa, K. (2000). Biochemical and genetic bases of microbial degradation of polychlorinated biphenyls (PCBs). *The Journal of General & Applied Microbiology, 46*(6), 283-296.

Furukawa, K., & Fujihara, H. (2008). Microbial degradation of polychlorinated biphenyls: biochemical and molecular features. *Journal of Bioscience & Bioengineering, 105*(5), 433-449.

Garcia-Lobo, J., & Ortiz, J. (1982). Tn2921, a transposon encoding fosfomycin resistance. *Journal of Bacteriology, 151*(1), 477-479.

Gibson, D. T., & Parales, R. E. (2000). Aromatic hydrocarbon dioxygenases in environmental biotechnology. *Current Opinion in Biotechnology, 11*(3), 236-243.

Gilmartin, N., Ryan, D., & Dowling, D. N. (2005). Analysis of the C-terminal domain of *Burkholderia* sp. strain LB400 BphK reveals a conserved motif that affects catalytic activity. *FEMS Microbiology Letters, 249*(1), 23-30.

Gilmartin, N., Ryan, D., Sherlock, O., & Dowling, D. (2003). BphK shows dechlorination activity against 4-chlorobenzoate, an end product of bph-promoted degradation of PCBs. *FEMS Microbiology Letters, 222*(2), 251-255.

Gisi, D., Willi, L., Traber, H., Leisinger, T., & Vuilleumier, S. (1998). Effects of bacterial host and dichloromethane dehalogenase on the competitiveness of *methylotrophic* bacteria growing with dichloromethane. *Applied & Environmental Microbiology, 64*(4), 1194-1202.

Glick, B. R. (2015). Introduction to plant growth-promoting Bacteria *Beneficial Plant-Bacterial Interactions*: Springer. Pp. 1-28.

Gomez-Cabrero, D., Abugessaisa, I., Maier, D., Teschendorff, A., Merkenschlager, M., Gisel, A., . . . Tegnér, J. (2014). Data integration in the era of omics: Current and future challenges. *BMC Systems Biology, 8*(2), I1-19.

Goodsell, D. S., Morris, G. M., & Olson, A. J. (1996). Automated docking of flexible ligands: applications of AutoDock. *Journal of Molecular Recognition, 9*(1), 1-5.

Guengerich, F. P., McCormick, W. A., & Wheeler, J. B. (2003). Analysis of the kinetic mechanism of haloalkane conjugation by mammalian theta-class glutathione transferases. *Chemical Research in Toxicology, 16*(11), 1493-1499.

Habash, M. B., Beaudette, L., Cassidy, M., Leung, K., Hoang, T., Vogel, H., . . . Lee, H. (2002). Characterization of tetrachlorohydroquinone reductive dehalogenase from *Sphingomonas* sp. UG30. *Biochemical & Biophysical Research Communications, 299*(4), 634-640.

Habig, W. H., & Jakoby, W. B. (1981). Assays for differentiation of glutathione S-Transferases. *Methods in Enzymology, 77*, 398-405.

Habig, W. H., Pabst, M. J., & Jakoby, W. B. (1974). Glutathione S-transferases the first enzymatic step in mercapturic acid formation. *Journal of Biological Chemistry, 249*(22), 7130-7139.

Hall, A., Robson, C. N., Hickson, I. D., Harris, A. L., Proctor, S. J., & Cattan, A. R. (1989). Possible role of inhibition of glutathione S-transferase in the partial reversal of chlorambucil resistance by indomethacin in a Chinese hamster ovary cell line. *Cancer Research, 49*(22), 6265-6268.

Hamilton, D. S., Zhang, X., Ding, Z., Hubatsch, I., Mannervik, B., Houk, K., & Creighton, D. J. (2003). Mechanism of the glutathione transferase-catalyzed conversion of antitumor 2-crotonyloxymethyl-2-cycloalkenones to GSH adducts. *Journal of the American Chemical Society, 125*(49), 15049-15058.

Harper, E. T., & Rose, G. D. (1993). Helix stop signals in proteins and peptides: The capping box. *Biochemistry, 32*(30), 7605-7609.

Harrad, S. (2010). *Persistent organic pollutants*. Wiley Online Library. *https://onlinelibrary.wiley.com/doi/book/10.1002/9780470684122.*

Harris, J. M., Meyer, D. J., Coles, B., & Ketterer, B. (1991). A novel glutathione transferase (13-13) isolated from the matrix of rat liver mitochondria having structural similarity to class theta enzymes. *Biochemical Journal, 278*, 137-141.

Hayes, J. D., Flanagan, J. U., & Jowsey, I. R. (2005). Glutathione transferases. *Annual Review in Pharmacology & Toxicology, 45*, 51-88.

Hayes, J. D., & McLellan, L. I. (1999). Glutathione and glutathione-dependent enzymes represent a co-ordinately regulated defence against oxidative stress. *Free Radical Research, 31*(4), 273-300.

Hayes, J. D., & Pulford, D. J. (1995). The glutathione S-transferase supergene family: Regulation of GST and the contribution of the lsoenzymes to cancer Chemoprotection and Drug Resistance Part II. *Critical Reviews in Biochemistry & Molecular Biology, 30*(6), 521-600.

Hegyi, H., & Gerstein, M. (1999). The relationship between protein structure and function: a comprehensive survey with application to the yeast genome. *Journal of Molecular Biology, 288*(1), 147-164.

Hiraoka, Y., Yamada, T., Tone, K., Futaesaku, Y., & Kimbara, K. (2002). Flow cytometry analysis of changes in the DNA content of the polychlorinated biphenyl degrader *Comamonas testosteroni* TK102: effect of metabolites on cell-cell separation. *Applied & Environmental Microbiology, 68*(10), 5104-5112.

Hofer, B., Backhaus, S., & Timmis, K. N. (1994). The biphenyl/polychlorinated biphenyl-degradation locus (bph) of *Pseudomonas* sp. LB400 encodes four additional metabolic enzymes. *Gene, 144*(1), 9-16.

Horikoshi, K. (1998). Barophiles: Deep-sea microorganisms adapted to an extreme environment. *Current Opinion in Microbiology, 1*(3), 291-295.

Hu, J., Su, X., Han, H., Shen, C., & Shi, J. (2014). Application prospect about bioremediation of polychlorinated biphenyls-contaminated soil with immobilized microorganism technique: a review. *The Journal of Applied Ecology, 25*(6), 1806-1814.

Huang, D. W., Sherman, B. T., & Lempicki, R. A. (2008). Bioinformatics enrichment tools: paths toward the comprehensive functional analysis of large gene lists. *Nucleic Acids Research, 37*(1), 1-13.

Hug, L. A., Maphosa, F., Leys, D., Löffler, F. E., Smidt, H., Edwards, E. A., & Adrian, L. (2013). Overview of organohalide-respiring bacteria and a proposal for a classification system for reductive dehalogenases. *Philosophical Transaction of the Royal Society B, 368*(1616), 2012-2022.

Humans, I. W. (2012). *Biological agents. A review of human carcinogens. IARC monographs on the evaluation of carcinogenic risks to humans*. WHO.

Hurst, R., Bao, Y., Jemth, P., Mannervik, B., & Williamson, G. (1998). Phospholipid hydroperoxide glutathione peroxidase activity of human glutathione transferases. *Biochemical Journal, 332*, 97-100.

Jaiswal, D. K., Verma, J. P., & Yadav, J. (2017). *Microbe induced degradation of pesticides in agricultural soils.* Springer.

Jakobsson, P.-J., Mancini, J. A., Riendeau, D., & Ford-Hutchinson, A. W. (1997). Identification and characterization of a novel microsomal enzyme with glutathione-dependent transferase and peroxidase activities. *Journal of Biological Chemistry, 272*(36), 22934-22939.

Jakobsson, P.-J., Morgenstern, R., Mancini, J., Ford-Hutchinson, A., & Persson, B. (1999). Common structural features of MAPEG—a widespread superfamily of membrane associated proteins with highly divergent functions in eicosanoid and glutathione metabolism. *Protein Science, 8*(03), 689-692.

Jakoby, W. B. (2012). *Enzymatic basis of detoxication*. Elsevier.

Janssen, D. B., Dinkla, I. J., Poelarends, G. J., & Terpstra, P. (2005). Bacterial degradation of xenobiotic compounds: evolution and distribution of novel enzyme activities. *Environmental Microbiology, 7*(12), 1868-1882.

Jiang, Y.-F., Wang, X.-T., Jia, Y., Wang, F., Wu, M.-H., Sheng, G.-Y., & Fu, J.-M. (2009). Occurrence, distribution and possible sources of organochlorine pesticides in agricultural soil of Shanghai, China. *Journal of Hazardous Materials, 170*(2), 989-997.

Johnson, B. L., Hicks, H. E., Cibulas, W., Faroon, O., Ashizawa, A. E., De Rosa, C. T., . . . Clark, M. (1999). *Public health implications of exposure to polychlorinated biphenyls*. Washington, DC: Agency for Toxic Substances & Disease Registry (USDHHS) and US Environmental Protection Agency.

Jurelevicius, D., Alvarez, V. M., & Seldin, L. (2016). *Molecular diversity of environmental prokaryotes*. Tailor & Francis. P. 327.

Kanaoka, Y., Ago, H., Inagaki, E., Nanayama, T., Miyano, M., Kikuno, R., Urade, Y. (1997). Cloning and crystal structure of hematopoietic prostaglandin D synthase. *Cell, 90*(6), 1085-1095.

Kanehisa, M., & Bork, P. (2003). Bioinformatics in the post-sequence era. *Nature Genetics, 33*, 305-310.

Kannan, K., Tanabe, S., Williams, R. J., & Tatsukawa, R. (1994). Persistent organochlorine residues in foodstuffs from Australia, Papua New Guinea and the Solomon Islands: Contamination levels and human dietary exposure. *Science of the Total Environment, 153*(1), 29-49.

Kaushik, P., & Kaushik, G. (2007). An assessment of structure and toxicity correlation in organochlorine pesticides. *Journal of Hazardous Materials, 143*(1), 102-111.

Kawano, S., Kida, T., Miyawaki, K., Noguchi, Y., Kato, E., Nakano, T., & Akashi, M. (2014). Cyclodextrin polymers as highly effective adsorbents for removal and recovery of polychlorobiphenyl (PCB) contaminants in insulating oil. *Environmental Science & Technology, 48*(14), 8094-8100.

Kearse, M., Moir, R., Wilson, A., Stones-Havas, S., Cheung, M., Sturrock, S., & Duran, C. (2012). Geneious Basic: an integrated and extendable desktop software platform for the organization and analysis of sequence data. *Bioinformatics, 28*(12), 1647-1649.

Keck, A., Conradt, D., Mahler, A., Stolz, A., Mattes, R., & Klein, J. (2006). Identification and functional analysis of the genes for naphthalenesulfonate catabolism by *Sphingomonas xenophaga* BN6. *Microbiology, 152*(7), 1929-1940.

Kelce, W. R., Stone, C. R., Laws, S. C., & Gray, L. E. (1995). Persistent DDT metabolite p, p'-DDE is a potent androgen receptor antagonist. *Nature, 375*(6532), 581.

Ketterer, B., Meyer, D., Taylor, J., Pemble, S., Coles, B., & Fraser, G. (1990). GSTs and protection against oxidative stress. *Biochemistry*, *212*, 97-109.

Kiefer, P. M., & Copley, S. D. (2002). Characterization of the initial steps in the reductive dehalogenation catalyzed by tetrachlorohydroquinone dehalogenase. *Biochemistry, 41*(4), 1315-1322.

Kiefer, P. M., McCarthy, D. L., & Copley, S. D. (2002). The reaction catalyzed by tetrachlorohydroquinone dehalogenase does not involve nucleophilic aromatic substitution. *Biochemistry, 41*(4), 1308-1314.

Kikuchi, Y., Nagata, Y., Ohtsubo, Y., Koana, T., & Takagi, M. (1995). *Pseudomonas fluorescens* KKL101, a benzoic acid degrader in a mixed culture that degrades biphenyl and polychlorinated biphenyls. *Bioscience, Biotechnology, & Biochemistry, 59*(12), 2303-2304.

Kikuchi, Y., Yasukochi, Y., Nagata, Y., Fukuda, M., & Takagi, M. (1994). Nucleotide sequence and functional analysis of the meta-cleavage pathway involved in biphenyl and polychlorinated biphenyl degradation in *Pseudomonas* sp. strain KKS102. *Journal of Bacteriology, 176*(14), 4269-4276.

Kimbara, K., Hashimoto, T., Fukuda, M., Koana, T., Takagi, M., Oishi, M., & Yano, K. (1988). Isolation and characterization of a mixed culture that degrades polychlorinated biphenyls. *Agricultural & Biological Chemistry, 52*(11), 2885-2891.

Kobe, B., & Kajava, A. V. (2001). The leucine-rich repeat as a protein recognition motif. *Current Opinion in Structural Biology, 11*(6), 725-732.

Komancová, M., Jurčová, I., Kochánková, L., & Burkhard, J. (2003). Metabolic pathways of polychlorinated biphenyls degradation by *Pseudomonas* sp. 2. *Chemosphere, 50*(4), 537-543.

Kong, K.-H., Inoue, H., & Takahashi, K. (1993). Site-directed mutagenesis study on the roles of evolutionally conserved aspartic acid residues in human glutathione S-transferase P1-1. *Protein Engineering, Design and Selection, 6*(1), 93-99.

Koppel, N., Rekdal, V. M., & Balskus, E. P. (2017). Chemical transformation of xenobiotics by the human gut microbiota. *Science, 356*(6344), 2770.

Kumar, J., Lind, P. M., Salihovic, S., van Bavel, B., Ingelsson, E., & Lind, L. (2014). Persistent organic pollutants and inflammatory markers in a cross-sectional study of elderly Swedish people: The PIVUS cohort. *Environmental Health Perspectives, 122*(9), 977-983.

Kumar, S., Sharma, A. K., Rawat, S., Jain, D., & Ghosh, S. (2013). Use of pesticides in agriculture and livestock animals and its impact on environment of India. *Asian Journal of Environmental Sciences, 1*, 51-57.

Kurashvili, M., Adamia, G., Amiranashvili, L., Ananiasvili, T., Varazi, T., Pruidze, M., & Khatisashvili, G. (2016). Targeting of detoxification potential of microorganisms and plants for cleaning environment polluted by organochlorine pesticides. *Annals of Agrarian Science, 14*(3), 222-226.

La Roche, S. D., & Leisinger, T. (1990). Sequence analysis and expression of the bacterial dichloromethane dehalogenase structural gene, a member of the glutathione S-transferase supergene family. *Journal of Bacteriology, 172*(1), 164-171.

Ladner, J. E., Parsons, J. F., Rife, C. L., Gilliland, G. L., & Armstrong, R. N. (2004). Parallel evolutionary pathways for glutathione transferases: Structure and mechanism of the mitochondrial class kappa enzyme rGSTK1-1. *Biochemistry, 43*(2), 352-361.

Laemmli, U. K. (1970). Cleavage of structural proteins during the assembly of the head of bacteriophage T4. *Nature, 227*(5259), 680-685.

Land, M., Hauser, L., Jun, S.-R., Nookaew, I., Leuze, M. R., Ahn, T.-H., & Wassenaar, T. (2015). Insights from 20 years of bacterial genome sequencing. *Functional & Integrative Genomics, 15*(2), 141.

Larkin, M. A., Blackshields, G., Brown, N., Chenna, R., McGettigan, P. A., McWilliam, H., & Lopez, R. (2007). Clustal W and Clustal X version 2.0. *Bioinformatics, 23*(21), 2947-2948.

Leisinger, T. (1996). Biodegradation of chlorinated aliphatic compounds. *Current Opinion in Biotechnology, 7*(3), 295-300.

Li, A., Qu, Y. Y., Pi, W. Q., Zhou, J. T., Gai, Z. H., & Xu, P. (2012). Metabolic characterization and genes for the conversion of biphenyl in *Dyella ginsengisoli* LA-4. *Biotechnology and bioengineering, 109*(2), 609-613.

Li, M. C., Chen, P. C., Tsai, P. C., Furue, M., Onozuka, D., Hagihara, A., & Guo, Y. L. (2015). Mortality after exposure to polychlorinated biphenyls and polychlorinated dibenzofurans: A meta-analysis of two highly exposed cohorts. *International Journal of Cancer, 137*(6), 1427-1432.

Lien, S., Larsson, A.-K., & Mannervik, B. (2002). The polymorphic human glutathione transferase T1-1, the most efficient glutathione transferase in the denitrosation and inactivation of the anticancer drug 1, 3-bis (2-chloroethyl)-1-nitrosourea. *Biochemical Pharmacology, 63*(2), 191-197.

Liu, H., & Naismith, J. H. (2008). An efficient one-step site-directed deletion, insertion, single and multiple-site plasmid mutagenesis protocol. *BMC Biotechnology, 8*(1), 1.

Liu, L.-Y., Ma, W.-L., Jia, H.-L., Zhang, Z.-F., Song, W.-W., & Li, Y.-F. (2016). Research on persistent organic pollutants in China on a national scale: 10 years after the enforcement of the Stockholm Convention. *Environmental Pollution, 217*, 70-81.

Lloyd-Jones, G., & Lau, P. (1997). Glutathione S-transferase-encoding gene as a potential probe for environmental bacterial isolates capable of degrading polycyclic aromatic hydrocarbons. *Applied & Environmental Microbiology, 63*(8), 3286-3290.

Loganathan, B. G., Khim, J. S., Kodavanti, P. R. S., & Masunaga, S. (2016). *Persistent organic chemicals in the environment: Status and trends in the Pacific Basin Countries II temporal trends*. ACS Publications.

Loman, N. J., & Pallen, M. J. (2015). Twenty years of bacterial genome sequencing. *Nature Reviews Microbiology, 13*(12), 787-794.

Lopez-Echartea, E., Macek, T., Demnerova, K., & Uhlik, O. (2016). Bacterial biotransformation of pentachlorophenol and micropollutants formed during Its production process. *International Journal of Environmental Research & Public Health, 13*(11), 1146.

Ludewig, G., & Robertson, L. W. (2013). Polychlorinated biphenyls (PCBs) as initiating agents in hepatocellular carcinoma. *Cancer Letters, 334*(1), 46-55.

Luscombe, N. M., Greenbaum, D., & Gerstein, M. (2001). What is bioinformatics? A proposed definition and overview of the field. *Methods of Information in Medicine, 40*(4), 346-358.

Mandal, A. K., Skoch, J., Bacskai, B. J., Hyman, B. T., Christmas, P., Miller, D., & Evans, J. F. (2004). The membrane organization of leukotriene synthesis. *Proceeding of the National Academy of Science, 101*(17), 6587-6592.

Mandelbaum, R. T., Allan, D. L., & Wackett, L. P. (1995). Isolation and characterization of a *Pseudomonas* sp. that mineralizes the s-triazine herbicide atrazine. *Applied & Environmental Microbiology, 61*(4), 1451-1457.

Mannervik, B., Helena Danielson, U., & Ketterer, B. (1988). Glutathione transferases—structure and catalytic activity. *CRC critical Reviews in Biochemistry, 23*(3), 283-337.

Mansouri, A., Cregut, M., Abbes, C., Durand, M.-J., Landoulsi, A., & Thouand, G. (2016). The environmental issues of DDT pollution and bioremediation: A multidisciplinary review. *Applied Biochemistry & Biotechnology*, 1-31.

Marnett, L. J. (1994). Generation of mutagens during arachidonic acid metabolism. *Cancer & Metastasis Reviews, 13*(3), 303-308.

Marnett, L. J., Riggins, J. N., & West, J. D. (2003). Endogenous generation of reactive oxidants and electrophiles and their reactions with DNA and protein. *Journal of Clinical Investigation, 111*(5), 583.

Marsh, M., Shoemark, D. K., Jacob, A., Robinson, C., Cahill, B., Zhou, N.-Y., & Hadfield, A. T. (2008). Structure of bacterial glutathione-S-transferase maleyl pyruvate isomerase and implications for mechanism of isomerisation. *Journal of Molecular Biology, 384*(1), 165-177.

Martin, A. C., Orengo, C. A., Hutchinson, E. G., Jones, S., Karmirantzou, M., Laskowski, R. A., . . . Thornton, J. M. (1998). Protein folds and functions. *Structure, 6*(7), 875-884.

Masai, E., Ichimura, A., Sato, Y., Miyauchi, K., Katayama, Y., & Fukuda, M. (2003). Roles of the enantioselective glutathione S-transferases in cleavage of β-aryl ether. *Journal of Bacteriology, 185*(6), 1768-1775.

McCarthy, D. L., Navarrete, S., Willett, W. S., Babbitt, P. C., & Copley, S. D. (1996). Exploration of the relationship between tetrachlorohydroquinone dehalogenase and the glutathione S-transferase superfamily. *Biochemistry, 35*(46), 14634-14642.

McEldowney, S., Hardman, D. J., & Waite, S. (1993). *Pollution: Ecology & biotreatment*. Longman Scientific & Technical.

McGlynn, K. A., Abnet, C. C., Zhang, M., Sun, X.-D., Fan, J.-H., O'Brien, T. R., & Weber, J.-P. (2006). Serum concentrations of 1, 1, 1-trichloro-2, 2-bis (p-chlorophenyl) ethane (DDT) and 1, 1-dichloro-2, 2-bis (p-chlorophenyl) ethylene (DDE) and risk of primary liver cancer. *Journal of the National Cancer Institute, 98*(14), 1005-1010.

McGlynn, K. A., Quraishi, S. M., Graubard, B. I., Weber, J.-P., Rubertone, M. V., & Erickson, R. L. (2008). Persistent organochlorine pesticides and risk of testicular germ cell tumors. *Journal of the National Cancer Institute, 100*(9), 663-671.

McGowan, C., Fulthorpe, R., Wright, A., & Tiedje, J. (1998). Evidence for interspecies gene transfer in the evolution of 2, 4-dichlorophenoxyacetic acid degraders. *Applied and Environmental Microbiology, 64*(10), 4089-4092.

McGuinness, M., Ivory, C., Gilmartin, N., & Dowling, D. N. (2006). Investigation of substrate specificity of wildtype and mutant BphK LB400 (a glutathione S-transferase) from *Burkholderia* LB400. *International Biodeterioration & Biodegradation, 58*(3), 203-208.

McGuinness, M., Mazurkiewicz, V., Brennan, E., & Dowling, D. (2007). Dechlorination of pesticides by a specific bacterial glutathione S-transferase, BphK LB400: Potential for Bioremediation. *Engineering in Life Sciences, 7*(6), 611-615.

McKay, D. B., Prucha, M., Reineke, W., Timmis, K. N., & Pieper, D. H. (2003). Substrate specificity and expression of three 2, 3-dihydroxybiphenyl 1, 2-dioxygenases from *Rhodococcus globerulus* strain P6. *Journal of Bacteriology, 185*(9), 2944-2951.

Messens, J., & Silver, S. (2006). Arsenate reduction: Thiol cascade chemistry with convergent evolution. *Journal of Molecular Biology, 362*(1), 1-17.

Mills, N. (2006). *ChemDraw Ultra 10.0*. ACS Publications.

Morel, F., Rauch, C., Petit, E., Piton, A., Theret, N., Coles, B., & Guillouzo, A. (2004). The human glutathione transferase Kappa: gene and protein characterization and evidence for a peroxisomal localization. *Journal of Biological Chemistry*, *199*(2), 1567-1574.

Morrow, C. S., Smitherman, P. K., Diah, S. K., Schneider, E., & Townsend, A. J. (1998). Coordinated action of glutathione s-transferases and multidrug resistance protein 1 (MRP1) in antineoplastic drug detoxification mechanism of GST A1-1-and MRP1-associated resistance to chlorambucil in MCF7 breast carcinoma cells. *Journal of Biological Chemistry, 273*(32), 20114-20120.

Mosialou, E., Piemonte, F., Andersson, C., Vos, R. M., van Bladeren, P. J., & Morgenstern, R. (1995). Microsomal glutathione transferase: Lipid-derived substrates and lipid dependence. *Archives of Biochemistry and Biophysics, 320*(2), 210-216.

Motoyama, N., & Dauterman, W. (1974). Role of nonoxidative metabolism in organophosphorus resistance. *Journal of Agricultural and Food Chemistry, 22*(3), 350-356.

Nagata, Y., Miyauchi, K., & Takagi, M. (1999). Complete analysis of genes and enzymes for γ-hexachlorocyclohexane degradation in *Sphingomonas paucimobilis* UT26. *Journal of Industrial Microbiology and Biotechnology, 23*(4), 380-390.

Nagata, Y., Tabata, M., Ohtsubo, Y., & Tsuda, M. (2016). *Biodegradation of organochlorine pesticides*. American Society of Microbiology.

Nilsson, A. I., Berg, O. G., Aspevall, O., Kahlmeter, G., & Andersson, D. I. (2003). Biological costs and mechanisms of fosfomycin resistance in *Escherichia coli*. *Antimicrobial Agents & Chemotherapy, 47*(9), 2850-2858.

Nishant, N., & Upadhyay, R. (2016). Interventions in handling of pesticides in agriculture: A Review. *Journal of Agriculture & Environmental Sciences, 5*(1), 113-133.

Oakley, A. J. (2005). Glutathione transferases: New functions. *Current Opinion in Structural Biology, 15*(6), 716-723.

Ohtsubo, Y., Kudo, T., Tsuda, M., & Nagata, Y. (2004). Strategies for bioremediation of polychlorinated biphenyls. *Applied Microbiology & Biotechnology, 65*(3), 250-258.

Ohtsubo, Y., Maruyama, F., Mitsui, H., Nagata, Y., & Tsuda, M. (2012). Complete genome sequence of *Acidovorax* sp. strain KKS102, a polychlorinated-biphenyl degrader. *Journal of Bacteriology, 194*(24), 6970-6971.

Ohtsubo, Y., Shimura, M., Delawary, M., Kimbara, K., Takagi, M., Kudo, T., . . . Nagata, Y. (2003). Novel approach to the improvement of biphenyl and polychlorinated biphenyl degradation activity: Promoter implantation by homologous recombination. *Applied & Environmental Microbiology, 69*(1), 146-153.

Oliveira, A. H., Cavalcante, R. M., Duaví, W. C., Fernandes, G. M., Nascimento, R. F., Queiroz, M. E., & Mendonça, K. V. (2016). The legacy of organochlorine pesticide usage in a tropical semi-arid region (Jaguaribe River, Ceará, Brazil): Implications of the influence of sediment parameters on occurrence, distribution and fate. *Science of the Total Environment, 542*, 254-263.

Pandey, T., Chhetri, G., Chinta, R., Kumar, B., Singh, D. B., Tripathi, T., & Singh, A. K. (2015). Functional classification and biochemical characterization of a novel rho class glutathione S-transferase in *Synechocystis* PCC 6803. *FEBS Open Bio, 5*(1), 1-7.

Passatore, L., Rossetti, S., Juwarkar, A. A., & Massacci, A. (2014). Phytoremediation and bioremediation of polychlorinated biphenyls (PCBs): state of knowledge and research perspectives. *Journal of Hazardous Materials, 278*, 189-202.

Pedersen, A. G., Jensen, L. J., Brunak, S., Stærfeldt, H.-H., & Ussery, D. W. (2000). A DNA structural atlas for *Escherichia coli*. *Journal of Molecular Biology, 299*(4), 907-930.

Pemble, S. E., & Taylor, J. B. (1992). An evolutionary perspective on glutathione transferases inferred from class-theta glutathione transferase cDNA sequences. *Biochemical Journal, 287*, 957-963.

Perito, B., Allocati, N., Casalone, E., Masulli, M., Dragani, B., Polsinelli, M., & Carmine, D. (1996). Molecular cloning and overexpression of a glutathione transferase gene from *Proteus mirabilis*. *Biochemical Journal, 318*(1), 157-162.

Pieper, D. H., & Seeger, M. (2008). Bacterial metabolism of polychlorinated biphenyls. *Journal of Molecular Microbiology and Biotechnology, 15*(2-3), 121-138.

Ponce, B. L., Latorre, V. K., González, M., & Seeger, M. (2011). Antioxidant compounds improved PCB-degradation by *Burkholderia xenovorans* strain LB400. *Enzyme & Microbial Technology, 49*(6), 509-516.

Portier, R. J., Zoeller, A. L., & Fujisaki, K. (1990). Bioremediation of pesticide-contaminated groundwater. *Remediation Journal, 1*(1), 41-60.

Prabhu, K. S., Reddy, P. V., Jones, E. C., Liken, A. D., & Reddy, C. C. (2004). Characterization of a class alpha glutathione-S-transferase with glutathione peroxidase activity in human liver microsomes. *Archives of Biochemistry & Biophysics, 424*(1), 72-80.

Raza, H. (2011). Dual localization of glutathione S-transferase in the cytosol and mitochondria: Implications in oxidative stress, toxicity and disease. *FEBS Journal, 278*(22), 4243-4251.

Rife, C. L., Pharris, R. E., Newcomer, M. E., & Armstrong, R. N. (2002). Crystal structure of a genomically encoded fosfomycin resistance protein (FosA) at 1.19 Å resolution by MAD phasing off the L-III edge of Tl+. *Journal of the American Chemical Society, 124*(37), 11001-11003.

Rigét, F., Vorkamp, K., Bossi, R., Sonne, C., Letcher, R., & Dietz, R. (2016). Twenty years of monitoring of persistent organic pollutants in Greenland biota. A review. *Environmental Pollution, 217*, 114-123.

Robertson, L. W., & Hansen, L. G. (2015). *PCBs: Recent advances in environmental toxicology & health effects*. University Press of Kentucky.

Robinson, A., Huttley, G., Booth, H., & Board, P. (2004). Modelling and bioinformatics studies of the human Kappa-class glutathione transferase predict a novel third glutathione transferase family with similarity to prokaryotic 2-hydroxychromene-2-carboxylate isomerases. *Biochemical Journal, 379*, 541-552.

Rossjohn, J., Polekhina, G., Feil, S. C., Allocati, N., Masulli, M., Di Ilio, C., & Parker, M. W. (1998). A mixed disulfide bond in bacterial glutathione transferase: Functional and evolutionary implications. *Structure, 6*(6), 721-734.

Sadowsky, M. J., Tong, Z., de Souza, M., & Wackett, L. P. (1998). AtzC is a new member of the amidohydrolase protein superfamily and is homologous to other atrazine-metabolizing enzymes. *Journal of Bacteriology, 180*(1), 152-158.

Saitou, N., & Nei, M. (1987). The neighbor-joining method: a new method for reconstructing phylogenetic trees. *Molecular Biology & Evolution, 4*(4), 406-425.

Šali, A., & Blundell, T. L. (1993). Comparative protein modelling by satisfaction of spatial restraints. *Journal of Molecular Biology, 234*(3), 779-815.

Samanta, S. K., Singh, O. V., & Jain, R. K. (2002). Polycyclic aromatic hydrocarbons: environmental pollution and bioremediation. *Trends in Biotechnology, 20*(6), 243-248.

Scholtz, R., Wackett, L. P., Egli, C., Cook, A. M., & Leisinger, T. (1988). Dichloromethane dehalogenase with improved catalytic activity isolated from a fast-growing dichloromethane-utilizing bacterium. *Journal of Bacteriology, 170*(12), 5698-5704.

Seah, S. Y., Ke, J., Denis, G., Horsman, G. P., Fortin, P. D., Whiting, C. J., & Eltis, L. D. (2007). Characterization of a C—C Bond Hydrolase from *Sphingomonas wittichii* RW1 with novel specificities towards polychlorinated biphenyl metabolites. *Journal of Bacteriology, 189*(11), 4038-4045.

Seah, S. Y., Labbé, G., Nerdinger, S., Johnson, M. R., Snieckus, V., & Eltis, L. D. (2000). Identification of a serine hydrolase as a key determinant in the microbial degradation of polychlorinated biphenyls. *Journal of Biological Chemistry, 275*(21), 15701-15708.

Seeger, M., & Pieper, D. (2010). Genetics of biphenyl biodegradation and co-metabolism of PCBs. *Handbook of hydrocarbon & Lipid Microbiology* (Pp. 1179-1199): Springer.

Sericano, J., Wade, T., Jackson, T., Brooks, J., Tripp, B., Farrington, J., & Goldberg, E. (1995). Trace organic contamination in the Americas: An overview of the US national status & Trends and the International 'Mussel Watch'programmes. *Marine Pollution Bulletin, 31*(4), 214-225.

Sheehan, D., Meade, G., Foley, V., & Dowd, C. (2001). Structure, function and evolution of glutathione transferases: Implications for classification of non-mammalian members of an ancient enzyme superfamily. *Biochemical Journal, 360*, 1-16.

Sherratt, P. J., & Hayes, J. D. (2001). *Glutathione S-transferases. Enzyme systems that metabolise drugs and other xenobiotics*. Chichester UK: John Wiley and Sons.

Shigeki Tsuchida, T. I., Takao Shimizu, T. I., & Ichiro Hayatama, K. S. (1987). Purification of a new acidic glutathione S-transferase, GST-YnlYnl, with a high leukotriene-C4 synthase activity from rat brain. *European Journal of Biochemistry, 170*, 159-164.

Sies, H. (1999). Glutathione and its role in cellular functions. *Free Radical Biology & Medicine, 27*(9), 916-921.

Sims, J. L., Suflita, J. M., & Russell, H. H. (2014). *Reductive dehalogenation of organic contaminants in soils and ground water*. Wiley Online Library. *https://onlinelibrary.wiley.com/doi/full/10.1111/j.1574-6941.2000.tb00693.x.*

Singh, P., Jain, R., Srivastava, N., Borthakur, A., Pal, D., Singh, R., & Mishra, P. K. (2017). Current and emerging trends in bioremediation of petrochemical waste: A review. *Critical Reviews in Environmental Science & Technology*, *6*(5), 389-397.

Skolnick, J., & Fetrow, J. S. (2000). From genes to protein structure and function: novel applications of computational approaches in the genomic era. *Trends in Biotechnology, 18*(1), 34-39.

Skopelitou, K., Dhavala, P., Papageorgiou, A. C., & Labrou, N. E. (2012). A glutathione transferase from *Agrobacterium tumefaciens* reveals a novel class of bacterial GST superfamily. *PLoS ONE, 7*(4), e34263.

Slater, T. F. (1988). Free radical mechanisms in tissue injury. *Cell Function & Disease*. Berlin: Springer.

Smith, D., Alvey, S., & Crowley, D. E. (2005). Cooperative catabolic pathways within an atrazine-degrading enrichment culture isolated from soil. *FEMS Microbiology Ecology, 53*(2), 265-273.

Sonoki, T., Iimura, Y., Masai, E., Kajita, S., & Katayama, Y. (2002). Specific degradation ofβ-aryl ether linkage in synthetic lignin (dehydrogenative polymerizate) by bacterial enzymes of *Sphingomonas paucimobilis* SYK-6 produced in recombinantEscherichia coli. *Journal of Wood Science, 48*(5), 429-433.

Stourman, N. V., Branch, M. C., Schaab, M. R., Harp, J. M., Ladner, J. E., & Armstrong, R. N. (2011). Structure and function of YghU, a nu-class glutathione transferase related to YfcG from *Escherichia coli*. *Biochemistry, 50*(7), 1274-1281.

Stourman, N. V., Rose, J. H., Vuilleumier, S., & Armstrong, R. N. (2003). Catalytic mechanism of dichloromethane dehalogenase from *Methylophilus* sp. strain DM11. *Biochemistry, 42*(37), 11048-11056.

Suenaga, H., Watanabe, T., Sato, M., & Furukawa, K. (2002). Alteration of regiospecificity in biphenyl dioxygenase by active-site engineering. *Journal of Bacteriology, 184*(13), 3682-3688.

Suk, W. A., Ahanchian, H., Asante, K. A., Carpenter, D. O., Diaz-Barriga, F., Ha, E.-H., . . . da Silva, E. R. (2016). Environmental pollution: An under-recognized threat to children's health, especially in low-and middle-income countries. *Environmental Health Perspectives, 124*(3), A41.

Sylvestre, M., Massé, R., Ayotte, C., Messier, F., & Fauteux, J. (1985). Total biodegradation of 4-chlorobiphenyl (4 CB) by a two-membered bacterial culture. *Applied Microbiology & Biotechnology, 21*(3-4), 192-195.

Tamura, K., Battistuzzi, F. U., Billing-Ross, P., Murillo, O., Filipski, A., & Kumar, S. (2012). Estimating divergence times in large molecular phylogenies. *Proceeding of the National Academy of Science, 109*(47), 19333-19338.

Tamura, K., Stecher, G., Peterson, D., Filipski, A., & Kumar, S. (2013). MEGA6: Molecular evolutionary genetics analysis version 6.0. *Molecular Biology & Evolution, 30*(12), 2725-2729.

Tew, K. D. (1994). Glutathione-associated enzymes in anticancer drug resistance. *Cancer Research, 54*(16), 4313-4320.

Thom, R., Dixon, D. P., Edwards, R., Cole, D. J., & Lapthorn, A. J. (2001). The structure of a zeta class glutathione S-transferase from *Arabidopsis thaliana*: characterisation of a GST with novel active-site architecture and a putative role in tyrosine catabolism. *Journal of Molecular Biology, 308*(5), 949-962.

Thompson, A. M. (1992). The oxidizing capacity of the earth's atmosphere: Probable past and future changes. *Science, 256*(5060), 1157-1165.

Thompson, L. C., Ladner, J. E., Codreanu, S. G., Harp, J., Gilliland, G. L., & Armstrong, R. N. (2007). 2-Hydroxychromene-2-carboxylic Acid Isomerase: A kappa class glutathione transferase from *Pseudomonas putida*. *Biochemistry, 46*(23), 6710-6722.

Thompson, M. K., Keithly, M. E., Sulikowski, G. A., & Armstrong, R. N. (2015). Diversity in fosfomycin resistance proteins. *Perspectives in Science, 4*, 17-23.

Tong, Z., Board, P. G., & Anders, M. (1998). Glutathione transferase zeta-catalyzed biotransformation of dichloroacetic acid and other α-haloacids. *Chemical Research in Toxicology, 11*(11), 1332-1338.

Vaillancourt, F. H., Labbé, G., Drouin, N. M., Fortin, P. D., & Eltis, L. D. (2002). The mechanism-based inactivation of 2, 3-dihydroxybiphenyl 1, 2-dioxygenase by catecholic substrates. *Journal of Biological Chemistry, 277*(3), 2019-2027.

van Hylckama Vlieg, J. E., Kingma, J., Kruizinga, W., & Janssen, D. B. (1999). Purification of a glutathione S-transferase and a glutathione conjugate-specific dehydrogenase involved in isoprene metabolism in *Rhodococcus* sp. strain AD45. *Journal of Bacteriology, 181*(7), 2094-2101.

van Hylckama Vlieg, J. E., Kingma, J., van den Wijngaard, A. J., & Janssen, D. B. (1998). A glutathione S-transferase with activity towards cis-1, 2-dichloroepoxyethane is involved in isoprene utilization by *Rhodococcus* sp. strain AD45. *Applied and Environmental Microbiology, 64*(8), 2800-2805.

van Hylckama Vlieg, J. E., Leemhuis, H., Spelberg, J. H. L., & Janssen, D. B. (2000). Characterization of the gene cluster involved in isoprene metabolism in *Rhodococcus* sp. strain AD45. *Journal of Bacteriology, 182*(7), 1956-1963.

Vargo, M. A., & Colman, R. F. (2004). Heterodimers of wild-type and subunit interface mutant enzymes of glutathione S-transferase A1–1: Interactive or independent active sites? *Protein Science, 13*(6), 1586-1593.

Vedler, E. (2009). *Megaplasmids and the degradation of aromatic compounds by soil bacteria*. Springer. Pp. 33-53.

Verhoeven, D. T., Verhagen, H., Goldbohm, R. A., van den Brandt, P. A., & van Poppel, G. (1997). A review of mechanisms underlying anticarcinogenicity by brassica vegetables. *Chemico-Biological Interactions, 103*(2), 79-129.

Vézina, J., Barriault, D., & Sylvestre, M. (2007). Family shuffling of soil DNA to change the regiospecificity of *Burkholderia xenovorans* LB400 biphenyl dioxygenase. *Journal of Bacteriology, 189*(3), 779-788.

Vignesvaran, K., & Alias, Z. (2016). Participation of Y89 and Y97 in the conjugating activity of *Drosophila melanogaster* glutathione s-transferase D3 (DmGSTD3). *Archives of Insect Biochemistry & Physiology, 92*(3), 210-221.

Vos, R. M., Rietjens, I. M., Stevens, L. H., & Van Bladeren, P. J. (1989). Methyl linoleate ozonide as a substrate for rat glutathione S-transferases: reaction pathway and isoenzyme selectivity. *Chemico-Biological Interactions, 69*(2), 269-278.

Vuilleumier, S. (1997). Bacterial glutathione S-transferases: What are they good for? *Journal of Bacteriology, 179*(5), 1431.

Vuilleumier, S., Ivoš, N., Dean, M., & Leisinger, T. (2001). Sequence variation in dichloromethane dehalogenases/glutathione S-transferases. *Microbiology, 147*(3), 611-619.

Vuilleumier, S., & Pagni, M. (2002). The elusive roles of bacterial glutathione S-transferases: New lessons from genomes. *Applied Microbiology and Biotechnology, 58*(2), 138-146.

Wackett, L. P. (2002). Mechanism and applications of Rieske non-heme iron dioxygenases. *Enzyme and Microbial Technology, 31*(5), 577-587.

Wadington, M. C., Ladner, J. E., Stourman, N. V., Harp, J. M., & Armstrong, R. N. (2009). Analysis of the structure and function of YfcG from *Escherichia coli* reveals an efficient and unique disulfide bond reductase. *Biochemistry, 48*(28), 6559-6561.

Wang, R. W., Newton, D., Huskey, S., McKeever, B., Pickett, C., & Lu, A. (1992). Site-directed mutagenesis of glutathione S-transferase YaYa. Important roles of tyrosine 9 and aspartic acid 101 in catalysis. *Journal of Biological Chemistry, 267*(28), 19866-19871.

Wang, X., Martínez, M.-A., Dai, M., Chen, D., Ares, I., Romero, A., & Martínez-Larrañaga, M.-R. (2016). Permethrin-induced oxidative stress and toxicity and metabolism. A review. *Environmental Research, 149*(5), 86-104.

Wang, X.-Y., Zhang, Z.-R., & Perrett, S. (2009). Characterization of the activity and folding of the glutathione transferase from *Escherichia coli* and the roles of residues Cys10 and His106. *Biochemical Journal, 417*(1), 55-64.

Watanabe, K. (2001). Microorganisms relevant to bioremediation. *Current Opinion in Biotechnology, 12*(3), 237-241.

Wheeler, J. B., Stourman, N. V., Thier, R., Dommermuth, A., Vuilleumier, S., Rose, J. A., . . . Guengerich, F. P. (2001). Conjugation of haloalkanes by bacterial and mammalian glutathione transferases: mono-and dihalomethanes. *Chemical Research in Toxicology, 14*(8), 1118-1127.

Wiktelius, E., & Stenberg, G. (2007). Novel class of glutathione transferases from *cyanobacteria* exhibit high catalytic activities towards naturally occurring isothiocyanates. *Biochemical Journal, 406*, 115-123.

Wilce, M. C., & Parker, M. W. (1994). Structure and function of glutathione S-transferases. *Biochimica et Biophysica Acta (BBA)-Protein Structure and Molecular Enzymology, 1205*(1), 1-18.

Wood, T. K. (2008). Molecular approaches in bioremediation. *Current Opinion in Biotechnology, 19*(6), 572-578.

Wu, B.-Z., Chen, H.-Y., Wang, S. J., Wai, C. M., Liao, W., & Chiu, K. (2012). Reductive dechlorination for remediation of polychlorinated biphenyls. *Chemosphere, 88*(7), 757-768.

Xu, K., & Thornalley, P. J. (2001). Involvement of glutathione metabolism in the cytotoxicity of the phenethyl isothiocyanate and its cysteine conjugate to human leukaemia cells *in vitro*. *Biochemical Pharmacology, 61*(2), 165-177.

Xun, L., Topp, E., & Orser, C. (1992). Purification and characterization of a tetrachloro-p-hydroquinone reductive dehalogenase from a *Flavobacterium* sp. *Journal of Bacteriology, 174*(24), 8003-8007.

Yamamoto, K., Shigeoka, Y., Aso, Y., Banno, Y., Kimura, M., & Nakashima, T. (2009). Molecular and biochemical characterization of a Zeta-class glutathione S-transferase of the silkmoth. *Pesticide Biochemistry & Physiology, 94*(1), 30-35.

Yamamoto, K., Zhang, P., Miake, F., Kashige, N., Aso, Y., Banno, Y., & Fujii, H. (2005). Cloning, expression and characterization of theta-class glutathione S-transferase from the silkworm, *Bombyx mori*. *Comparative Biochemistry and Physiology Part B: Biochemistry and Molecular Biology, 141*(3), 340-346.

Yu, B., Jin, X., Kuang, Y., Megharaj, M., Naidu, R., & Chen, Z. (2015). An integrated biodegradation and nano-oxidation used for the remediation of naphthalene from aqueous solution. *Chemosphere, 141*, 205-211.

Yu, J., Liu, Q., Liu, L., & Chen, J. (2017). Cloning and characterization of dichloromethane dehalogenase from *Methylobacterium rhodesianum* for dichloromethane degradation. *Bioremediation Journal, 21*(2), 71-80.

Zablotowicz, R. M., Hoagland, R. E., Locke, M. A., & Hickey, W. J. (1995). Glutathione-S-transferase activity and metabolism of glutathione conjugates by rhizosphere bacteria. *Applied and Environmental Microbiology, 61*(3), 1054-1060.

Zaffar, H., Irshad, U., Pervez, A., & Naqvi, T. A. (2016). Mode of action, toxicity and biodegradation of organchlorinated pesticides: A Mini Overview. *Journal of Applied and Environmental Biological Sciences, 6*(8), 1-6.

Zeen, T., Philip, G., & Anders, M. (1998). Glutathione transferase zeta catalyses the oxygenation of the carcinogen dichloroacetic acid to glyoxylic acid. *Biochemical Journal, 331*(2), 371-374.

Zhang, H., Jiang, X., Lu, L., & Xiao, W. (2015). Biodegradation of polychlorinated biphenyls (PCBs) by the novel identified *Cyanobacterium Anabaena* PD-1. *PLoS ONE, 10*(7), 131-145.

Zhao, B., & Poh, C. L. (2008). Insights into environmental bioremediation by microorganisms through functional genomics and proteomics. *Proteomics, 8*(4), 874-881.

Zielinski, M., Kahl, S., Standfuß-Gabisch, C., Cámara, B., Seeger, M., & Hofer, B. (2006). Generation of novel-substrate-accepting biphenyl dioxygenases through segmental random mutagenesis and identification of residues involved in enzyme specificity. *Applied and Environmental Microbiology, 72*(3), 2191-2199.

LIST OF PUBLICATIONS AND PAPERS PRESENTED

PUBLICATIONS

(1) Shehu, D., & Alias, Z. (2018). Functional Role of Tyr12 in the Catalytic Activity of Novel Zeta-like Glutathione S-transferase from *Acidovorax* sp. KKS102. *The protein journal*, *37*(3) 261-269.

(2) Shehu, D., & Alias, Z (2018). Dechlorination of polychlorobiphenyl (PCB) degradation metabolites by a recombinant glutathione transferase from *Acidovorax* sp. KKS102. *FEBS open bio*.

PAPERS PRESENTED

(1) Dayyabu Shehu & Zazali Alias. Molecular cloning, Expression and Role of Cytosolic Glutathione S-transferase from *Acidovorax* sp. KKS 102 in the biodegradation of polychlorobiphenyls, 21st Biological Sciences Graduate Congress (BSGC), December 2016. University of Malaya, Kuala Lumpur, Malaysia.

(2) Dayyabu Shehu & Zazali Alias. Site-directed mutagenesis, characterization and study of the interaction of organochlorine pesticides with wild-type and mutant glutathione S-transferases from *Acidovorax* sp. KKS102, 43nd Annual Conference of the Malaysian Society for Biochemistry and Molecular Biology (MSBMB), August 2017-Kuala Lumpur, Malaysia.